Genetic and molecular mechanisms of early embryonic patterning in *Danio rerio, Oryzias latipes* and *Kryptolebias marmoratus*

Submitted by

Hussein Abed Saud Almatwari

To the University of Exeter as a thesis for the degree of

Doctor of Philosophy in Biological Sciences,

July 2017

I certify that all material in this thesis which is not my own work has been identified and that no material has previously been submitted and approved for the award of a degree by this or any other University.

Signature: ……

Summary

The aim of this project is to investigate genetic mechanisms of early development of vertebrate embryos using model fish species. Zebrafish (*Danio rerio*) and medaka (*Orizias latipes*) have been used extensively for molecular genetics and developmental biology studies because these fish produce many eggs, which can be manipulated from the 1 cell stage and are ideally suited for analysing gene expression, function, and embryonic phenotypes. These species have already been extensively used to generate many mutants which show clear phenotypes during early embryonic development. The development of other model species for mutant screening and analyses is likely to provide scope to analyse gene function from uncharacterised/under-characterised genes. Therefore we have developed and tested a small number of early developmental mutants from the mangrove killifish (*Kryptolebias marmoratus*).

To achieve my aim, embryos from zebrafish, medaka and the mangrove killifish have been used as models to study gene function and understand the molecular mechanisms for early patterning genes. We focused in particular on development of neural ectoderm and non-neural ectoderm (epidermis) and anterior-posterior patterning (head, trunk and tail development). As different model animals have different advantages, we used these model animals for different purposes. Zebrafish and medaka were used with chemical treatment (specific inhibitors of target genes) and morpholino analyses because they give many synchronized eggs every morning allowing highly replicated analyses. On the other hand, the mangrove killifish were used for developing and testing novel mutants and associated loss (or gain) of gene function.

Firstly, zebrafish was used to study maternal fibroblast growth factor (FGF) signaling at pre-maternal zygotic transition (Pre-MZT) and consequent neural induction at the gastrula stage (Chapter 3). This study found the important role of acquiring maternal FGF signaling in stem cells to achieve neural induction during the zygotic gene expression stage. An FGF signaling inhibitor SU5402 was tested using RNA–seq, ATAC-seq, *in situ* hybridization and immunohistochemistry methods. Through these techniques, we found that the maternal FGF signaling provides competence to the ectodermal stem cells for neural induction possibly via epigenetic modification of histone trimethylation. To examine the role of a specific FGF molecule (FGF2), gene knockdown was conducted to study *fgf2* gene function during early development in zebrafish (Chapter 4). *In situ* hybridization and immunostaining with tissue-specific markers at the gastrula stage were used to discover a novel role for *fgf2* in development of the epidermis.

The final stage of my project involved characterization of mutations underlying two mutant phenotypes (*short tail/stl* and *ball tail/stl*), that exhibit defects in tail development using the self-fertilizing mangrove killifish (Chapter 5). Using a small scale RNA-seq, the mutated genes responsible for the *stl* and *btl* mutations were instantly identified as *noto* and *msgn1* respectively. The mutant phenotype was phenocopied by morpholino injections in medaka. This study revealed crucial roles of the two genes in tail bud development. Defects of these genes affected the motility of progenitor cells in the tail bud by suppressing cell translocation to the axial mesoderm in the *noto* mutation and to the paraxial mesoderm in the *msgn1* mutation. The study demonstrated similarity of gene function and redundancy in the mangrove killifish and medaka that is different from the function of these genes in zebrafish, revealing the importance of

research on different model animals to fully characterise the gene function. From these data, it can be considered that mangrove killifish is very powerful model for mutation screening, suggesting that this animal model can be applied in various genetic studies alongside or in addition to other vertebrate models.

Acknowledgements

I would like to thank the Iraqi Ministry of Higher Education and Scientific Research and Iraqi Cultural Attaché for their continued support. I would like to thank the funding body, University of Basrah-Iraq, for their assistance and financial support. I would also like to thank my supervisor Dr.Tetsu Kudoh for the proposition and guidance My PhD project. Many Thanks for ARC team and sequencing team who aided me over research period. Thanks are also for Dr. John Dowdle, manager of lab 201, Dr. Anke Lange, and Dr. Jonathan Ball for the helpful advice. A special thanks to Dr. Ross Brown for his assistance. Thanks are also for my Colleagues in 201 lab who gave me time and assistance.

Table of contents

Chapter 1: General Introduction

Chapter 2: Materials and Methods

Results Chapter 3

Results Chapter 4

Results Chapter 5

Chapter 6: General Discussion

Appendix . ……..169

List of Figures

CHAPTER 1

CHAPTER 3

CHAPTER 4

CHAPTER 5

List of Tables

CHAPTER 1

CHAPTER 2

CHAPTER 3

CHAPTER 4

CHAPTER 5

List of General Abbreviations

ATAC-seq	Assay for Transposase Accessible Chromatin with high throughput sequencing
BMP	Bone Morphogenic Protein
BSA	Bovine Serum Albumin
CDNA	Complementary DNA
CHAPS	3-[(3-Cholamidopropyl)dimethylammonio]-1-propanesulfonate hydrate
CE	Convergent Extension
Chip-seq	Chromatin Immunoprecipitation followed by sequencing
CNS	Central Nervous System
CRISPR/Cas9	Clustered Regularly Interspaced Short Palindromic Repeats
DEG	Differentially expressed Genes
DESeq	Differential Expression Sequencing
DIG	Digoxigenin
DM	Dorsomorphin
DMSO	Demethylsulphoxide
DNA	Deoxyribonucleic Acid
DNase	Deoxy ribonuclease

dNTP	deoxy Nucleoside Triphosphate
dpf	day post fertilization
EDTA	Ethylene Diamante Tetra acetic Acid
ENU	N-Ethyl –N-nitroso Urea
ES	Embryonic Stem cells
F1, 2, 3….	Filial 1, 2, 3….
FBS	Fetal Bovine Serum
FDR	False Discovery Rate
FGF	Fibroblast Growth Factor
FGFR	Fibroblast Growth Factor Receptor
GB	Giga Base Pair
GO	Gene Ontology
HI-BS	Heat Inactivated-Bovine serum
hpf	hours post fertilization
HTSeq	High Throughput Sequencing
MB	Mega Base Pair
MBT	Mid- Blastula Transition
MHB	Mid-Hind Brain
M-MLV	Moloney Murine Leukemia Virus enzyme

MO	Morpholino
MT	Methyl Testosterone
MZT	Maternal zygotic Transition
PBS	Phosphate Buffered Saline
PBST	Phosphate Buffered Saline Triton
PCR	Polymerase Chain Reaction
PFA	Paraformaldehyde
PPT	Parts Per Thousand
RAD- seq	Restriction site Associated DNA markers sequencing
RIN^e	RNA integrity number is an algorithm for assigning integrity values to RNA measurements
RNA	Ribonucleic Acid
RNA-seq	Ribonucleic Acid sequencing
SSC	Saline Sodium Citrate
TBS	Tris Buffered Saline
TFs	Transcription Factors
UV	Ultra Violet
YSL	Yolk Syncytial Layer

Chapter 1: General Introduction

Introduction

1- Model fish species in developmental genetic

1.1-Zebrafish, *Danio rerio*

The zebrafish, *Danio rerio* (Family: Cyprinidae; Order: Cypriniformes) is endemic to eastern India, it is considered as a unique and strong model because of its small size (30-40mm in adults) and its capacity to develop rapidly (hatching period 2 days post fertilization (dpf) (table1), facilitating live imaging, transgenesis and genetics experiments (Nusslein-Volhard *et al*., 2002; Veldman and Lin, 2008; Mork and Crump, 2015). During early development, the yolk is confined within a restricted area that enables adequate viewing of cells during cleavage. The rapid embryonic development also enables the body plan to be investigated in a short time (Kimmel, 1989). Sexual maturity of zebrafish is attained in three months. Zebrafish are easy to maintain and breed. They can survive temperatures between 25-33C° and salinity 0.1-0.6 ppt. (Kimmel 1995 *et al*.; Lawrence, 2007). Hundreds of eggs can be obtained weekly. All of these features are rarely available in other model vertebrates (Driever *et al.*, 1994) which means that zebrafish are highly suitable for developmental and genetic analysis (Mendieta -Serrano *et al.*, 2013).

One of the important aspects in zebrafish studies is the large number of genetic screens, matching with many human clinical disorders. The genomic resemblance between zebrafish and other vertebrates, including humans, make zebrafish an ideal model for human medical research (Veldman and Lin, 2008). Substantial progress has been gained in human pathophysiology through characterization and identification of zebrafish genetic mutant phenotypes (Dooley and Zon, 2000).

1.2- Medaka, *Oryzias latipes*

Medaka, *Oryzias latipes*, (Family: Adrianichthyidae; Order: Beloniformes) is a fresh water fish that is native to Japan; it is considered a worthy model for genetic and developmental studies (Inoue and Takei, 2003). The small size of fish, surviving ability to grow in small aquaria under the normal laboratory conditions, the large and transparent eggs and their small genome size commend this species as a good model for genetic studies (Iwamatsu, 2004; Ozato and Wakamatsu, 1994).

Medaka possess the same requirements as the zebrafish in terms of water quality and light period, but there are differences in temperature tolerance at early stages of development versus late stages. For example medaka embryos can tolerate temperature between 4-35°C, but the tolerable range is 18-35°C at the heart beating stage (stage 22); medaka can also tolerate a wide range of salinity between 0.1-15 ppt (Kang *et al*., 2008). Hatching occurs within 10 dpf and the generation time in medaka is between 6-8 weeks, which is less than for zebrafish (table1). Each female spawns between 20-40 eggs in a day in the early morning (Furutani-Seiki and Wittbrodt, 2004).

1.3- The mangrove killifish, *Kryptolabias marmoratus*

The Mangrove killifish, *Kryptolabias marmoratus* (Family: Rivulidae; Order: Cyprindontiformes) was originally known as *Rivulus marmoratus* (Poey, 1880). The natural habitat of *K. marmoratus* is mangrove areas, which are found in tropical and subtropical regions in brackish water from Brazil to Florida (Harrington & Rivas, 1958). *K*. *marmoratus* can also live in marine water, in brackish water and in hypersaline swamps; it is known for its ability to survive and resist the extreme changes in the environment (Lee *et al.*, 2008). It can

remain alive in humid leaves for more than one month (Nordlie, 2006). Oxygen carbon dioxide gases and sodium, chloride ions exchange across the mangrove killifish skin. It can perform cutaneous respiration from air at low levels of oxygen in the water (Wright, 2012). *K. marmoratus* is extremely euryhaline; it can survive in salinities ranging from fresh water to 32 ppt (King *et al.*, 1989) and can tolerate temperatures between 7°C to 38°C (table1) (Taylor *et al.*, 2001; Elison *et al.*, 2012), and oxygen deficiency. In addition, it is resistant to high levels of ammonia. *K. marmoratus* can volatilise a considerable amount of ammonia from its cutaneous surface (Litwiller *et al.*, 2006) and is more resistant to external parasites compared with other species (Taylor, 2012). All of these characters have enabled researchers to maintain the fish easily under laboratory conditions.

The mangrove killifish reaches 45mm total length in the wild (Grageda *et al.*, 2005). A unique characteristic of this species is its reproductive biology; it is a self-fertilising hermaphrodite; its eggs are self-fertilized. This event was recorded in 1961 for the first time by Robert Harrington (Avise, 2008).

In the wild only hermaphrodites and males have been observed. Hermaphrodites can be recognized by their brownish colour and spots on the caudal fin, whereas the males have orange colour in their fins. Both hermaphrodites and males have been observed among laboratory cultured individuals (Grageda *et al.*, 2005). Like numerous species of fishes that change their sex during part of their life, hermaphrodites of *K. marmoratus* become secondary males by loss of ovarian tissue. In contrast primary males develop directly without passing through the hermaphrodite stage (Harrington, 1967).

After 3-4 years of *K*. *marmoratus* life about 60% of hermaphrodite phenotypes change into secondary males that produce sperm only (Lee *et al.*, 2008).

Gonadal development and sexual maturity of *K*. *marmoratus* were examined through histological study of gonads by Cole and Noakes (1997); the study illustrated development of gonads in mature and immature individuals aged between 1-150 days. Cole and Noakes have proved that there are female mangrove killifish, as opposed to other researchers who mentioned there are no pure females reported in natural or laboratory populations. They ascribed that, due to biased sampling for old or large adults, sexual maturity of males is indicated clearly by orange coloration expression, but adult females are less easily recognized. Some aspects of *K*. *marmoratus* were studied by Sakakura and Noakes (2000): age, growth and sexual development. They reported the relationship between the age and total length, between age and otolith annuli radius, and they also recorded that mature ovarian gonads were seen between 60-100 dpf, according to histological sections. The hatching period of fertilized eggs is between 12-21dpf, and embryos become mature after 12 weeks post hatch (Taylor *et al*., 1995). Lee *et al.* (2008) studied the morphology, ecology and distribution of *K*. *marmoratus,* they described its reproductive cycle, and mention in their review paper the potential use of mangrove killifish in toxicological studies alongside other common species, such as zebrafish and medaka. Sakakura *et al.* (2006) studied the morphology and histology of *K*. *marmoratus* gonads: They mentioned that three hormones (oestrogen, androgen and progestin) are secreted by this species which is considered a special case in such teleost. Sex determination studies on *K*. *marmoratus* were conducted by Kanamori *et al.* (2006), who treated late stage *K*. *marmoratus* embryos (10 dpf) with 0.025 mg/ml of Methyl testosterone (MT), and reported

that the rate of changing to male was about 97%, but the underlying mechanisms were not identified.

Outcrossing between males and hermaphrodites in nature has been shown by Mackiewicz *et al.* (2006a), through isolation of 36 microsatellite loci from several strains. Their work confirmed that successful outcrossing generated heterozygous progenies. Microsatellite markers also provided evidence of high diversity of DNA fingerprints in Twin Cays and Belize strains, confirming outcrossing events between *K*. *marmoratus* males and hermaphrodites in nature. The observed mixed mating strategy that involves such solitary self-fertilizing species for generating a variety of genotypic characters is a classic example of adaptive evolution (Mackiewicz *et al.* 2006b).

Mourabit *et al.* (2011) described the development of *K*. *marmoratus* embryos from the one cell stage after fertilization until the hatching stage, showing 32 stages over 310 hours of development, and this work provides a sound basis for studying early developmental process in this species. Mourabit and Kudoh (2012) showed applications of many methodological processes in *K*. *marmoratus* experiments, such as manipulation of the dechorionated embryo, microinjection, controlling cell development and imaging, concluding that *K*. *marmoratus* is an excellent model for developmental biology.

Several studies have been conducted on *K. marmoratus,* which exploit certain features that make it ideal for molecular research. Self-fertilization facilitates the generation of homozygous progeny lines, as well as the possibility of harvesting many generations from one adult parent. The short life cycle of this species is an important feature for genetic studies; larvae mature in to adults within three months under laboratory conditions. The ability of this species to survive in

extreme conditions, including a wide range of water salinities also makes it an amenable model for biological studies. There are some disadvantages of using *K*. *marmoratus,* including their small and infrequent (weekly) broods of around 10-20 eggs. The earliest stages of divisions of eggs may occur inside the fish before spawning, therefore collecting suitable numbers of one-cell-stage embryos for DNA and RNA injection is not easy. However, by using sufficiently large numbers of fish stock, it is possible to obtain enough embryos to study, and therefore the power of the self-fertilising animal for studying genetics can be still be applied in developmental biology research. The powerful feature of *K*. *marmoratus* i.e. generating homozygous progeny from the first line of offspring makes it a unique model for genetic studies. New investigations of this species present great prospects for many biomedical, phylogenetic and mutagenesis experiments. Mutation studies reveal different functions of the genes and the time of their expression during configuration of the embryo.

Fish model	*D. rerio*	*O. latipes*	*K. marmoratus*
Temperature (°C)	25-33	18-35	7-38
Salinity (PPT)	0.1-0.6	0.1-15	0.1-32
Total length (mm)	30-40	25-35	45
Fecundity (eggs)	≤ 100/daily	20-40/daily	10-20/weekly
Hatching period (dpf)	2	10	12-21
Generation time (week)	8-10	6-8	12
Genome size	1.42 Gb	800 Mb	680 Mb
References	Kimmel *et al*. (1995) Lawrence (2007)	Iwamtsu (2004) Kang *et al*. (2008)	Taylor *et al*. (1995) Rhee *et al*. (2017)

Table 1. Comparison of key characteristics among fish models used in genetic studies

2- Employment of different model species to study embryonic development in fish

Three fish species were selected as complementary models for studying gene function. The zebrafish has a fully sequenced and comprehensively annotated

genome. It is ideally suited for studying embryo-larval development, since it regularly produces externally fertilised eggs, which can be readily injected at the one cell stage to study the effects of morpholinos or chemical inhibitors of gene function. Although not fully sequenced, mangrove killifish is highly isogenic (due to self-fertilisation) and therefore offers the possibility of reducing the number of generations necessary to generate genetic lines for the study of specific gene mutations. However, since mangrove killifish eggs develop internally for several cell stages they are not injectable at the one cell stage for studying gene function. Medaka have a similar genome size to mangrove killifish (as opposed to zebrafish, which have a larger genome), but like zebrafish their eggs are fertilised externally and embryos are injectable at the one cell stage. Therefore medaka were used to phenocopy mangrove killifish mutants and the results were compared.

Embryonic development of the zebrafish has been reported in detail by Kimmel *et al.* (1995); After fertilization, the zygote initiates a series of cell divisions; this stage represents cleavage that ends at the onset of a new stage called blastula (512 cells) when the spherical blastodisc and the yolk syncytial layer (YSL) develop. The blastula stage is subdivided into the high stage (1000 cells), oblong stage (elliptical shape), sphere stage (spherical shape but the boarder of blastodisc still equable), dome stage (yolk cells twist across the animal pole) and 30% epiboly (cells spreading and forming an envelope layer). The gastrula stage starts at 50% epiboly. At the beginning of gastrula, the germ ring and the shield (it is easily to distinguish dorsal side from ventral side through the thickness of germ ring) are formed. The blastoderm expands toward the vegetal pole as epiboly progresses. With the progress of epiboly, the blastoderm covers the yolk. According to the level of coverage of blastoderm, the gastrula stage

may be defined as 75% epiboly (mid gastrula) or 90% epiboly (late gastrula) and the bud stage, the end of gastrula (tail bud present). Soon after the bud stage, somitogenesis initiates and is accompanied by organ development (organogenesis) (Kimmel *et al.*, 1995). Somitogenesis starts at around 10h and finishes at 22hpf. From somitogensis to hatching, organs began to develop such as optic vesicle, otic vesicle, brain segments and visceral organs. (Fig.1, Kimmel *et al*., 1995).

In the mangrove killifish, developmental pattern and speed is more similar to medaka. However the hatching period takes two weeks or more. Due to its unique reproductive strategy, self-fertilization, embryos are laid at various stages and the number of eggs produced each week is around 20. Mourabit *et al*. (2011) divided embryonic development into 32 stages, which begins with a one cell stage (stages 1, takes 2h 30min), cleavage (stage 2, 3h 30min). Blastula stages continues until stage 9 (10h 30min), early gastrula starts at stage 10 (15hpf) and ends at 100% epiboly at stage 15 (31hpf). The tail bud is recognizable at stage 16 (34h 30min), along with a discernible head. Optic vesicle and somite formation occur at stage 17 (36hpf). At stage 18 (43h 30min) brain segmentation for fore-mid-hind brain become visible (Fig. 2).

In medaka, fertilisation occurs by mating of males and females in the morning. The females carry eggs in chains attached to their belly (15 to 30 eggs). The chorion has hair; therefore the embryo is not suitable for imaging without removing the chorion. Embryonic development has been described within 39 stages (Iwamatsu, 2004). The first cleavage occurs at around 1hpf. Blastula starts and ends at stage 10-11 (6h - 8h15min. pf). Gastrula began at stage 12 (10 h 20 min pf) and late gastrula at stage 16 (21hpf), 2 somite starts at stage

19 (1 day 3h 30 min pf) and somite completion at stage 32 (4 days 5hpf) during these stages many organs begin developing such as the optic lobe, optic vesicles, after somite completion the swim bladder can be recognized. (Fig.3, Iwamatsu, 2004).

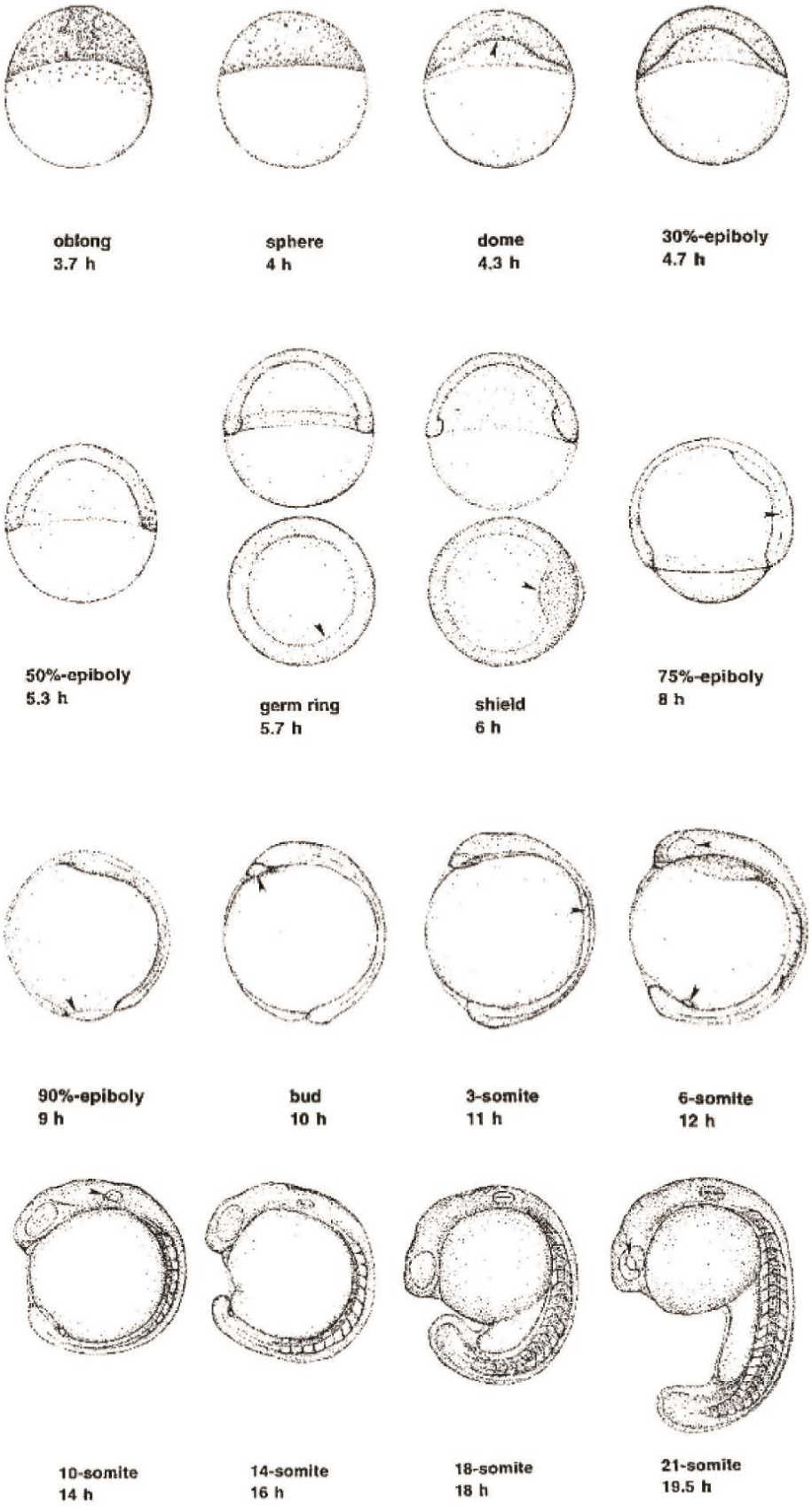

Figure 1. Embryonic development of zebrafish from blastula to somite (Kimmel *et al*., 1995)

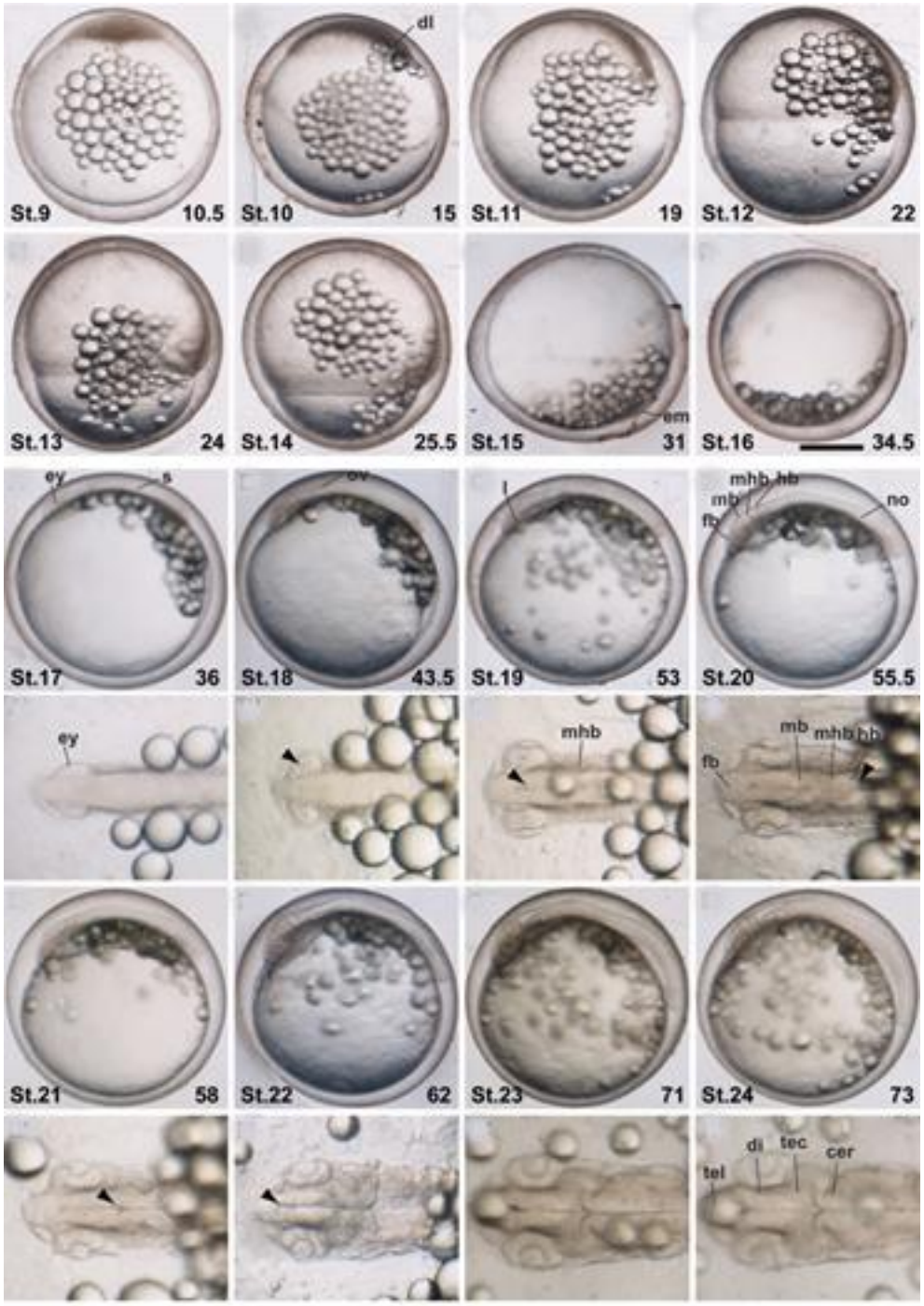

Figure 2. Embryonic development of mangrove killifish from blastula to somite (Mourabit *et al*., 2011)

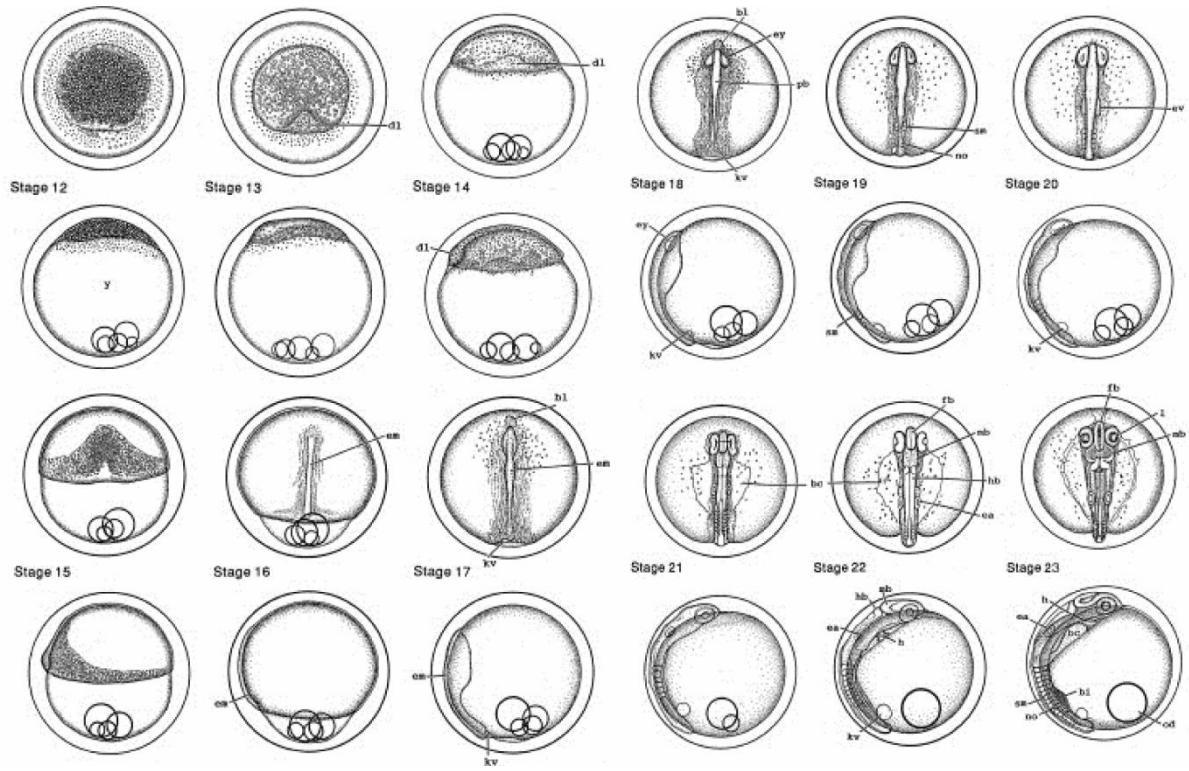

Figure 3. Embryonic development of medaka from blastula to somite (Iwamatsu, 2004)

3- Maternal–Zygotic Transition (MZT)

Initially the embryonic development at the cleavage stage is coordinated by deposited maternal agents such as mRNA and proteins stored in the egg (Baroux *et al.,* 2008). In lower vertebrates, at mid-blastula, there is transition from maternal to zygotic gene activity. This mode of development is named Maternal-Zygotic Transition (MZT), which marks initiation of zygotic gene transcription (zygotic genome activation/ZGA) and the decay of maternal RNAs (Schier, 2007). In zebrafish, MZT occurs at the 500 to 1000 cell stage ~ 3 hours post fertilization (hpf). Messenger RNAs for many key genes regulating embryonic development are maternally supplied and also zygotically expressed, including *bmp, fgf, nodal* and downstream genes of these pathways.

The pluripotency transcription factor in mammalian, Oct4 (which has a homologue pou5f3 in zebrafish) has the role of activation of early zygotic genes via Sox-Pou binding site; in vertebrates Oct4/Pou5f3, Nanog and Sox2 are considered as the connection agents between the zygotic gene activation (ZGA) and embryonic stem cells pluripotent state (Leichsenring *et al*., 2013). Pou5f3, Nanog and sox2 or all redundant soxB1 members are maternally derived in zebrafish eggs and ubiquitously expressed at early embryonic stages (Okuda *et al*., 2010; Xu *et al*., 2012). In zebrafish, it was observed that *nanog, pou5f3* and *soxB1* have a primary role in maintaining pluripotency (Lee *et al.*, 2013). 74% of the first wave of zygotic gene expression is regulated by DNA binding of Nanog, and around 40% accomplished through Pou5f3 and sox2 (Leichsenring *et al*., 2013). At later stages, pou5f3 and sox2 also regulate dorso-ventral patterning (Okuda *et al*., 2010; Belting *et al*., 2011), whereas *nanog* is important in endoderm development (Xu *et al.*, 2012).

4- Epigenetic regulation of early development via histone modification

Histones are proteins that package the genomic DNA. Histone modification is a process that changes chromatin packaging leading to altered gene expression. The regulation of histone modification, so called epigenetic regulation, includes methylation, phosphorylation, acetylation, ubiquitylation and sumoylation (Egger *et al*., 2004). Histones are classified into five groups: core histones are H2A, H2B, H3 and H4; group five contains linker histones (H1/H5) (Draizen *et al*., 2016). Methylation occurs through transfer of one, two or three methyl groups to lysine or arginine residues. H3K4me3 methylation around the promoter region is associated with initiation of transcription, subsequently tri-methylation of H3K36 occurs in the gene body (Vastenhouw *et al*., 2010). Depending on the site of

methylation, methylation associated with gene activation or inactivation for instance, mono and tri-methylation of K4 are associated with active enhancers/promoters whereas H3K9 and H3K27 methylation is associated with repression of enhancers/promoters (Hublitz *et al*., 2009; Ostrup *et al*., 2013). Using chromatin immunoprecipitation sequencing (ChIP-seq), it has been shown that bivalent marks, H3K4me3 and H3K27me3 are present prior to ZGA in zebrafish (Vastenhouw *et al*., 2010; Lindeman *et al*., 2010). Post ZGA, more than 80% active genes are marked by H3K4me3 and many inactive marked by H3K27me3 (Vastenhouw *et al*., 2010; Lindeman *et al*., 2010).

5- Germ layer formation

At the late blastula stage, soon after the MZT, three germ layers are generated: i) ectoderm that develops into the epidermis (skin) and neural ectoderm (all central nervous system and sense organs), ii) mesoderm (origin of muscles, bones, heart, blood, kidney and notochord), and iii) endoderm (origin of intestine, pharynx and liver) (Figure 4) (Kimmel *et al.*, 1990).

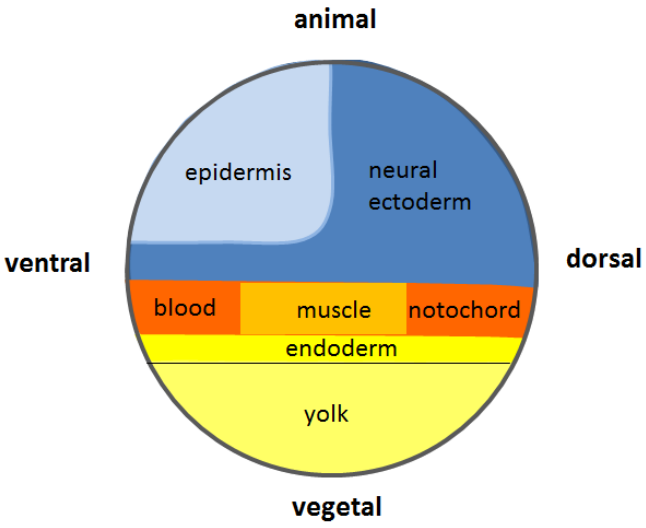

Figure 4. Fate map of zebrafish embryo from Wolpert *et al*. *"Principles of Development"* (2011) with modification according to Kudoh *et al.* (2004)

6-The organizer

The organizer is an activity located in the dorsal blastoderm margin of the fish embryos at blastula to gastrula stage; it is an equatorial part of embryo that has maternal genes for controlling body axis development (Harland and Gerhart, 1997). The activity was initially discovered in the Amphibian studies by Spemann and Mangold (Gurdon, 1987) and confirmed as a conserved activity in other vertebrate model animals including mice, chick and fish species (Dawid, 2004). The organizer is an activity which can induce most of the tissues specific to the dorsal side of the embryo at blastula to gastrula stage, including neural ectoderm, axial and paraxial mesoderm and anterior endoderm. Therefore, the lack of the organizer induces loss of these structures, causing a ventralised embryo, which mainly consists of epidermis, blood and undeveloped tail (Saúde *et al.*, 2000).

Defects of the organizer in zebrafish result in severe ventralized phenotypes; one of these mutations was named *Ichabod. Ichabod* mutant is lethal and often generates headless embryos with a missing notochord (Kelly *et al.*, 2000). *Ichabod* was identified as a maternal effect mutant that has suppression of the *β-catenin 2* gene. The lack of β-Catenin in dorsal nuclei fails to form the organizer (Kelly *et al.*, 2000). Downstream of β-Catenin, the organizer expresses many signaling molecules including Chordin, Noggin, FGF and Nodal (Shimizu *et al.*, 2002; Vagra *et al.*, 2007; Dawid, 2004). Among these genes, Chordin and Noggin are secreted antagonists of the BMP signaling (Anderson *et al*., 2002). As these genes are expressed in the dorsal side during blastula and gastrula stages, BMP gene (e.g. *bmp2b, bmp4 and bmp7*) expression is restricted to the ventral side (Kishimoto *et al*., 1997; Dick *et al.* 2000), creating a

gradient of BMP activity, highest in the ventral side, intermediate in the lateral side and low in the dorsal side of the gastrula embryo (Kishimoto *et al*., 1997). This gradient specifies the cell fate in the embryo in different cell layers; in the animal pole, the dorsal side which has low BMP activity differentiates into the central nervous system, whereas in the ventral side, where BMP is high, it differentiates to form epidermis (skin) (Kudoh *et al*., 2004). In the mesoderm, the dorsal side develops into axial and paraxial mesoderm, whereas the ventral mesoderm mainly develops to form blood, kidney and posterior paraxial mesoderm (tail muscle) (Ramel *et al.*, 2005). Thus the BMP gradient is the key for the gastrula cells to be specified to differentiate to different cell lineages localized in different positions. A *bmp2* defect in zebrafish results in a *swirl* mutant that features an enlarged notochord and somites, and failure in ventral specification (Kishimoto *et al.,* 1997; Dick *et al.* 2000), indicating the crucial role of BMP in dorsal-ventral specification.

7- Neural induction

Organizer-derived BMP antagonists (e.g. Chordin and Noggin) and FGF are required for neural induction, Suppression of BMP by Chordin and Noggin induces the dorsal neural ectoderm, whereas FGF emanating from the blastoderm margin activates neural cells in the vegetal ectoderm; the combination of these two neural inducing activities leads to formation of the whole central nervous system in the embryo (Figure 5, Kudoh *et al.*, 2004; Schmidt *et al*., 2013). As a consequence of these neural inducing activities, neural ectoderm specific genes are expressed at the gastrula stage, including *sox3*, *zic2*, *otx2* and *hoxb1b*. These neural genes subsequently activate

neuronal genes and glial genes and induce the central nervous system in the forebrain, midbrain, hindbrain and spinal cord (Stern, 2006; Jia *et al.*, 2009).

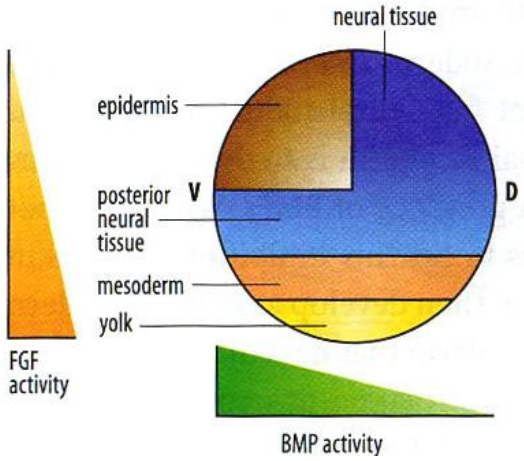

Figure 5. Neural induction of zebrafish embryo from Wolpert *et al*.

"Principles of Development" (2011)

8- Trunk and tail development

8.1- Tissue development

The continuous structure of the trunk and tail consists of the spinal cord, somite muscle, notochord and some other cells. The position of the trunk and tail in the fish embryo is distinguished by the position of the anus which is the border between the trunk and tail.

After gastrulation, the bud stage represents emergence of the tail bud. The mechanism of the tail bud formation in zebrafish was described by Kanki and Ho (1997). At the end of gastrulation (9-10hpf) aggregation of cells at the

ventral and dorsal side of the blastoderm margin constitute the posterior and anterior parts of the tail bud, respectively. At 12-17hpf the initial tail bud dilates over the ventral side to the midpoint to become prominent. After 18hpf, the tail bud segregates from the yolk to produce the tail appendage. Many genes are involved in tail and trunk development. The lack of these genes leads to defects in the posterior part of the body. The roles of genes that target the tail and trunk at early stages of development are summarised as follows.

8.2- Genes involved in the trunk/tail development – T-box genes

To study trunk and tail development, many genetic mutants have been generated from large scale zebrafish mutant screening. Halpern *et al.* (1993) examined the no tail (*ntl*) mutant in zebrafish, showing an embryonic lethal phenotype with a short tail and abnormal trunk and without a notochord. In *ntl* mutants, notochord precursor cells in the trunk and tail were unable to develop a notochord, this inability to develop tail somites is caused by missing the crucial role of *ntl* for maintaining the mesodermal progenitor cells during somitogenesis by regulating *wnt* and *cyp26a1* consequently the tail elongation was suppressed in the posterior part of the body (Martin and Kimelman, 2010). Schulte-Merker *et al.* (1994) found that *ntl* encodes a T-box protein (homologue of brachyury in *Xenopus* and T in mice) which possibly acts as a transcription factor. Griffin *et al.* (1998) studied the role of T-box genes, *tbx6, spt* (*tbx16*) and *ntl,* on regulation of trunk and tail mesoderm formation in zebrafish; they found that FGF signalling was necessary for mesoderm formation in the trunk and tail through spade tail (*spt*) signalling regulation. *Spt* expression required FGF signalling at mid gastrula and onwards, whereas *ntl* expression required FGF signalling at early gastrula. *Ntl* signalling is required for *tbx6* and *spt* at an early

stage. *Tbx6* is expressed in the trunk, whereas *spt* and *ntl* targets the tail bud. Therefore several T-box genes have specific and crucial roles in trunk and tail development.

8.3- Genes involved in the trunk/tail development – FGFs

FGF signalling is also required for trunk and tail development. It is a master regulator for trunk and tail development, both in the neural ectoderm and mesoderm, regulating many key transcription factors as downstream effectors. FGF signalling is required for inducing posterior neural gene *hoxb1b* (Kudoh *et al*., 2002). FGF acts in regulating many T-box genes in mesodermal trunk and tail induction (Amaya *et al*., 1993; Griffin *et al*., 1995). For instance, *fgf8* acts with *oep* cooperatively in trunk and tail paraxial mesoderm development, through regulation of T-box genes *spt* and *ntl* (Griffin and Kimelman, 2003).

Yokoi *et al.* (2007) undertook analyses of mutant head fish (*hdf*) medaka (*Oryzias latipes*). The medaka head fish (*hdf*) phenotype (i.e. loss of most of the trunk and tail structure) is due to the null mutation of *fgfr1*. This study suggested the requirement of FGFR1-mediated signalling for trunk and tail mesoderm patterning and development of the embryo. The orthologues of FGFR1 in zebrafish and medaka are similar but, loss of function results in different phenotypes: In zebrafish null mutants showed normal trunk and tail and defective mid-hind brain (MHB), but in medaka FGFR1 hdf mutants displayed normal MHB, but the trunk and tail were absent. Therefore the same gene from different species can have different functions or at least different levels of redundancy to their related genes.

After the analysis of the *hdf* zygotic mutant, a valuable model of maternal-zygotic (MZ) medaka *hdf* mutant was generated by Shimada *et al.* (2008) for

discovering the FGFR1 mediated signalling in early embryonic development. *MZ_hdf* (FGFR1) was reproduced in *hdf* germ cells, which were then transplanted into sterile interspecific hybrids. The authors demonstrated the necessity of FGFR1 for interior movement of axial mesoderm; by using anterior neural markers use to visualize axial mesoderm movement and reveal the essential role of FGFR1 mediated signalling in pre-chordal plate movement. At the same time, FGFR1 was shown to have no essential function for initial mesoderm induction. As seen in these examples, mutant animals allowed identification of genes that are crucial in development of specific tissues such as the notochord and somites in the trunk and tail. In addition, maternally derived materials are crucial in early development and therefore maternal-zygotic mutants often show more severe phenotypes than zygotic mutant.

8.4- Genes involved in the trunk/tail development – *noto*

Talbot *et al.* (1995) studied the function of a homeobox gene *floatinghead (flh)* in zebrafish; their study elucidated that the *flh* mutant generates an embryo lacking a notochord. *Flh* in zebrafish is homologous to the *noto* gene in mouse. *Flh* is expressed in notochord precursor during gastrulation (Melby *et al*., 1997). Zebrafish *flh* mutant embryo lack a notochord (Talbot *et al.*, 1995; Halpert *et al.*, 1995; Melby *et al*., 1997) creating embryos with a shorter tail than the wild type (Amacher and Kimmel, 1998). The role of *noto* in the mouse is regulation of posterior notochord, organizer (node morphogenesis) and ciliogenesis in the posterior notochord (Beckers *et al., 2007*).

8.5- Genes involved in the trunk/tail development – *msgn1*

Mesogenin1 is essential for tail development in vertebrates. Yoon and Wold (2000) studied the *msgn1* homozygous mutant in mouse that showed

disturbance of the posterior paraxial mesoderm. In zebrafish loss of function of *msgn1* is less severe than in the mouse, limiting transition of progenitor cells from the tail bud, resulting in less somites and an expanded tail bud; lack of both *msgn1* and *spt* making progenitor cells in tail bud unable to migrate anteriorly subsequently generates an embryo fails to form trunk and tail somites (Fior *et al*., 2012). In *Xenopus*, Joseph and Cassetta (1999) isolated and characterized mesogenin1 in the tail bud and paraxial mesoderm. It is initially expressed at gastrula stage in mesoderm and continues in paraxial mesoderm and tail bud. They also found the gene is involved in somite segmentation (Joseph and Cassetta, 1999).

8.6- Genes involved in the trunk/tail development – other genes and signaling

There are also other genes and signaling pathways involved in tail development including *bmp*, *nodal, wnt* and *eve1*. Although BMP is important in neural vs non-neural specification, another role of BMP was discovered in its function in tail development. Agathon *et al.* (2003) pointed out the role of triple signalling of *bmp*, *nodal and wnt8* for the origination of the caudal part of zebrafish, indicating that the activity of these genes initiates after mid-blastula in the ventral margin of the embryo called the tail organizer, in which *bmp, nodal and wnt8* signalling induce stem cells surrounding ventral margin to form the tail.

The role of the BMP was also examined in early stages of *K*. *marmoratus* embryos by Mourabit *et al.* (2014). Bmp is known as a crucial regulator for vertebrate dorso-ventral patterning, as well as for tail development (Kudoh *et al*., 2004; Cruz *et al*., 2010). The authors reduced BMP activity using the Bmp inhibitor, dorsomorphin (DM) in mangrove killifish. They demonstrated that

inhibition of BMP produced a severe phenotype characterised by a short anterior-posterior axis with bilateral division in notochord, spinal cord and somite. Furthermore, the caudal neural plate was separated into cell islands in the posterior part of embryo. Kudoh *et al*. (2004) reported that in a chordin mutant (*din* zebrafish mutation), in which Bmp activity is elevated, the cell fate in the trunk is transferred to tail cell fate. These results suggest that Bmp is an important morphogenetic signal which is essential for gastrula cell movement along the dorsal-ventral and anterior-posterior axes. In addition to the role of *eve1* in reducing BMP to induce neural induction in the posterior ectoderm, it is also involved in *aldh1a2* induction that is essential in trunk-tail development (Cruz *et al*., 2010).

Nodal signaling in the zebrafish organizer is necessary to activate floating head (*flh*) and no tail (*ntl*) (Chen and Schier, 2001). Both *flh* and *ntl* mutants exhibit missing notochords and fusion of tail somites at the early somite stage. However, in the *ntl* mutant notochord precursor cells exist initially and subsequently fail to differentiate (Schulte-Merker *et al.*, 1994; Odenthal *et al.*, 1996).

Spade tail (*spt*) and *trilobite* (*tri*) mutants displayed the deterioration of convergent extension movement of cells from ventrolateral to dorsal midline at the gastrula stage. *Pipe tail* (*ppt*) and *kugelig* (*kgg*) mutants showed failed detachment of the tip of the tail from the yolk (Hammerschmidt *et al.,* 1996).

These data suggest that many genes are involved in trunk and tail formation. Some genes are involved in specifying cell lineages (e.g. *ntl* and *flh*) and some are involved in cell movement (e.g. *tri* and *kgg*).

Gouti *et al*. (2015) proposed that in the tail bud, neuromesodermal progenitors are the source of posterior body elongation that is considered to generate the spinal cord and mesoderm tissues (Tzouanacou *et al*., 2009; Gentsch *et al*., 2013; Gouti e*t al.,* 2017). Neural cell differentiation supresses T/Bra and maintains *sox2* expression, which is a pluripotent stem cell factor (Gouti *et al.,* 2015). The authors investigated transcriptional factor networks in the caudal lateral epiblast in mouse embryo and found that the cell fate of neuromesodermal progenitors is specified through two pathways: i) differentiation of mesodermal progenitors into neural progenitor cells, following increased retinoic acid (RA) levels induced by expression of *bra*, *msgn1* and *tbx6* genes that upregulate *aldh1a2*; ii) increase in RA levels triggered by *sox2* expression (Gouti *et al*., 2017). T-box genes, *ntla* and *spt* control and supply and movement of cells into paraxial mesoderm during gastrulation and tail bud outgrowth by modifying *deltaC* expression (Jahangiri *et al*., 2012). In zebrafish, Manning and Kimelman (2015) described mesodermal cell morphogenesis during gastrulation and somitogenesis: During gastrulation, the prospective mesodermal cells generate a highly blebbing intermediate prominent region to become migratory from epiblast to hypoblast (Figure 6A). Later during somitogenesis, neuromesodermal progenitors that exist in the posterior zone (PZ) are in a transition state and are mobilised by lamellipodia into the anterior zone, inducing mesodermal (MZ) cell to become presomitic mesoderm (PSM) and later somite (Figure 6B). However, in the absence of *tbx16* (*spt*) during gastrulation, the cells are unable to become migratory (Figure 6C). During somitogenesis the absence of *tbx16* and *msgn1* expression in cells also renders them unable to migrate anteriorly, after they have left the neuromesodermal

progenitor epithelium or mesodermal zone (MZ) (Manning and Kimelman, 2015, Figure 6D).

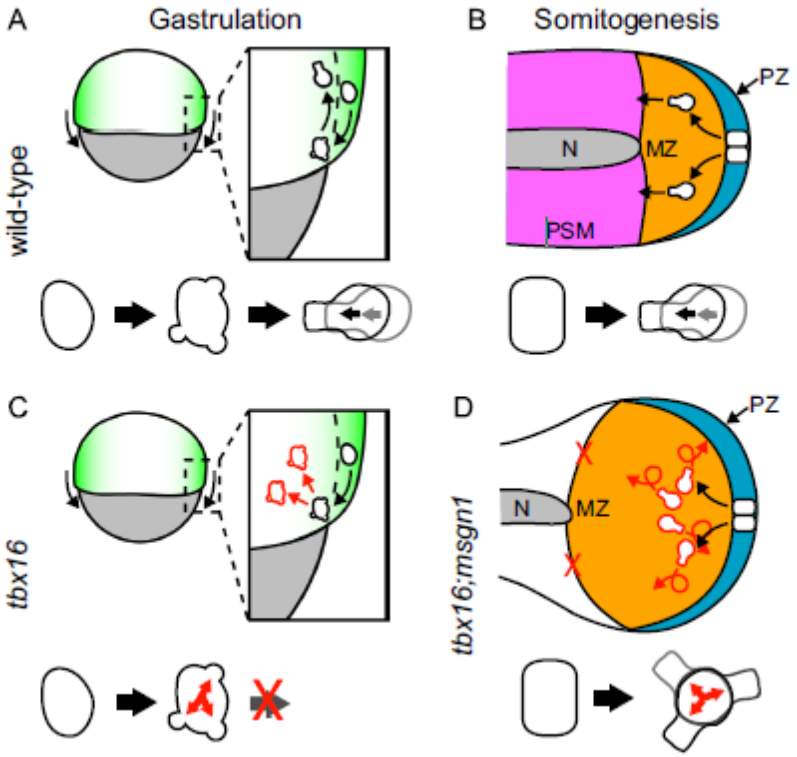

Figure 6. Tail bud formation from Manning and Kimelman (2015)

9- Genetics studies in fish

Advancements have been made in information and knowledge recently in molecular biology, these data and facts come from studies using animal models considered ideal for genetic and cell biology research such as *Drosophila*, mice (*Mus musculus*), and zebrafish (*Danio rerio)*. The zebrafish was used in genetic studies for the first time in the 1980s (Howe *et al.*, 2013). The zebrafish genome sequence project was reported in 2001; the total size of genome is 1,421 Mega bases (Mb). It has 69% orthology with the human genome, enabling understanding of the function of many human genes, including disease related

genes (Howe *et al.*, 2013). In 1996, Nusselin-Volhard started a large scale project on generating zebrafish mutations that characterized 1500 phenotypes linked to more than 400 genes. This project included two large screening experiments accomplished in Tubingen and Boston, which resulted in 37 papers (Nusselin-Volhard, 2012).

Medaka (*O. latipes*) has a small sized of genome, which is about 800 Mb offering a considerable advantage over other models for genetic screening (Ishikawa, 2000). Medaka genetic investigations started with spontaneous mutations that were analyzed in Nagoya University 1960 (Wittbrodt *et al.*, 2002). The Whole genome sequencing was published by National Institute of Genetics (NIG) in Japan in 2002 (Naruse *et al.*, 2004). The team led by Kondoh and Furutani-Seiki conducted large scale mutagenesis using N-ethyl-N-nitroso urea (ENU) (Furutani-Seiki, 2004). This was the 2nd largest mutagenesis and screening study in fish species after the zebrafish mutant screening study reported in 1996 (Nusslein-Volhard, 2012). The team generated and characterized 126 mutations (Furutani-Seiki *et al.*, 2004). Genetic analysis and genome mapping have greatly advanced Medaka genetic studies, and enabled rapid progress in the fields of developmental biology and genetics. Zebrafish and medaka are renowned as genetic model organisms to understand the characterization and function of genes.

K. *marmoratus* has also been used as a unique fish model for genetic studies. It has 24 diploid chromosomes (Scheel, 1972) with a genome size of around 680 Mb (Rhee *et al*., 2017). A genetic map for *K. marmoratus* has been published recently by Kanamori *et al.* (2016) and will support further genetic studies in *K. marmoratus*: Kanamori *et al.* (2016) mapped 24 linkage groups

from 9904 polymorphic DNA markers using RAD-seq to query genomic DNAs from parental lines, and using Medaka and platyfish (*Xiphophorus*) genomic sequences for comparison.

Moore *et al.* (2012) described *K*. *marmoratus* as an exemplar model organism for developmental genetic screens. They established the developmental genetics in *K*. *marmoratus* by using ENU mutagen doses to obtain zygotic mutants. Eight abnormal phenotypic classes have been identified from first filial (F1) offspring and similar phenotypes occurred in the generation F2, which represented different defects in embryos such as skull defect, eye defect, curly tail, short tail, dwarf body, unresolved gastrulation and oedema. Sucar *et al.* (2016) screened *K. marmoratus* mutations and considered this species a powerful model for genetic studies to identify the mutation causing sterility. They confirmed zygotic mutants from three generations of genetic screening. From 307 individuals, they identified 16 sterile and 189 carrying zygotic mutant alleles. Zygotic recessive alleles produced 25% of mutations that were previously identified in zebrafish. The new phenotypes include golden yolk, no trunk, short tail and sterile as well as the wild type heterozygous or homozygous. The study included the third generation (F3) of 284 siblings, which included 83 sterile individuals, therefore confirming heritability of zygotic mutant alleles.

As seen in the examples mentioned above, many gene functions have been discovered using zebrafish and medaka mutants. However many genes have different levels of redundancy, and therefore mutant phenotypes may be different depending on the model animals being studied. The self-fertilising fish, *K.marmoratus* allows us to generate and screen mutants with one generation

earlier, allowing us to screen novel mutants in a more efficient way. Therefore we aimed to analyse *K.marmoratus* mutants to discover novel gene functions involved in early embryo development in this species.

10- Gene loss-of-function analyses using genetic mutations

A gene mutation is a permanent change in a DNA sequence. Mutation may occur in two ways; one is inherited from parents; the second occurs during the life time of an individual that creates new (*de novo*) mutations (Genetic Home Reference, 2015). The methods that enable genetic screening have diverged and expanded for investigating the genetic basis of a phenotype. Forward genetic screening includes the studies that use mutagens to create mutations or naturally occurring mutants. Alternatively reverse genetic screening involves mutations by using specific chemical inhibitors or morpholinos to known genes (Crocetta *et al*., 2015). Alternatively gene editing using CRISPR/Cas9 can be used for both forward and reverse genetics (Ota *et al.*, 2014; Kimura *et al*., 2014). Both forward and reverse genetics have widely contributed to developmental and genetic studies, principally on biomedical animal models.

N-ethyl-N-nitrosourea (ENU) is a chemical mutagen used to induce functional mutation in many animal models in genetic studies (Jiang *et al.*, 2011). Zebrafish, Medaka, and mice are common animal models that have been employed in functional genome analyses through mutagenesis exposure (Mullins *et al.*, 1994; Loosli *et al.*, 2000). ENU was used for the first time in mice by Russell in Oak Ridge National Laboratories in the late 1970s; the author had found it is a useful agent to induce mutation (Acevedo-Arozena *et al.*, 2008). Using ENU has several advantages including: changing a single gene in a manner which is independent of positional effects, providing clear interpretation

of protein function, discovering the level of mutation, i.e. whether there is complete or partial loss gene function, and finding out the gene function neutrality (Justice *et al.*, 1999).

ENU acts through its ethyl group transferring it to nucleophilic oxygen or nitrogen on the DNA during the replication process and causing base mismatch (Jiang *et al.*, 2011). The method of ENU exposure was not only confined to adults, but was also applied to reproductive products, such as mature sperm in grass carp *Ctenophryngodon idellus* (Jiang *et al.*, 2011 study), and in mammalian models such as mice. ENU has been injected with sufficient concentration to create the mutation in the first generation (Acevedo-Arozena *et al.*, 2008 study).

11- Gene loss-of-function analyses using other methods

Genetic mutant animals are useful tools for understanding gene function. But there are also other methods to analyse gene function, including antisense morpholino oligonucleotide injection, mRNA injection of a dominant-negative form of a gene (Griffen *et al*., 1995) and chemical inhibitor treatment. Gene knockdown using morpholino is widely used to study gene function in zebrafish (Draper *et al.*, 2001). Loss of gene function methods has positive and negative issues. Mutagenesis can generate obvious phenotypes and can lead to complete loss of function of a gene, but it takes a long time to establish a mutant. Knock down of a gene using a morpholino produces results in a short time, but loss of gene function may be partial and have side effects (general toxicity or off target effect) (Fiset and Gounni, 2001). Recently the CRISPR/Cas9 system has become popular in generating gene knock out animals. In zebrafish, CRSIPR/Cas9 is widely applied to create genetic mutants

and transgenic fish (Ota *et al.*, 2014; Kimura *et al*., 2014). Therefore it is possible to compare the loss of functional phenotype created by morpholino and CRISPR/Cas9 to confirm the result.

Besides these techniques, chemical inhibitors can give quicker results, allowing investigation of stage-specific effects, but they may also have partial and off target effects, for example, SU5402 can block FGFR (Mohamadi *et al*., 1997), but also block vascular endothelial growth factor (VEGF), that is important for stimulating vasculogenesis and angiogenesis (Fong *et al*., 1999).

12- Fibroblast growth factor (FGF) signalling pathway

Fibroblast growth factors (FGFs) are secreted proteins including several members that possess different functions. FGF signal controls multi-biological function during different stages of embryonic development starting from cell proliferation and morphogenesis to regulation of tissue regeneration and wound healing after injury (Saera-Vila *et al.*, 2016). FGFs are a large family and have vital roles in many organisms, but there are still some vague aspects requiring further study.

The zebrafish FGF family contains twenty-eight genes: *fgf1, fgf2, fgf3, fgf4,fgf5, fgf6a, fgf6b, fgf7, fgf8, fgf9, fgf10, fgf11, fgf12, fgf13,fgf14, fgf16, fgf17a, fgf17b, fgf18a, fgf18b, fgf19, fgf20a,fgf20b, fgf21, fgf22, fgf23, fgf24 and fgf25*, the last two genes are homologs of *fgf8* and *fgf10* human genes respectively (Fischer *et al*. ,2003), with several paralogs (a and b) for the above genes, originating during evolution by a gene duplication event in zebrafish (Sasaki *et al.*, 2011*).* There are also four FGF receptors: *fgfr1*, *fgfr2*, *fgfr3* and *fgfr4* (Thisse *et al*., 1995).

At least three intracellular FGF signalling pathways via ligand-dependent dimerization of FGFR are known, which regulate different biological processes in a cell during early development. The first pathway is Ras /ERK which is necessary for cell division, cell fate specification and differentiation (Krens *et al.*, 2008; Dorey and Amaya, 2010). This pathway is initiated by binding growth factor receptor-protien2 (Grb2) with fibroblast growth factor receptor substrate2 (FRS2) following creation of the protein complex Grb2/SOS. This cascade activates Harvey Rat Sarcoma Virus Oncogene homologue (Ras), then phosphorylation of Rapidly Accelerated Fibro sarcoma (Raf), mitogen activated protein kinase (Map2k) and extracellular –signal related kinase (ERK).

The second pathway is PI3 kinase /Akt which involves mesoderm induction (Carballada *et al.*, 2001). Akt can be activated via PI3 kinase activation, which is stimulated through the Ras/Mapk pathway or from P85 catalytic subunit P13 kinase. The former can be activated by Grb2/SOS complex or the phosphorylated FRS2 (Bottcher and Niehrs, 2005; Dorey and Amaya, 2010).

The third pathway of FGF signalling which is initiated from FGFR1 activation is the PLCγ/Ca^{+2} pathway. The PLCγ/Ca^{+2} cascade signalling is important for neurite development (Hall *et al.*, 1996). Plcγ activates protein kinase C (PKC) through Diacylglycerol formation, and also contributes to release intracellular Ca^{+2} by inosito1-1, 4, 5-triphosphate creation (Bottcher and Niehrs, 2005) (Figure 7).

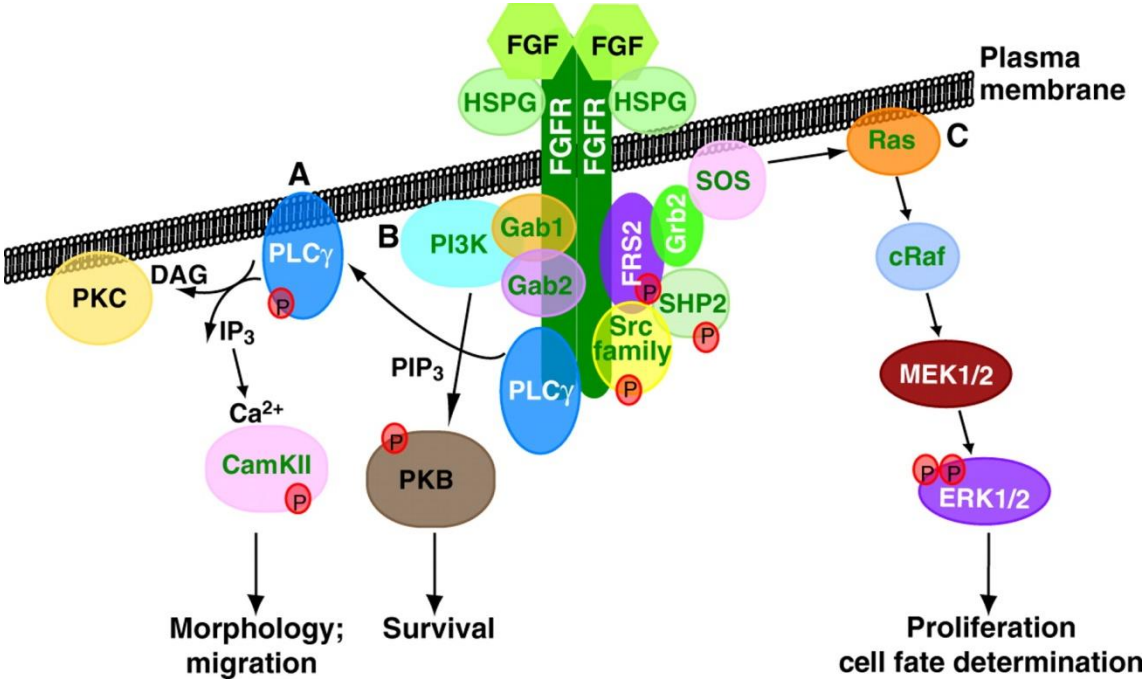

Figure 7. FGF signaling pathways by Dorey and Amaya (2010)

13- Project aims

This project aims to elucidate molecular mechanisms of early embryonic patterning along the antero-poterior axis (head, trunk and tail) by using three different fish species, zebrafish, medaka and mangrove killifish which can provide different and complementary approaches to achieve the goal. In the first two result chapters, the research focuses on the molecular mechanisms of an FGF signalling pathway involved in the neural and epidermal cell fate specification and differentiation. The third chapter describes how a new model species, mangrove killifish, can be used to characterise mutant strains which show specific defects in tail development. Throughout these chapters, molecular mechanisms of cell fate specification and methodologies to analyse the gene function using different model animals are discussed.

Chapter 2: Materials and Methods

Materials and methods

1- Fish husbandry

Fishes (zebrafish and medaka) were maintained in the laboratory in containers (50 x 50 x 30 cm) supplied with aerated and circulated fresh water containing artificial sea salt (0.2 ppt), 28°C ± 1°C (for zebrafish) or 26°C ± 1°C (for medaka). ENU-induced Mangrove killifish, *K. marmoratus* mutant strains (Moore *et al.*, 2012) and the parental wild-type strain, *Hon9* (Tatarenkov *et al,* 2010) were maintained in the laboratory in water: 14-15 ppt salinity at 26°C ± 1°C, a 1500 cm^3 plastic container was used for each individual. As the mangrove killifish tank was not circulated and aerated, weekly changes of water were undertaken. Photoperiod was maintained at 12 hours light: 12 hours dark. Food requirements: live *Artemia salinus* were provided as food once a day. Egg collection in zebarafish was carried out by placing a small container filled with glass balls in each aquaria, each morning before dawn. Eggs were collected from the containers after half an hour, being washed with system water using a sieve and recovered in a plastic petri-dish with the system water. Mangrove killifish eggs were collected from sponge beds where the fish attached their eggs during spawning. Medaka female fish carry their eggs attached to their belly during the first hours of spawning. The medaka eggs were collected during the early morning by removing their eggs from their body by hand. Fertilized eggs were incubated at 28°C for zebrafish or 26°C for mangrove killifish and medaka.

2- Gene markers for *in situ* hybridization

2.1- Gene cloning of *Km_Col9a1b* and *Km_hsp90aa*

To obtain *in situ* probes for the mangrove killifish *col9a1b* and *hsp90aa*, we cloned these genes using the fish embryos. Total RNA was extracted from 20 mangrove killifish embryos with Trizol solution (Sigma-Aldrich) Schulte-Merker *et al*. (1992) and subsequently reverse-transcribed to cDNA using the oligo dT primer. DNase treatment was performed using 0.5 µg of total RNA, 1µl of RQ buffer (Promega), 1µl RQ DNase (Promega) and molecular water to a final volume 10µl. The mixture was briefly spun down and incubated at 37°C for 30min. Subsequently the reaction was mixed with 1µl of RQ stope solution (Promega) and incubated at 65°C for 10min. The content was briefly centrifuged and chilled on ice. Reverse transcription was initiated by adding 1µl of oligo dT (Promega) to the reaction mixture with incubation at 70°C for 5min, then immediately cooled on ice for 2min. On ice, the reaction was mixed gently with 5µl of M-MLV buffer (Promega), 1µl of M-MLV reverse transcriptase (Promega), 2µl of dNTP mix (10mM, Promega) and 5µl molecular water and incubated at 42°C for 60min. The synthesised cDNA was cooled down and amplified by PCR using primers specific to the *Km_Col9a1b* and *Km_hsp90aa* genes. PCR primers were designed according to the RNA-seq information generated in the host lab (Table1).

Gene	Forward primer (F)	Reverse primer (R)
Km_col9a1b	F1: CTCACTTGTGGGCGCCTGACA F2: ATGGAGATGCAAAGGTGGTCC	R1: CTCCGGAGCAACAGGAGGGGC R2: GCGGTGACAAACGCACCGTCG
Km_hsp90aa	F1: ATGCCTGAAGAAATGCACCAA F2: GGAGGAGGTTGAGACCTTCGC	R1: CAGATCAAAAGGTGCACGGCG R2: GGAATAAAGAGCAGGGCCCTG

Table 1. PCR primers of *Km_Col9a1b* and *Km_hsp90aa* genes

PCR condition: 94°C 2min., [49°C 30sec, 58 °C 1min, 72°C 1min] X30, 72°C 5min. For the c*ol9a1b*, nested PCR was used to clone the DNA fragment. However, for the hsp90, the band of the first PCR using F1 and R1 primers was clear and strong enough, therefore the 2nd PCR was not conducted. The PCR products were inserted into a plasmid vector (pGM T easy) with a ligation reaction and transformed into JM109 *E.coli* high efficiency competent cell (Promega). JM109 *E.coli* was cultured in LB/ampicillin/IPTG/X-Gal plates and left overnight. The next day, 10 white colonies were selected to culture in 2ml LB Amp. The plasmid was mini-prepped, digested with EcoR1 and a positive clone having the correct size of insert was selected. The positive colony was amplified again with 100ml LB Amp from which the plasmid was purified using Genes JET plasmid Midiperp Kit (Thermo).

2.2- Preparation of *in situ* probes

To make *in situ* probes, the template DNAs were prepared using plasmid digestion or PCR. All genes, plasmids, primers, enzymes used for probe synthesis were listed in the Table 2. For preparation of the template using plasmid digestion, 5 to 10 µg/µl of DNA plasmid were digested at 37°C for 2h in a water bath, then extracted using phenol/chloroform. To do this, digested DNA was placed in 200ul phenol/chloroform, vortexed for 15 sec and the aqueous phase was isolated. DNA in the aqueous phase was precipitated with 18ul 3M Na Acetate, 450ul absolute ethanol then mixed and kept at -80°C (1 hour). Subsequently, it was centrifuged at 4°C 14,000rpm (20min). The supernatant was discarded and the precipitated DNA was washed with 180ul of 70% Ethanol and centrifuged at room temperature (14,000rpm 5min). The

supernatant was discarded and DNA pellets left to dry for 10min and then dissolved in molecular water.

In the PCR method for DNA amplification, 1µl of 1ng/µl DNA was used as a template and mixed with 38µl molecular water, 4 µl of 2.5mM of dNTP (Promega), 1/10 buffer, Dream Taq DNA polymerase (Thermo) and T3 or T7 as a forward primer and Sp6 as a reverse primer. The mixture was run in a PCR machine under the following conditions: 94°C 2min. [94°C 30sec, 58°C 1min, 72°C 1min] x25, 72°C 5min., 4°C~. Antisense RNA probe was synthesised with 1.5µg of the template DNA in a mixture of 4 µl of 1/5 transcription buffer (Thermo), 2µl of digoxygenin RNA labelling mix (Roche), 1µl of RNAse inhibitor (Roche) and 1µl of RNA polymerase. The ingredients were incubated at 37°C for 3h in a water bath and mixed with 2µl of DNase for an additional hour. The RNA was precipitated with 10µl of LiCl 4M, 80µl H_2O, 300µl absolute ethanol. The ingredients were centrifuged at 4°C 14,000rpm (20min). After discarding the supernatant, the precipitated RNA was washed with 180ul of 70% ethanol and centrifuged at room temperature (14,000rpm 5min). The supernatant was discarded while the RNA was sediments left to dry for 10min and then dissolved in 20µl molecular water. The RNA was diluted (1/200) with 20µl hybridization buffer (50% formamide, 1/5 SSC, 5mM EDTA, 0.1% Tween20, 0.1% 3-[(3-Cholamidopropyl) dimethylammonio]-1-propanesulfonate hydrate (CHAPS), 50ug/ml heparin, 1mg/ml torula RNA) and store in -20°C until use.

Gene marker name	Plasmid name	Source	Digestion Enzyme	PCR F -primer	PCR R -primer	RNA polymerase
Dr_sox3	pSORT1	Kudoh	EcoR1	-	-	Sp6
Dr_hoxb1b	pBluescript	Kudoh	Xba1	-	-	T7
Dr_otx2	-	S. WIlson	EcoR1	-	-	T7
Dr_p63	pBluescript	Kudoh	Sal1	-		T7
Dr_ntl	-	Halpern	Xho	-	-	T7
Dr_zic2.1	pCS2+	Toyama	HindIII	-	-	T7
Dr_id1	pDNR-LIB	Invitrogen	-	T7	T3	T3
Dr_dusp6	PME18S-FL3	Source Bioscience	Sal1	-	-	T7
Dr_pricle1b	pBluescript	Tada	EcoR1	-	-	T3
Dr_fgf2	PMK-RQ-FGF2	Saud	Not1	-	-	Sp6
Dr_spt	-	S. WIlson	EcoR1	-	-	T7
Dr_aldh1a2	pGM T easy	Kudoh	Sal1	-	-	T7
Dr_sox17	-	Stainier	EcoR1	-	-	T7
Dr_dlx3	pBluescript	Kudoh	Sal1	-	-	T7
Dr_tfap2a	pGMT Easy	Source Bioscience	Not2	-	-	T7
Km_Col9a1b	pGMT Easy	Saud	Sac2	-	-	T7
Km_hsp90aa	pGMT Easy	Saud	Sac2	-	-	T7
Km_sox3	pMK (KanR)	Mourabit	Sal1	-	-	T7
Km_spt	pMK(KanR)	Saud	EcoR1	-	-	T3
Km_noto	pMA-T	Saud	-	Sp6	T3	T3
Km_msgn1	pMA-T	Saud	-	Sp6	T3	T3

Table 2. Gene markers (probes) information

3- Microinjection

Embryos from the zebrafish and medaka were used for microinjection. For zebrafish injection, embryos were lined up in a glass slide in a Petri-dish. For medaka, embryos were lined up in a Petri-dish with an agarose bed containing groves. A 1mm OD glass capillary tube (Harvard Apparatus ltd.) was loaded with mRNA or morpholino that was used for injection: about 1nl of mRNA was injected in the 1 cell stage blastomere, or 2nl of morpholino was injected in the yolk near the blastomere at the 1-4 cell stage. The same glass capillary was used for medaka embryo injection, but the end of capillary was made slightly shorter and wider shape (Porazinski *et al*., 2010). A WPI Injector (World Precision Instruments) was used for embryo injection.

4- Morpholino injection

4.1- The bmp2bMO

The BMP2bMO (GeneTools, LLC) 5'- GCGGACCACGGCGACCATGATC -3' targets the transcription start site; it was used at 5ng/nl and 1-2 nl of solution was injected into the yolk as close as possible to the cell(s) at the one to two cell stage (Kudoh *et al.,* 2004).

4.2- Fgf2MO

1µg/ µl of *fgf2* Morpholino (*fgf2* MO) oligonucleotide 5´CCATCCCTCA GTC TGTCGGTCTCTG´3 was designed and synthesized by Gene Tools LLC.
About 2nl was injected into one to two cells stage into the yolk near the blastomere.

4.3- NotoMO and msgn1MO

MOs of *Ol_msgn1* (5-ACAGGATTTCAGCTTCCACGTCCAT-3) and *Ol_noto* (5-CCTGCCTTTGCTGTCCTGTGGATC-3) were generated by Gene Tools LLC. To create *stl* and *msgn1* morphants, 2nl of 2µg/µl morpholino was injected at the one cell stage in medaka embryos. For the phenotypic rescue experiment, 1nl of 25ng/µl mRNAs were co-injected with *noto* or *msgn1* morpholinos. For cell lineage analysis, Kaede mRNA (100ng/µl) was also co-injected with a morpholino.

5- Chemical treatment

For knockdown of FGF signalling, specific FGF receptor inhibitors SU5402 and PD173074 (Sigma-Aldrich) were used. The chemicals were dissolved in demethylsulphoxide (DMSO) at a concentration of 40mM and embryos were incubated with these chemicals after further dilution (to 60µM) in system water.

Dorsomorphin (DM), a selective inhibitor of the BMP type I receptors (Sigma-Aldrich), was used for BMP signalling knockdown. DM was dissolved in DMSO at a concentration of 10mM and embryos were incubated in Dorsomorphin further diluted (to 100µM) in system water.

6- Animal cap assay

Embryos were treated with 1mg/ml Pronase (Sigma) diluted with 1/100 Ringer solution at stage 125 cells in 6 cm Petri- dish with agarose bed. Immediately after the rupture of the chorion, a wash process was performed by replacing 80% of liquid with clean Ringer solution, avoiding contact of the embryos with the water surface. The wash was repeated for three times. Cutting the animal pole of the embryo was achieved at 500 cells stage using Tungsten Wire (0.05mm Diameter), and took place in a 10cm Petri-dish containing agarose bed with 0.5% methylcellulose in 1/100 Ringer solution + Gentamycin (200µg/ml, Gibco). After 30min of cutting process, 10 animal caps were transferred into a well in 12 well plates (30 embryos in total) with agarose filled with 2ml Ringer/Gentamycin. 1ml of liquid was replaced with 1ml 5/1000 Ringer/Gentamycin and this process was repeated, and the processed samples were incubated at 28C° overnight. The animal caps were photographed at 24hpf and examined for morphology and lethality. To examine the Pre-MZT FGF in neural induction, animal caps from embryos were injected with *bmp2b* MO, *noggin1* or treated with DM and PD173074 or SU5402 then fixed with 4%PFA/PBS at late gastrula stage. Caps were tested via *in situ* hybridisation using *sox3*, *p63* and *ntl* probes. For *fgf2*MO examine, animal cap from embryos that injected *fgf2*MO only, *bmp2b* mRNA only, *fgf2*MO and *bmp2b* mRNA, treated with DM only, injected with *fgf2*MO and treated with DM and control non

injected nor treated incubated (28C° overnight) to investigate survival and lethality.

7- In situ hybridization

In situ hybridization (as described by Schulte-Merker *et al* (1992) with some modifications) was applied to different stages of embryos, depending on the type of gene markers. Embryos were fixed with 4%Paraformaldehyde (PFA)/Phosphate Buffered Saline (PBS) at room temperature and left overnight for zebrafish and for two-four days for medaka and mangrove killifish, and subsequently washed with PBS and the chorions were removed manually. PBS was replaced with 100% methanol for at least 1 hour at -20°C, then embryos were washed with PBTW (10min), and then with Hyb buffer (1h, 65°C). The Hyb buffer was replaced with diluted probe (probe /Hyb buffer 1/200), which was re-heated 85°C (10min) and then chilled immediately on ice (5min). A series of washes were carried out as follows: 30min. 65°C 50% Formamide 1/2 SSC, 0.1% Tween20, 30min. 65°C 1/2 SSC, 0.1 % Tween20, 30min. 65°C 2/10 SSC, 0.1%Tween20 and 10min room temperature PBTW. After that samples were blocked by blocking solution +5% NGS for 1 hour or more, then transferred to anti-DIG antibody (1/5000 dilute 1/100 with pre-absorbed 1/50 antibody for 2 hours or more, then washed with PBT 30min 1/4 on a shaker and with AP buffer (Tris pH 9.5 0.1M, NaCl 0.1M, $MgCl_2$ 50mM, Tween20 0.1% /50ml) (10min). Then the samples were transferred to BM-purple (Roche) to 24 well plates in a box, to shut off the light. The samples were kept in the dark for as long as required, depending on staining condition, to stop the staining, embryos were washed with PBTw and fixed with 4%PFA/PBS.

8- mRNA Synthesis

mMACHINE SP6 Transcription Kit (Thermo fisher scientific) was used for mRNA syntheses, Plasmids names, Digestion enzyme ,PCR primers and polymerase of mRNAs are listed in table 3.

mRNA	Plasmid name	Digestion enzyme	PCR F- primer	PCR R- primer	RNA Polymerase
Dr_bmp2b	Psp64t+BMP2b	EcoR1	-	-	Sp6
Dr_noggin1	pCS2+Noggin1	Not1	-	-	Sp6
Dr_fgf2	pMK-RQ-FGF2	Not1	-	-	Sp6
Km_noto	pMA-T	-	Sp6	T3	Sp6
Km_msgn1	pMA-T	-	Sp6	T3	Sp6
Km_ Mu_noto	pMK	-	Sp6	T3	Sp6
Km_ Mu_msgn1	pMK	-	Sp6	T3	Sp6
Kaede	pCS2	Not1	-	-	Sp6

Table 3. mRNA information

9- RNA-seq

9.1- RNA extraction

Total RNA was extracted using RNA easy Mini Kits (Qiagen) as described below: 20 embryos were homogenized with 600µl lysate buffer RLT, and then centrifuged for 3 min. at full speed. The supernatant was removed carefully by pipetting. Then 350µl of 70% ethanol was added and mixed for clearing the lysate. 700µl of the sample, including any precipitate, was transferred to an RNeasy spin column and centrifuged for 15sec. (10,000 rpm), then the flow through was discarded. 700µl of RW1 Buffer was added to the RNeasy spin column and the mixture was centrifuged for 15sec (10,000 rpm) and the flow through was discarded. 500µl of RPE buffer was added to the RNeasy spin column and spun for 2min. (10,000 rpm). Finally 30–50µl RNase-free water was added then centrifuged for 1min. (10,000 rpm) for RNA elution.

9.2- RNA-seq of zebrafish embryos treated with SU5402

The qualities of total RNAs were tested using an Agilent RNA 6000 Nano instrument before commencing the sequencing process. Only the RNA with RIN^e values ≥ 8.5 were used, whereas samples having less than 8.5 were discarded. The RNA-seq was conducted with Illumina HiSeq 2500 v3 with 100bp paired end reading. Then the data were sequenced (see appendix chapter).

9.3- RNA-seq of zebrafish animal cap

Animal caps that were taken from injected embryos with *fgf*2MO and control (50 caps each) were subjected to RNA-seq, the same kit and method was used as described above.

9.4- RNA-seq of the mangrove killifish, *stl* and *btl* mutant embryos

RNA easy Mini Kits (Qiagen) were used to extract total RNA from 20-25 embryos (st.16-18) in each strain: Wt progenitor (Hon9), *btl*, *stl* and their non-mutant siblings. All samples were duplicated. RNA quality of samples was confirmed using an Agilent RNA 6000 Nano Kit before sequencing.

10- Whole mount immunohistochemistry

10.1- H3K36 and phospho-Erk immunohistochemistry

Embryos were fixed with pre warmed 4% PFA/PBS overnight and dechlorinated manually in PBST0.1 (PBS, 0.1% Triton 100X). Embryos were then treated with methanol at -20’C for more than 1 hour and washed with PBST for 10min then treated with blocking solution (5% Bovine Serum Albumin (BSA), 5% Fetal Bovine Serum (FBS) in PBS) for 30min. The primary antibody (anti-H3K36 abcam, 1/300, anti-phospho-Erk Sigma, 1/300, in blocking solution) was applied overnight at 4°C. The embryos were washed with PBST 3/100 15min., treated

with the secondary antibody (Anti-mouse-Alexa594, Life Technology 1/200 dilution in blocking solution) for 60min, washed with PBST, stained with Hoechst (Life Technology) 15min. and finally washed with PBST for 15min.

10.2- P63, Phalloidin and Hoechst immunohistochemistry

Control and morphant embryos were fixed with pre-warmed 4%PFA/PBS at 28°C and subsequently left at 4°C overnight. Embryos were incubated with PBST0.5 (PBS, 0.5%Triton) for 1h two times after removing the chorion. Embryos were then blocked with blocking buffer (5%BSA, 5%Heated Inactivated Bovine Serum (HI-BS) in PBS) 1h at RT. Primary antibody with 1/300 dilution of p63 (Santa Cruz) was applied overnight at 4C°. Washing with PBST was done 4 times for 30min each. Secondary antibody Alexa 594 (1/200) was applied for 1 hour, and then samples were washed with PBST0.5 three times for 30min each. 0.2µg/ml Hoechst (Life technology) (1/100) in PBST was applied for 30min. at room temperature, then embryos were washed with PBST 3 times for 20min each. For Actin staining-Phalloidin-Alexa488 (Life technology) (1/200) was used and followed by Hoechst for nucleus staining for 30min. each. Embryos were kept in the dark at 4C°until photos were taken.

11- Western Blotting

50 embryos were homogenized and lysed using a plastic homogeniser in 300µl LDS sample buffer (Invitrogen) and applied (30µl/lane) to the precast gel (Invitrogen). The proteins were transferred to the nitrocellulose membrane (Bio-Rad). The membrane was blocked with 5% skimmed milk in TBST (Tris Buffered Saline (TBS) and 0.1% triton) for 1h. The primary antibodies (Histone H3, H3K4, H3K36 (abcam) 1/300 dilution) were applied overnight. After washing with TBST (3 times for 30min each), the secondary antibodies, anti-mouse-HRP

(Roche) (1/2000), were added for 2 hours. The membranes were washed with TBST (3 times 30min) and developed using the staining kit (GE Healthcare).

12- Histology

The mangrove killifish embryos at the hatching stage were fixed in 4%PFA/PBS (4 days), and dehydrated with series of rising in methanol (50% 1 time, 70% 2 times, 80% 1time, 90% 1time, 100% 1 time and with 100% ethanol 1 time) for 1.5 hour each, followed by histoclear for 4.5 hours using a Shandon Citadel Tissue Processor 2000 (Thermo Scientific), after that embryos were embedded in paraffin wax (Sigma–Aldrich, Gillingham, U.K.). Samples were sectioned at 5µm thickness using a rotary microtome (Leica Biosystems, RM2125RTS) and stained with haematoxylin and eosin (Sigma Aldrich) using a Shandon Varistain 24-4 automatic slide strainer (Thermo Scientific). Programmes of staining included: clearing with histoclear 5min 2 times, rehydration (100-80% ethanol, 6min, raising with water 2min, Harris Haematoxylin stain 15min, washing with water 2min, washing with acid alcohol 30sec, washing with water 30sec, washing with 70%methanol/Ammoniated alcohol 30sec, washing with running water 30sec, Eosin Y stain 15sec and washing with running water 30sec. Slides were dehydrated with methanol (80-100%) 4.5min, 100% ethanol 2min and clearing with histoclear. Mounting was done with mounting medium, and then left overnight. Photograph images were taken using a Zeiss Axioskop 40 microscope.

13- Cell lineage analysis using *Kaede* mRNA in the medaka embryo

2nl of 100ng/µl Kaede mRNA was injected to 1 cell stage medaka embryos with or without morpholinos for Ol_*noto* or Ol_*msgn1*. The tail bud was ‘spot-labelled’ by photo-conversion by UV exposure for 1min with DAPI filter: the

aperture was narrowed down within the tail bud region at 28 hpf - when the tail bud was clearly recognized using an inverted microscope (Zeiss-Axio Cam MRm). Photos were taken at 28hpf, 51hpf and 75hpf to track the cells movement.

14- Reagents Recipes

LB Agar plates

20g LB Agar (Miller) is dissolved in 500ml of deionised water, then it is autoclaved, the agar cooled down to 55-65°C, then 500ul of 100mg/ml antibody is mixed gently with agar , and the medium is poured into a 10cm diameter petri dish and stored at 4°C.

LB Broth medium

25g of LB powder (Miller) is dissolved in 1000ml, and then it is autoclaved. After cooling, Ampicillin antibiotic (500ul of 100mg/ml) is mixed with the medium.

Phosphate Buffered Saline (Tween) (PBTw)

PBS (Roche), 0.1%Tween20 (Sigma).

1X PBS

100 ml 10X PBS (Sigma) in 900ml deionised water.

4%PFA/PBS

2g of PFA (Sigma) in 50ml PBS. The solution is dissolved in PBS at 60°C, then pH adjusted to 7 -7.3. PFA/PBS is stored at –20°C. The solution can be thawed and kept at 4°C for 2 weeks (half-life time).

Hyb-buffer

Formamide 50% (Qbiogene), 5XSSC (Sigma), 5mM EDTA (Sigma), 0.1% Tween20 (Sigma), 0.1% CHAPS, 50µg/ml heparin (50mg/ml -20'C) and 1mg/ml torula RNA (50mg/ml -20°C). Stored at -20°C.

Malic Acid B (MAB)

Maleic acid 0.1M (Sigma) is prepared from 0.5M stock (29g Maleic acid/500ml H_2O) and NaCl 150mM, pH is adjusted to 7.5.

Blocking Solution for *in situ* Staining

1g blocking reagent (Roche) is heated up to 50°C to 80°C in 50ml MAB (using a water bath or microwave) for 30 min. Then 2.5ml bovine serum albumin (BSA) is added, after reducing the solution temperature to room temperature.

Pre-absorption of antibody

10ul Anti-Dig (or Flu) antibody, conjugated with alkaline phosphatase, is mixed with 500µl Blocking solution added with 20 fixed embryos (fixed in PFA/PBS at bud, somitogenesis or 24hpf stage, then methanol treated and PBS rehydrated). The final mixture is gently rotated at 4°C for 4 hours or longer, to be ready for using.

3% Methylcellulose

1.5g of methylcellulose (Sigma) is dissolved in 50ml deionized water and frozen at -20°C overnight, until the powder is totally dissolved.

Blocking buffer for immunohistochemistry

2.5g of BSA, 47.5ml PBS and 2.5ml HI-BS (bovine serum).

Ringer Solution

7.2g NaCl, 0.37g KCl and 0.17g CaCl are dissolved in 1L water and pH is adjusted to 7.3-7.4, then the solution is filtered using 0.22-µm filter paper.

Tris Buffered Saline (TBS)

6.05g Tris and 8.76 g NaCl are dissolved in 800 ml H_2O and pH adjusted to 7.6 using 1M HCl, then the volume is made up to 1L. TBS is stable at 4°C for 3 months.

TBST buffer

1XTBS, 0.5% Triton (Sigma).

10X TBS

24.2g Tris and 84g NaCl (PH 7-7.6) in 1L deionised water.

1X TBS

100 ml 10X TBS in 900 ml deionised water.

10X Running buffer

250mM Tris, 192mM Glycine and 0.5%SDS.

10X Transfer buffer

144.1g Glycine and 30.3g Tris base in 1L deionised water.

1X Transfer buffer

100ml 10X transfer buffer, 100 ml methanol and 800 ml deionised water.

Ponceau S solution

0.5g Ponceau S (Sigma), 2.5ml Acetic acid (100% glacial) and 47.5ml deionised water.

Results Chapter 3

Maternal FGFR signalling regulates the competence for neural induction in the zebrafish embryo

Abstract

Vertebrate cell lineage specification occurs through the activity of various growth factors, initially maternally supplied and subsequently generated in the embryo from the Maternal-Zygotic Transition (MZT). We have investigated the relative contribution of maternal and zygotic FGFR signalling to neural induction and report that blocking maternal FGFR signalling in zebrafish suppresses many post-MZT gene transcriptions and consequently suppresses development of the central nervous system (CNS). We show that there is a time gap (3h) between the pre-zygotic FGF taking a role in development and the post-zygotic stage, when gene expression changes occur as a consequence of the pre-MZT FGF activity. We propose that pre-MZT FGF modifies the histone methylation and DNA binding of the pluripotent factors without immediately activating gene transcription, instead making the ectoderm competent to respond to neural induction and other cell differentiation signals after the MZT. This provides a novel mechanism of gene regulation at the earliest stage of embryonic development.

Introduction

Development of animal embryos starts from fertilisation of the egg, which supplies maternal factors including mRNAs, proteins and other small molecules. In the zebrafish, zygotic transcription is mostly silent from fertilisation to the mid-blastula (around the 500 to 1000 cell stage, 2-3 hpf) and early embryonic development is regulated primarily by maternal factors (Bruce *et al*., 2003; Lee *et al*., 2014; Shimada *et al*., 2008; Kelly *et al*., 2000). Zygotic transcription begins at the so-called mid-blastula transition (MBT), more broadly defined as the maternal-zygotic transition (MZT) (Tadros and Lipshitz,2009). Soon after the MZT, embryonic cells initiate differential zygotic gene expression, leading to spatially and temporally localised production of signalling molecules and initiating cell lineage specification. Among secreted molecules, Chordin, a BMP antagonist, suppresses BMP signalling on the dorsal side of blastula to gastrula stage embryos, thereby promoting neural cell fates. In addition, zygotically produced FGF, emanating from the blastoderm margin, also induces neural character in the vegetal ectoderm. This combination of organiser-derived BMP antagonists and marginal-cell-derived FGF induce the neural plate, which gives rise to the central nervous system (CNS), including the entire brain and trunk and tail spinal cord (Kudoh et al.,2004; Rentzsch *et al*.,2004; Dee *et al*.,2007; Londin *et al*.,2005; Streit *et al*.,2000; Wilson *et al*.,2000; Delaune *et al*.,2005).

Although the roles of key signalling pathways post-MZT have been extensively studied, it remains largely unclear how these pathways act on embryonic development pre-MZT. Since tissue-specific gene expression is silent before the MZT, it has generally been assumed that cells at this stage do not go into lineage specification but simply proliferate to increase cell numbers. However,

recent studies have revealed that prior to MZT, epigenetic changes have already begun and that these changes are crucial for cells to be primed for appropriate zygotic gene expression after the MZT. For instance, patterns of DNA methylation are globally modified during the cleavage to blastula stages (Andersen *et al*.,2012). Histone tri-methylation at residues K4 and K27 mark a gene-specific manner prior to initiation of zygotic gene expression early post-MZT (Vastenhouw *et al*., 2010).

Methylation of histones plays a significant role chromatin remodelling and the regulation of transcriptional events, including during stem cell specification; histone methylation is considered as an essential epigenetic modification for neural differentiation from embryonic stem cells (Shimomura and Hashino, 2013). Methylation generally takes place in histones H3 and H4, and can occur at Lysine or Arginine residue. Methylation of both histones H3 and H4 can affect transcriptional activation or repression, depending on the site of methylation (Hublitz *et al*., 2009; Ostrup *et al*., 2013). Lysine methylation is divided into mono, di or tri-methylation, and both mono and tri-methylation of K4 are 'activational marks' activating transcription e.g. for H3K4me1 at enhancer sites and for H3K4me3 in promoters regions of genes. Tri-methylation of K36 (H3K36me3) is associated with transcriptional activation in gene body regions (Gupta *et al*., 2010; Ostrup *et al*., 2013). In general Arginine methylation is associated with transcriptional activation, including via H3K4me3 (Zhang and Reinberg, 2001). In zebrafish H3K4me3 methylation occurs during the start of zygotic transcription and is then followed by methylation of H3K36me3 (Vastenhouw *et al*., 2010).

Conversely, tri-methylation of K9 and K27 are repressive marks, such as H3K27me3 at promoters regions and H3K9me3 at poor regions (satellites) (Gupta *et al*., 2010; Ostrup *et al*., 2013).

It has recently been shown that the pluripotency factor, Pou5f3, binds to the target DNA sequence before the MZT and is important for the initiation of many earliest zygotic gene expressions (Leichsenring *et al*.,2013; Lee *et al*.,2013). These data suggest that cells acquire a competence before the initiation of the zygotic gene expression and cell fate specification. However, it is still not clear how these changes are triggered and regulated.

In this paper, we have investigated the role of maternal (pre-MZT) FGF signalling in the initiation of zygotic and tissue-specific gene expression. We propose a novel role for maternal FGF in regulating histone modification and DNA binding of the Pou5f3 and other pluripotent stem cell transcription factors, thus making the ectoderm competent to respond to neural induction signals and other cell differentiation signals after the MZT.

Results

Pre-MZT FGFR signalling is required for anterior neural induction

To investigate potentially differential and/or synergistic roles of pre and post-MZT FGFR signalling on neural induction, zebrafish embryos were incubated with an FGFR inhibitor, SU5402, at pre-MZT (0-3hpf) and/or post-MZT (3hpf-) stages, fixed at late gastrula and examined for neural ectoderm marker genes (Kudoh *et al*., 2004). To our surprise, suppression of FGFR signalling at the pre-MZT stage led to a strong reduction in the expression of anterior neural genes

(*otx2* and anterior *sox3*) while *hoxb1b* and *sox3* remained expressed in posterior prospective neural cells (Fig.1B,G,L and Supp.Tab.1). In contrast, and as previously reported, suppression of FGFR signalling post MZT (3hpf to fixation at late gastrula) showed specific reduction in the expression of posterior neural genes (*hoxb1b* and posterior *sox3*) (Fig.1 C,H,M and Supp.Tab.1) (Kudoh *et al*.,2004; Rentzsch *et al*.,2004; Dee *et al*.,2007). Consistently, inhibition of FGFR signalling throughout cleavage to gastrula stages suppressed both anterior and posterior neural genes (Fig.1D, I, N and Supp.Tab.1). To further confirm the specificity of the chemical inhibitor, we overexpressed the mRNA encoding a dominant-negative FGFR, XFD, inducing the same phenotype as the inhibitor treatment throughout cleavage to gastrula stages (Fig.1E, J, O). In all conditions tested, the domain within which neural markers are suppressed shows expansion of the non-neural (epidermal) gene, *p63* (Fig.1P-T and Supp.Tab.2). These data suggest that pre-MZT FGFR signalling has a crucial role in induction of the anterior neural ectoderm.

In this experiment, to examine the role of pre-MZT FGFR signalling, SU5042 was added from fertilisation to 3hpf when the chemical was removed and the embryo washed. However, it is possible that the inhibitor may bind to the receptor and still suppress signalling after the MZT. To confirm that the pre-MZT specific treatment of SU5402 (0-3hpf) indeed specifically suppressed pre-MZT FGF only; we examined FGFR activity by immunostaining for phosphor-Erk (p-Erk) (Shinya *et al*., 2001). At 3hpf, p-Erk is seen in cell nuclei of untreated embryos, but is absent in embryos treated with SU5402 pre-MZT (Fig.1U, Supp.Tab.3). However, when the inhibitor is washed off at 3hpf, p-Erk levels are partially restored in the nucleus after 30min and restored to the level of normal

embryos after 1 hour (4hpf). These data suggest a tight correlation between the timing of SU5402 treatment and the suppression of FGFR activity.

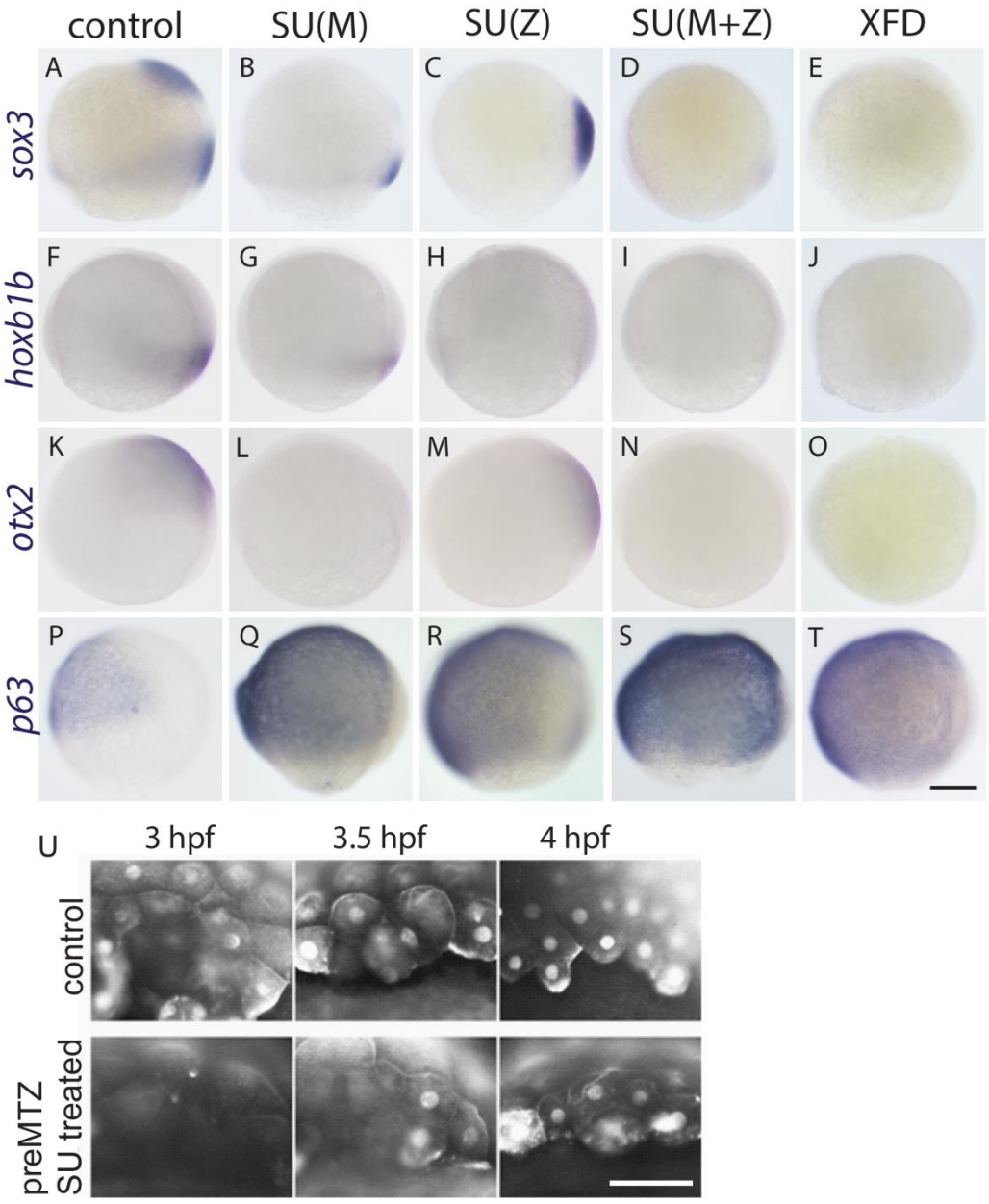

Figure 1. Pre-MZT FGFR signalling is necessary for anterior neural induction. Late gastrula stage embryos exposed to SU5402 in a stage-specific manner or injected with XFD mRNA as shown at the top of the columns. Lateral views, dorsal to the right (where discernible). Probes used are shown to the left of the rows. Control embryos (A, F, K, P). Embryos exposed to SU5402 (B, G, L, Q) at pre-MZT period (0-3hpf). *Sox3* anterior expression domain and *otx2* was abolished (B, L) while the *sox3* posterior

domain and *hoxb1b* was not suppressed (B, G). Epidermis was expanded as observed with *p63* staining (Q). Exposure to SU5402 from the MZT (C, H, M, R). Posterior *sox3* expression is lost, as is the expression of *hoxb1b* (H) but anterior *sox3* expression remains largely unaffected although shifted toward vegetal pole (C), similar to the effects on the expression of *otx2* (M). *P63* expression is expanded posteriorly and dorsally (R). Exposure to SU5402 throughout the pre-MZT and post-MZT stages (D, I, N, S). Embryos injected with XFD mRNA (E, J, O, T). In these embryos, both anterior and posterior neural genes are suppressed (D, E, N, O, I, J) and epidermis gene, *p63* is expanded (S, T). U. Immunostaining with Phospho-Erk antibody indicate active FGFR signalling pathway occurring at around MZT. Upper panel shows control embryo. Lower panel shows SU5402 treated embryos at 0-3hpf. At 3hpf, the inhibitor was washed off. The embryos were fixed at the indicated time (U). Scale bars are 200µm.

Maternal FGFR function is crucial for anterior neural induction independently of BMP inhibition

The whole-mount *in situ* data suggest that maternal FGFR signalling is essential for neural induction (Fig. 1). However, since suppression of the BMP pathway dorsally has been postulated as a precondition for neural induction (e.g. Kudoh *et al*.,2004; Rentzsch *et al*.,2004; Dee *et al*.,2007; Londin *et al*.,2005), it is possible that the observed maternal FGFR neuralising activity occurs via disruption of the BMP pathway. To address this question, we co-treated embryos with the BMP inhibitor, Dorsomorphin and an FGF inhibitor, SU5402 or PD173074. However, treated embryos had severe epiboly defects and died before the mid-gastrula stage (data not shown). Instead, we made use of blastula caps excised from the animal pole of zebrafish embryos and fixed at

the late gastrula stage. This experiment allowed us to examine if, by simply modifying FGF and BMP signalling, neural fates could be induced in ectodermal explants without influence from other cell layers such as mesendoderm and the yolk syncytial layer. In this experiment, to examine the most effective loss of function of FGFR, two inhibitors, SU5402 and PD173074, were tested. We found both inhibitors showed similar dose effect on the tested marker genes (Fig.2 and Supp. Fig.1). However, PD173074 easily precipitates causing difficulty in testing high dose effects. Therefore in all other experiments SU5402 was used as the primary tool.

As wild type caps may still receive signals from a presumptive early organiser, which expresses BMP antagonists such as Chordin (capable of maintaining neural induction) (see Fig. 2A), we used both wild type Wik and *ichabod* mutant embryos for the animal caps (Kelly *et al*., 2000). The *ichabod* mutant is devoid of maternal Beta-catenin 2 activity, does not form an organiser (Kudoh *et al*., 2004; Kelly *et al*., 2000), and neural induction in isolated *ichabod* caps does not occur (Fig. 2B). However, when BMP signalling is suppressed through the addition of Dorsomorphin at 3hpf onward, both wild type (Fig2A, Supp.Fig.1) and *Ichabod* (Fig.2E) caps show activation of the neural marker *sox3* with concomitant suppression of the non-neural (epidermal) marker *p63* (Fig.2L, Supp.Fig.1). In this condition, we tested whether suppressing pre-MZT FGFR signalling could suppress neural induction. We found that WT or *ichabod* caps treated from 0 to 3 hpf with both the FGFR inhibitor and Dorsomorphin failed to induce neural markers (Fig. 2F, Supp.Fig.1). For comparison, bmp2MO, *noggin1* (BMP antagonist) mRNA were injected at the one cell stage to induce neural tissues. The results of this work suggested that BMP antagonism alone is not sufficient to induce neural markers if pre-MZT FGFR signalling is blocked.

For comparison, an FGFR inhibitor was added post-MZT and, at this stage, it failed to suppress neural markers induced by Dorsomorphin (Fig.2G, Supp.Fig.1). This further confirms that maternal FGFR signalling is required for anterior neural induction, and that this requirement is independent of BMP antagonism.

These data suggest that maternal FGFR is crucial for rendering pre-MZT cells competent to receive later neural induction signals, with BMP antagonism.

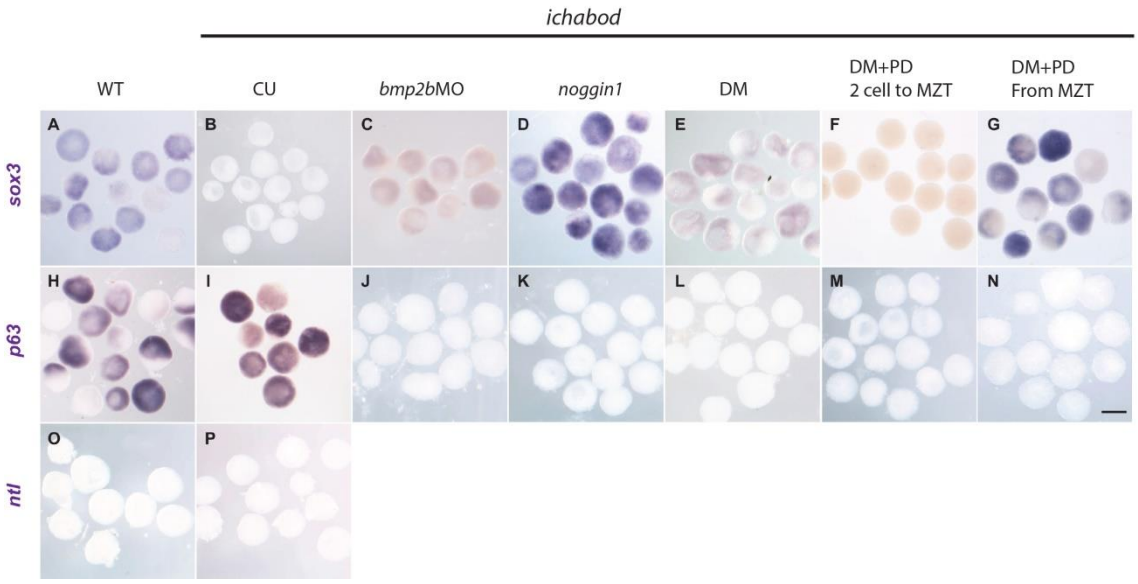

Figure 2. Anterior neural induction does not occur in *ichabod* caps exposed to both DM and PD173074. *In situ* staining of wildtype and *ichabod* animal caps fixed when control embryos were at the late gastrula stage. (WT, wild type uninjected/unexposed caps; CU, control uninjected/unexposed *ichabod* caps). A, H. In WT animal caps, expression of *sox3* and *p63* respectively is patchy indicating both neural and epidermal fates co-exist within an explant. However, in control *ichabod* caps *sox3* expression is absent (B) while *p63* is expressed ubiquitously (I), consistent with the embryo data (Fig.1Q-T). O, P. *ntl* expression is absent in both WT and *ichabod* control caps, suggesting there is no mesoderm/posterior contamination in our experiments. C-E, J-L. *Ichabod* caps exposed to, or injected with, three different inhibitors of the BMP pathway. C-E. *Sox3* expression is induced in all the caps when compared to controls (see B), while as expected with loss of BMP signalling,

expression of the epidermal marker, *p63,* is lost (J-L). F,G,M,N *Ichabod* caps exposed in a stage-specific manner to PD173074, while also being exposed to DM from the 2 cell stage to fixation. F. When *ichabod* caps are exposed to PD173074 until the MZT, *sox3* expression is absent while with exposure from the MZT *sox3* expression is present (G) although weakly in some of the caps. In both conditions, there is no *p63* expression (M, N). Scale bar is 200µm.

RNA-seq and ATAC-seq identify potential competence genes regulated by the maternal FGF signalling pathway

As we showed that pre-MZT FGFR signalling is crucial for neural gene expression at later gastrula stages, we hypothesised that some early post-MZT gene expression would be altered by pre-MZT FGFR inhibitor treatment. In order to examine the function of maternal FGFR-dependent signalling in gene expression and cis-regulatory activity at the genome-wide level, we performed RNA-seq and ATAC-seq from cells taken from dome stage embryos exposed or not to the, SU5402 pre-MZT.

RNA-seq data produced a list of differentially expressed genes (DEG, FDR < 0.05). From these, 130 genes were downregulated in the treated sample (log2 fold change < -1), while 173 showed upregulation (log2 fold change > 1). Gene ontology (GO) enrichment analysis of the downregulated genes showed enrichment terms related to early development processes such as regionalization, pattern formation, pattern specification and mesoderm development (Appendix Fig.1A). However, no GO enrichment terms were found for the upregulated genes.

We next evaluated the impact of FGFR-dependent signalling depletion at cis-regulatory regions by performing ATAC-seq experiments in unexposed and SU-

5402 treated zebrafish embryos, also at the dome stage. ATAC-seq is used to identify genome-wide maps of open chromatin regions, which include active enhancers and gene promoters (Buenrostro *et al*.,2015). Using these data, we determined the genomic regions that showed differences in ATAC signal between control and SU5402 treated embryos. We found 1070 ATAC-seq peaks that showed differential accessibility. To determine if these differentially upregulated and downregulated peaks represented biologically meaningful classes of regulatory elements, we performed motif discovery analyses in both groups. We found very few motifs enriched in the group of upregulated peaks, and these did not belong to any clearly specific group of transcription factors. On the contrary, in the downregulated peaks, we found a clear enrichment for several motifs that correspond to binding sites for pluripotency transcription factors such as Nanog, Sox2, Klf5 and Pou5f3 (e.g. Appendix Fig. 1D).

Next, using the web tool GREAT (Hiller *et al*.,2013), we assigned the differentially regulated peaks to their potential target genes and looked for GO term enrichment in these genes. Genes associated with the upregulated peaks were very heterogeneous and did not show any enriched biological function. On the contrary, those genes associated with downregulated ATAC peaks showed strong enrichment for GO terms related to chromatin assembly and nuclear organization (Appendix Fig. 1B). This is likely due to the fact that many peaks around histone genes showed reduced ATAC signal in embryos with reduced FGF signalling.

We then intersected the list of differentially expressed genes and the list of genes associated to ATAC peaks downregulated after SU5402 treatment and found 49 common genes (Appendix Fig.1C). These correspond to a group of

genes that show differential expression likely as a consequence of changes to cis-regulatory elements in their vicinity. Most of these genes are downregulated when FGFR signalling is impaired pre MZT (0-3hpf) (Appendix Fig.1C). Many of these genes showed multiple ATAC peaks in their vicinity affected by the reduction in FGFR signalling (Appendix Fig.1C). Appendix Fig.1D shows examples of genes having differential ATAC peaks which contain DNA binding sequence of Nanog, Sox2, Klf5 and Pou5f3. These data suggests that these pluripotent transcription factors acting downstream of the pre-MZT FGFR signalling pathway.

The RNA-seq and ATAC-seq data revealed that many late blastula genes are suppressed in embryos treated with SU5402 pre-MZT. To confirm the result, these suppressed genes were re-examined using *in situ* hybridisation on dome stage embryos treated with SU5402 at pre-MZT. The expression of *zic2.1, id1, dusp6 and prickle1b* which are usually expressed widely in the blastoderm at early post-MZT stage was suppressed by pre-MZT SU5402 treatment (Fig.3B, E, H, K). To validate the specificity of the chemical inhibitor treatment, FGF Receptor signalling was also suppressed by injecting the dominant-negative FGFR1 receptor, XFD (Kudoh *et al*., 2004). Consistent with the drug inhibitor result, XFD injection also caused reduction in the expression of the same post-MZT genes (Fig.3C, F, I, L). These data suggest that pre-MZT FGFR signalling regulates DNA binding of the pluripotent stem cell transcription factors and impacts the ability of cells to become competent to express many zygotic genes post-MZT.

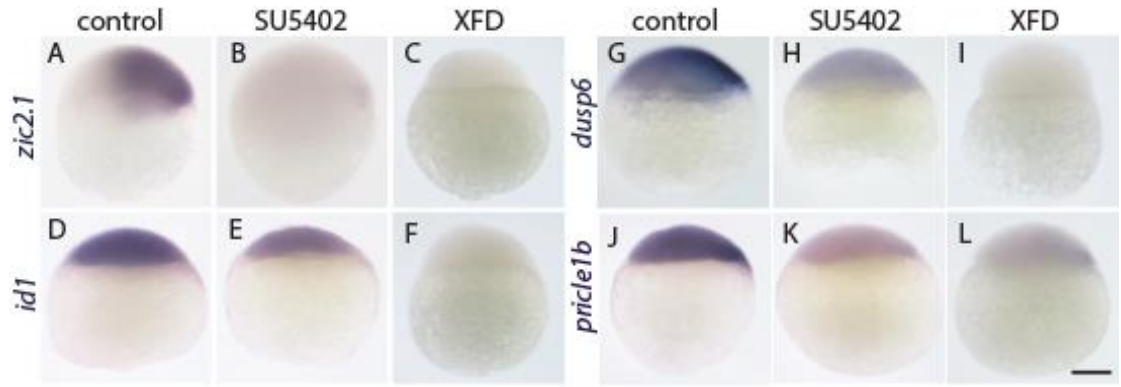

Figure 3. In situ hybridization in zebrafish embryos treated with FGF inhibitor SU5402 or injected with XFD, a dominant negative receptor of *fgfr1*. Candidate genes (identified from the RNA-seq and ATAC-seq as downstream of FGFR signalling) were examined for expression in dome stage control and SU5402 treated embryos. Lateral views of dome stage embryos showing expression of genes (indicated to the left of the columns) in controls (A, D, G, J), pre-MZT treatment with SU5402 from 0-3phf (B, E, H, K) and XFD injected embryos (C, F, I, L). Note that expression of all genes shown is reduced following Su5402 treatment. *zic2.1* (A,B,C), *id1* (D,E,F), *dusp6* (G,H,I), *prickle1b* (J,K,L). Scale bar is 200µm.

Blocking Pre-MZT FGFR signalling suppresses histone methylation at H3K36 and H3K4

Pre-MZT SU5402 treatment led to alterations in gene expression post-MZT but there is a time gap between when the inhibitor presumably induced a change in the cells (0-3hpf), and the first gene expression changes which occur post-MZT around the sphere to dome stages (4 to 4.5hpf). This suggests that the effect of the pre-MZT SU5402 treatment is not to directly modulate gene expression but rather to change competence to express specific genes when they are induced subsequent to the MZT. We suspected that the change occurring in cells pre-MZT by suppression of FGFR function might involve Histone modifications, as this is an established epigenetic signature change occurring at, or prior to, zygotic gene expression (Vastenhouw *et al*.,2010). To test this possibility, the

extent of Histone H3 and tri-methylated HistoneH3 (H3K36 and H3K4) were examined using Western Blotting (Fig. 4A, B). Although pre-MZT SU5402 treatment did not overtly change total Histone H3 protein level, methylation in H3K36 was suppressed both at dome and shield stage. H3K4 trimethylation was also clearly reduced at shield stage. These results are consistent with the RNA-seq and ATAC-seq data, both suggesting that the role of FGFR signalling pre-MZT is not to regulate a small number of specific genes. Rather, it mediates global chromatin structure thereby influencing the expression of a large number of genes after the MZT. To confirm this result, whole mount immunohistochemistry was conducted on H3K36, which indicated that suppression of pre-MZT FGF signalling widely reduced H3K36 methylation in the majority of cell nuclei at dome stage (Fig. 4C).

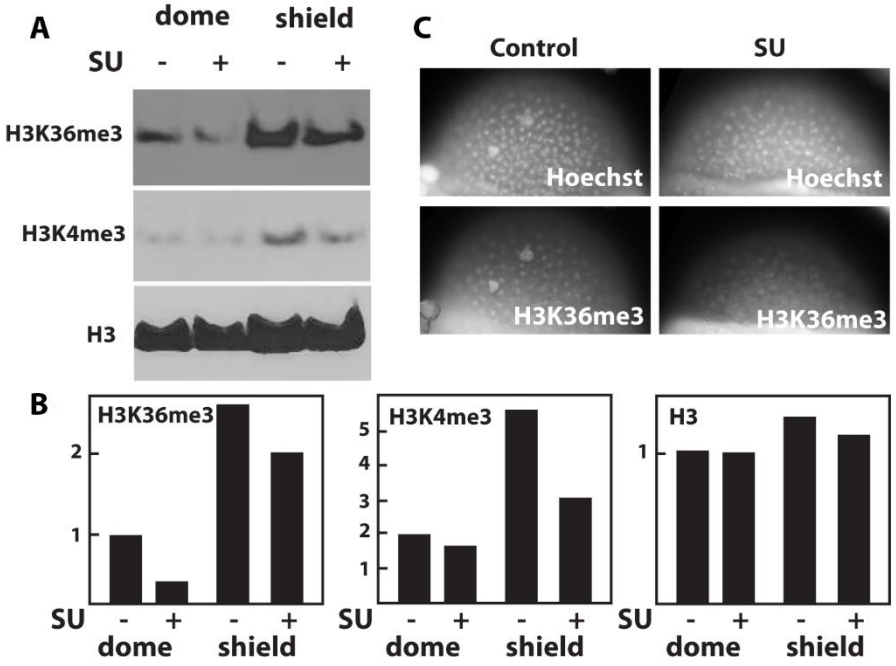

Figure 4. Pre-MZT FGFR signalling induces Histone methylation at H3K36 and H3K4. A,B. Western blotting of dome and shield stages embryos treated with SU5402 pre-MZT. Suppression of Histone H3K36 histone trimethylation by pre-MZT SU5402 was also confirmed with whole mount immunohistochemistry. In this figure, Hoechst stains all cell nuclei. H3K36 staining shows H3K36 trimethylation in the cell nuclei of the control embryo at dome stage whereas pre-MZT SU5402 treated embryos shows reduction of H3K36 positive nuclei (C). Scale bar is 200µm.

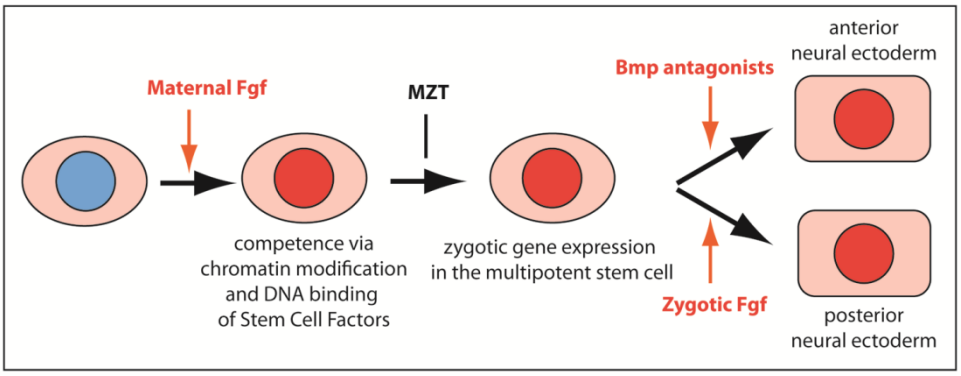

Figure 5. Model for differential role of FGFR signalling at maternal and zygotic periods. FGFR signalling in the pre-MZT period (0-3hpf) imparts competence for cells to respond to later signals possibly via chromatin modification. At late blastula to gastrula stage, dorsal BMP antagonists and marginal FGF signals (zygotic FGF) further induce these cells to become anterior and posterior neural tissues respectively (Kudoh *et al.*,2004).

Discussion

Maternal FGFR signalling imparts competence for acquiring neural identity

We examined the stage-specific contribution of FGFR signalling to neural induction by treatment with FGFR inhibitors, and observed different phenotypes upon suppression of maternal or zygotic FGFR signalling: inhibitor treatment until the MZT strongly suppressed anterior neural induction, whereas treatment from the MZT primarily suppressed trunk/tail, but not head, neural induction.

We interpret the differential roles of maternal and zygotic FGFR dependent signalling with a “competence and induction” concept (Fig. 5). In this model, maternal FGFR signalling is a pre-requisite for neural induction, but is not sufficient to specify neural identity and is not localised only to those cells that will later form neural tissue. The function of maternal FGFR activity pre-MZT could then be interpreted as giving “competence”, i.e., sensitising cells to future neuralising signals. The transcription factors Pou5f3, Nanog and SoxB1 have been studied in zebrafish (Xu *et al*., 2012; Leichsenring *et al*., 2013). Nanog acts during the early stage of MZT to control the activation of many zygotic genes and subsequent regulation is by Pou5f3 and Sox2. Thus, these factors work together to activate the first wave of zygotic transcription in the zebrafish embryo (Lee *et al*., 2013). The maternal factor Pou5f3 is involved in envelope layer formation (Lachnit *et al*., 2008; Sabel *et al*., 2009). We suggest that this competence could potentially be acquired by the epigenetic modifications of Histone proteins and the DNA binding of pluripotent factors such as Pou5f3. On the other hand, zygotic FGFs emanating from the blastoderm margin (e.g. FGF3) or Bmp-antagonists, such as chordin emanating from the organiser can induce neural tissues (Fig.5) (Kudoh *et al*., 2004; Rentzsch *et al*.,2004; Dee *et*

al.,2007). Therefore, the role of zygotic FGF is primarily in neural induction, particularly in the posterior (trunk and tail) neural tissue. We have previously shown that in embryos in which zygotic (including organiser) FGF signalling is suppressed, anterior neural markers are still expressed (Kudoh *et al*., 2004). Furthermore, when BMP signalling was blocked in organiser-deficient *ichabod* embryos by treatment with Dorsomorphin, both anterior and posterior neural markers were restored in their correct position along the animal-vegetal axis (Varga *et al*.,2011). These data indicate that BMP antagonism is sufficient to restore both anterior and posterior neural induction independently of zygotic FGF function and support the idea that the role of FGF signalling in anterior neural induction (independent of BMP-antagonism) is due to the ubiquitous, FGFR dependent pathway imparting neural competence. If pre-MZT FGFR activity provides competence to cells before neural induction, it would be possible that such a mechanism may also operate for posterior neural induction. However, pre-MZT SU5402 treatment primarily suppressed anterior neural induction and this is possibly due to the overlapping roles of maternal and zygotic FGF signalling. As zygotic FGF is expressed after the MZT in the blastoderm margin, competence for, and induction of posterior neural tissue may both be achieved by zygotic FGF signalling.

Our “competence and induction” model is consistent with previous data from other species; in *Xenopus* and Chick, it has been shown that FGF signalling is required for neural induction both in the anterior and posterior neural ectoderm, independently of the Bmp antagonism (Streit *et al*.,2000; Wilson *et al*.,2000; Delaune *et al*.,2005). In the ES cell studies, it has also been shown that FGF signalling pathway is required for neural induction but not for self-renewal of the stem cells (Kunath *et al*.,2007).

FGFR function regulates post-MZT expression of stem cell related genes which is accompanied with epigenetic modification.

ATAC-seq showed that Stem Cell Factors (e.g. Nanog, Pou5f3 and Sox2) binding sequences are among the most obvious changes in promoter-enhancer regions affected by SU5402 treatment. RNA-seq and in situ hybridisation identified many blastula genes which promoter-enhancer regions contain Stem Cell Factor motifs and show reduced gene expression in pre-MZT FGFR suppression. As inhibitor treatment occurred at pre-MZT but gene expression changed only after the MZT, it is possible that pre-MZT FGFR signalling may not regulate these Stem Cell Factor-related cis elements directly, but rather the epigenetic chromatin signature that would consequently alter the accessibility of Stem Cell Factors to the promoter sequence to initiate expression of genes subsequent to the MZT (Fig. 5). Indeed we observed decreased trimethylation of Histone H3K4 and H3K36, using western blotting and immunohistochemistry (Fig. 4). The H3K36 data was confirmed by duplicated immunohistochemistry (Fig. 4 A, C), suggesting a decrease of H3K36me3 in SU5402 treated embryos. To further quantify the level of methylation, we would require more detailed stage-dependent analyses, replicated analysis and improvement of the immunostaining quality and imaging. As the expression of a large number of blastula genes is dependent on pre-MZT FGFR signalling, it is possible that competence for neural induction by pre-MZT FGF is only a part of the role of pre-MZT FGF. It is likely that pre-MZT FGF has a more fundamental role on post-MZT gene expression and cell differentiation via chromatin modification.

It is not clear how FGFR signalling regulates the observed histone modifications. It is possible that FGF/MapK may activate transcription factors (Po5f1, Nanog and/or Sox2) to bind to DNA, and then when MZT occurs,

transcription may start and may (or may not) be mediated subsequently by histone methylation. In either case, the transcription does not start until MZT. Another possibility is that FGF/MapK may directly activate methylation or deactivate demethylation enzymes. Further screening and analyses of maternal effect mutants are required (Pelegri and Mullins, 2004). ChIP-seq has been used to detect active transcription factors in DNA binding sites (Wardle and Tan, 2017). ChIP seq could be undertaken with Sox2, Pou5f3 and Nanog to examine the timing and location (loci) of DNA binding before and after MZT, with and without FGF signalling (e.g.SU5402 treatment and XFD injection). Advances in techniques for epigenomic analyses and genome editing technology (e.g. CRISPR-Cas9) would also facilitate.

Supplementary

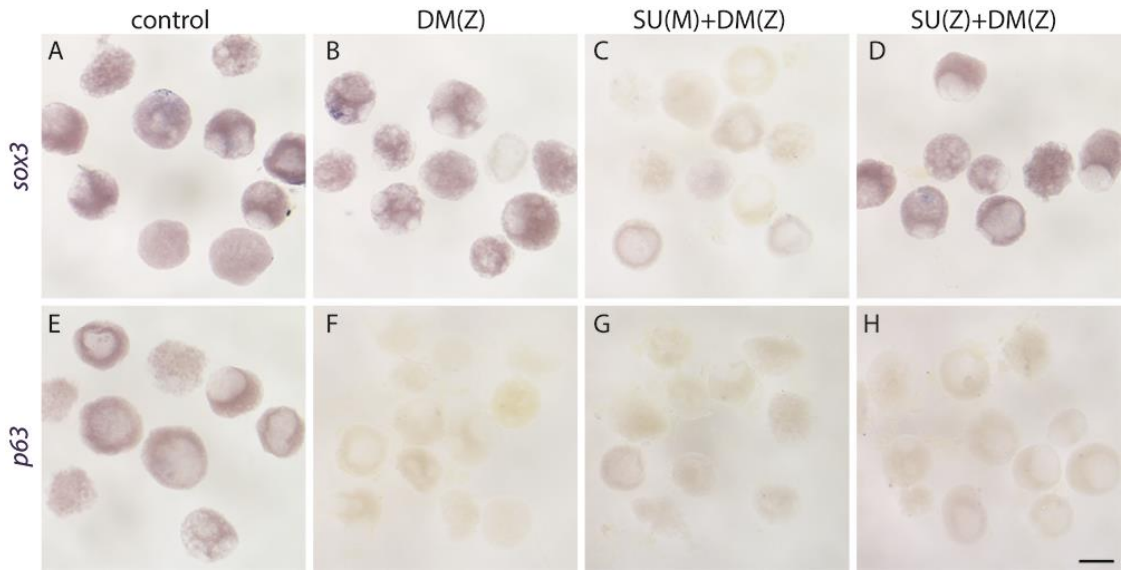

Supplementary figure1. Anterior neural induction does not occur in animal caps exposed to SU5402 at maternal stage. In situ hybridisation of wildtype animal caps fixed when control embryos were at the late gastrula stage. A and E unexposed embryos show the expression of *sox3* and *p63* respectively. B and D show expression of *sox3* in embryos unexposed or exposed to SU5402 at post-MZT stage respectively. C. missing of *sox3* expression in embryos exposed to SU5402 at pre-MZT (0-3hpf). F-H shows the missing of expression in *p63* in both unexposed and exposed to SU5402 at pre or post-MZT. Embryos were exposed to DM at post-MZT stage in all condition except control. Scale bar is 200µm.

Gene marker	control			SU(M)			SU(Z)			SU(M+Z)			XFD		
	N	+	%	N	+	%	N	+	%	N	+	%	N	+	%
Sox3(A)	25	25	100	20	0	0	20	18	90	24	0	0	11	2	18
Sox3(P)	25	25	100	20	15	75	20	0	0	24	3	21	11	2	18
hoxb1b	25	25	100	22	22	100	19	0	0	15	0	0	10	2	20
otx2	20	20	100	23	0	0	18	17	94	14	0	0	12	4	33

Supplementary Table1. In situ staining of gene markers at 80% epiboly in SU5402 treated and XFD injected embryos. (A) anterior expression, (P) posterior expression. Images of the treated embryos are shown in Fig.1.

Gene marker	control				SU(M)				SU(Z)			
	N	+	++	%	N	+	++	%	N	+	++	%
P63	17	17	0	0	23	0	23	100	14	0	14	100

Supplementary Table 2. In situ staining of *p63* at 80% epiboly in SU5402 treated and XFD injected embryos. (+) normal expression, (++) overexpression. Images of the treated embryos are shown in Fig.1

Time	control			Pre MTZ SU treated			
	N	+	-	N	+*	+	-
3 hpf	15	15	0	15	0	0	15
3.5 hpf	15	15	0	15	7	0	8
4 hpf	15	15	0	15	6	5	4

Supplementary Table 3. Immunostaining with Phospho-Erk antibody shows SU5402 treated embryos at 0-3hpf. At 3hpf, the inhibitor was washed off**.** (+) normal p-Erk signal or totally restored, (+*) p-Erk levels are partially restored (-) negative signals. Images of the treated embryos are shown in Fig.1

Gene marker	control			SU5402			XFD		
	N	+	%	N	+	%	N	+	%
zic2.1	10	10	100	15	0	0	8	1	12
id1	7	7	100	16	0	0	12	3	25
dusp6	15	15	100	13	0	0	10	2	20
pricle1b	6	6	100	16	0	0	11	1	9

Supplementary Table 4. In situ staining of gene markers at dome stage in control and SU5402 treated and XFD injected embryos. (+) normal expression, (N) number of embryos. Images of the treated embryos are shown in Fig.3.

Results Chapter 4

Fgf2 regulates differentiation and survival of the skin cells in the zebrafish embryo

Abstract

In vertebrates, it has been known that FGF signaling has crucial roles in the early embryo development particularly in mesoderm induction, neural induction and gastrulation cell movement. However due to the size of the *fgf* gene family (28 known genes, including some duplicates) and associated redundancies in the zebrafish (Ref), the role of each *fgf* gene has not yet been fully understood. Here we investigated the function of *fgf2* in zebrafish embryo development. The gene knock down of *fgf2* did not show an abnormality at gastrula stage except a mild delay in epiboly. However a synchronized degeneration of epidermal progenitor cells occurred at the early somite stage, leading to sudden lethality at the mid-somite stage. Zebrafish animal cap assays further confirmed that cell death primarily occurs at the epidermis. RNA-seq analyses followed by *in situ* hybridization staining of selected gene probes revealed that many epidermis specific genes are down-regulated following knock down of the *fgf2* gene. As *fgf2* knock down suppressed epidermis marker genes, but did not expand neural markers, the data suggest that there are two steps in differentiation of the epidermis: Firstly presence or absence of a neural inductive signal specifying the ectoderm to neural and non-neural fates respectively in an FGF2-independent manner. Subsequently the non-neural ectoderm is differentiated by an FGF2 dependent signaling pathway. Our data, for the first time, revealed that *fgf2* is crucial for the survival of the early stage embryo, especially by regulating the differentiation of the primordial epidermal cells in the embryo.

Introduction

Fibroblast Growth Factor 2 (FGF2) is an important signalling molecule for cell growth and differentiation: It belongs to a large growth factor family, Fibroblast Growth Factors which have crucial roles in cell proliferation, differentiation, embryonic patterning, and morphogenesis (Powers *et al.*, 2000; Coumoul and Deng, 2003; Quarto *et al.*, 2005; Thisse and Thisse, 2005). FGF2 binds to FGF Receptors FGFR1, 2, 3 and 4 (Nugent and Iozzo, 2000) and sends signals via RTK-Map kinase pathway and/or PI3 kinase pathway (Dailey *et al.*, 2005; Thisse and Thisse, 2005; Vinuela, 2008). FGF2 plays several significant roles in the growth and differentiation of many tissues (Zhou *et al.,* 1998). FGF2 was extensively studied in mammalian culture cells and was proposed as a crucial factor regulating angiogenesis by regulating cell migration and proliferation of endothelial cells via the Map Kinase pathway (Pintucci *et al*., 2002; Tanaka *et al*., 2004), FGF2 is also involved in the process of wound healing and many other cell events (Basilico and Moscatelli, 1992; Gibran *et al.,* 1994; Ortega *et al.,* 1998; Pintucci *et al.,* 2002). Fgf2 is involved in cardiomyocyte growth (Schultz *et al.,* 1999). Ortega *et al.* (1998) and Raballo *et al.* (2000) found a significant reduction in neuron number in brain neocortex in mice lacking FGF2. In *Xenopus*, *fgf2* acts as a mesoderm inducer; it acts to maintain cell propagation of mesenchyme in the epical ectodermal limb during development (Fallon *et al.,* 1994).

In zebrafish, *fgf2* plays an essential role in inducing angiogenesis. Injection of human recombination *fgf2* (rFGF2) in zebrafish embryos at 48hpf between the yolk and the periderm, induced the formation of blood vessels (Nicoli *et al.,* 2009). *Fgf2* shows effects on primordial germ cells. It was cited by Wong and

Collodi (2013) that expression of *fgf2* in zebrafish considerably increases primordial cell number at stage 14-21dpf.

On the other hand, the roles of FGF2 in fish embryonic development remain largely unknown Several studies have been conducted on *fgf2* function in zebrafish, but there has been no focus on *fgf2* function at early stages of development, except for studying its role in Kupffer's vesicle (KV) morphogenesis, that is important for organ asymmetry in zebrafish (Arrington *et al*., 2013). The discrepancy between crucial effects of FGF2 in cell culture systems and its relatively minor defects in embryonic systems may be explained by a potential redundancy between the FGF molecules in embryos. Depending on species, such genetic redundancies can be diversified: For instance, loss of function of *fgfr1* showed different phenotypes in the zebrafish and medaka. The zebrafish *fgfr1* knock down shows a specific defect in the midbrain-hindbrain boundary with normal trunk and tail formation (Scholpp *et al.,* 2004), whereas the FGFR1 mutant in medaka showed global reduction of the posterior structure, including the whole trunk and tail with a comparatively normal head (Yokoi *et al.,* 2007). As seen in this example, testing loss of function using different model animals often facilitates understanding of the roles of genes in developmental and cellular processes.

In this study, we investigated the role of *fgf2* in zebrafish by injecting a gene specific morpholino. Here we report the crucial role of *fgf2* in survival of the embryo, which is distinct from known phenotype obtained in the knock-out mice. Our finding reveals a novel role of *fgf2* in the development of the epidermal primordia and the survival of the early vertebrate embryo.

Zebrafish epidermis is composed of a surface layer, enveloping layer (EVL) that is generated during the blastula stage and an inner layer, epidermal basal layer (EBL) (Chang and Hwang, 2011). The epidermal basal layer forms during gastrulation when the main germ layers ectoderm, mesoderm and endoderm are organized (Heisen-berg and Tada, 2002).

It is known that ectoderm cell fate consists of neural and non-neural tissues. Non-neural ectoderm is specified into epidermis that becomes skin (Lee and Kimelman, 2002). At the gastrula stage, BMP gradient along the dorso-ventral region drives cell specification to neural or non-neural ectoderm, the high level of BMP in the ventral domain leads to specification of the epidermis (e.g. Kudoh *et al*., 2004). BMP induces transcription factors *foxi1*, *tfap2*, *gata3* and *p63* that express in prospective epidermis; *foxi1*, *tfap2* and *gata3* during late blastula are necessary for preplacodal ectoderm (Kwon *et al*., 2010), while *p63* is required for epidermal differentiation (Lee and Kimelman, 2002). Here in we investigated the role of FGF2 in inducing epidermal transcription factors. We injected a morpholino which shows a synchronized embryonic lethality at early somite stage. In situ data suggested that *fgf2* knock down did not affect cell fate specification in mesoderm, endoderm and neural ectoderm. However, *fgf2*MO suppressed epidermis marker p63 as RNA and protein level, causing apoptosis of the epidermal layer at early somite stage. From these result we concluded that f*gf2* has significant role in epidermis differentiation and early embryonic development.

Results

Fgf2 is ubiquitously expressed from the early developmental stage

Expression of *fgf2* at the cleavage to gastrula stages was examined using *in situ* hybridisation. *Fgf2* is widely expressed at a pre-zygotic (256 cell stage) and early zygotic (high) stages (Fig.1 A, B). It was initially observed a weak expression from the pre-zygotic stage. At blastula to gastrula, the staining become more intense (Fig.1 C, D). At the end of gastrula to early somitogenesis stage (Fig.1 E-H), ubiquitous staining of *fgf2* is decreased and the expression becomes specific to the forerunner cells as previously reported (Arrington *et al*., 2013). The ubiquitous expression of *fgf2* during the gastrula stage implies an important role of this gene during early embryonic development.

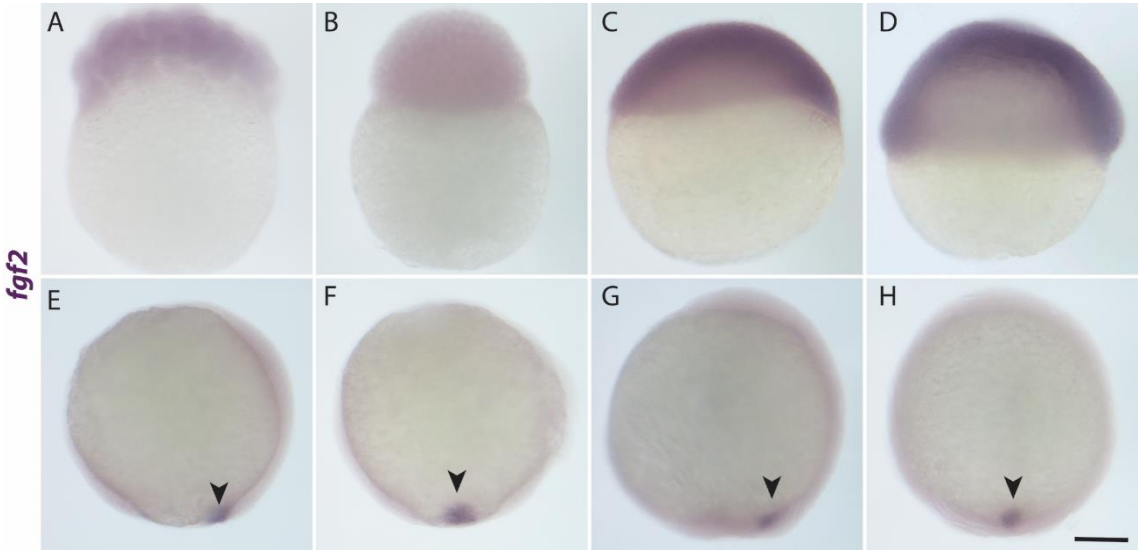

Figure 1. *Fgf2* is widely expressed at blastula to gastrula stage. A-D ubiquitous expression of *fgf2* at blastula and gastrula stages. Elevated expression was observed at gastrula stage (C and D). *Fgf2* is specifically expressed in forerunner cell at late gastrula (90% epiboly, E and F) and bud stage (G and H) (Arrington *et al*. 2013). Scale bar is 200µm.

Fgf2-knockdown shows severe morphological abnormalities and embryonic lethality at early to mid-somite stage

To investigate the role of *fgf2* at early embryonic stages, loss of function of *fgf2* was achieved by injecting *fgf2* morpholino (fgf2MO). *Fgf2* morphant embryos showed mild delay in epiboly at late gastrula stage (Fig.2). At the early somite stage, the embryo exhibited abnormal morphologies including failure of germ ring closure, irregular shape of the blastoderm margin and small head (Fig.2B). Time lapse video shows a striking embryonic lethality at mid somite stage (Fig.2D, and Supplementary video). These data suggest that *fgf2* has crucial role in the survival of the embryo by regulating cell movement, cell adhesion and/or cell differentiation at late gastrula to early somite stage.

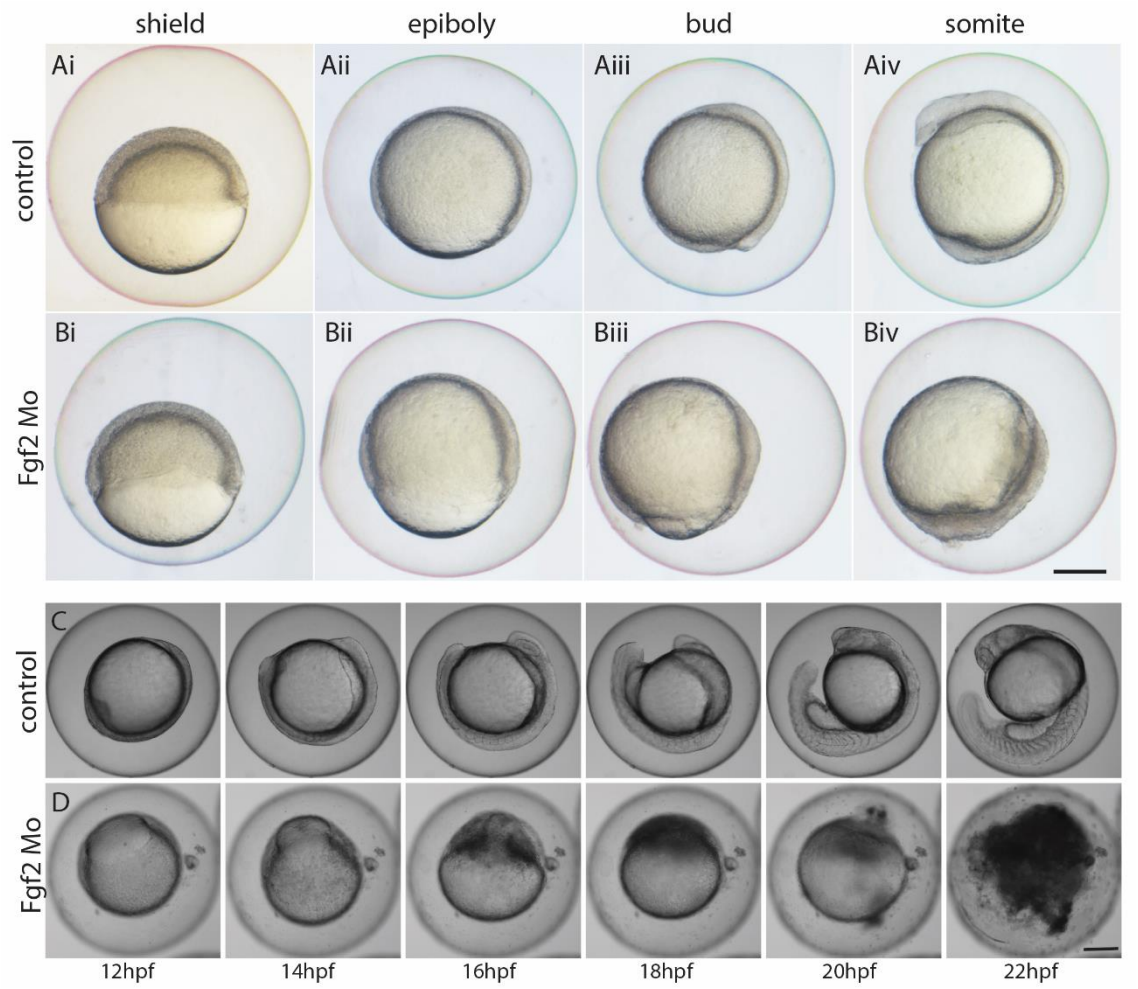

Figure 2. Morphological change and lethality of the *fgf2* knock-down embryo. Control (A and C) and fgf2MO injected at 1 to 2 cell stage embryos (B and D). B. Live images of the embryo at gastrula to 3 somite stage. D. Live images were selected from time lapse video taken overnight, showing fgf2MO embryo degradation and dying at early somite stage, fgf2MO showed 93% (±7) mortality. Scale bars are 200μm.

Fgf2 mRNA rescues *fgf2* morphants

To confirm the specificity of the fgf2MO, *fgf2* mRNA was co-injected with fgf2MO at 1 cell stage (Fig.3). Indeed *fgf2* mRNA significantly rescued the embryo in both lethality and morphological abnormality (Fig.3C): The data shows high survival ratio with *fgf2* mRNA rescuing 63.4% (±26) of embryos, compared to only 1.5% (±2.6) of survival of embryos injected with fgf2MO (Fig.3I). The data indicate that the phenotype of fgf2MO is specific to the loss of

function of the *fgf2*. The data also suggest that overexpression of *fgf2* at 1 cell stage is not embryonically lethal.

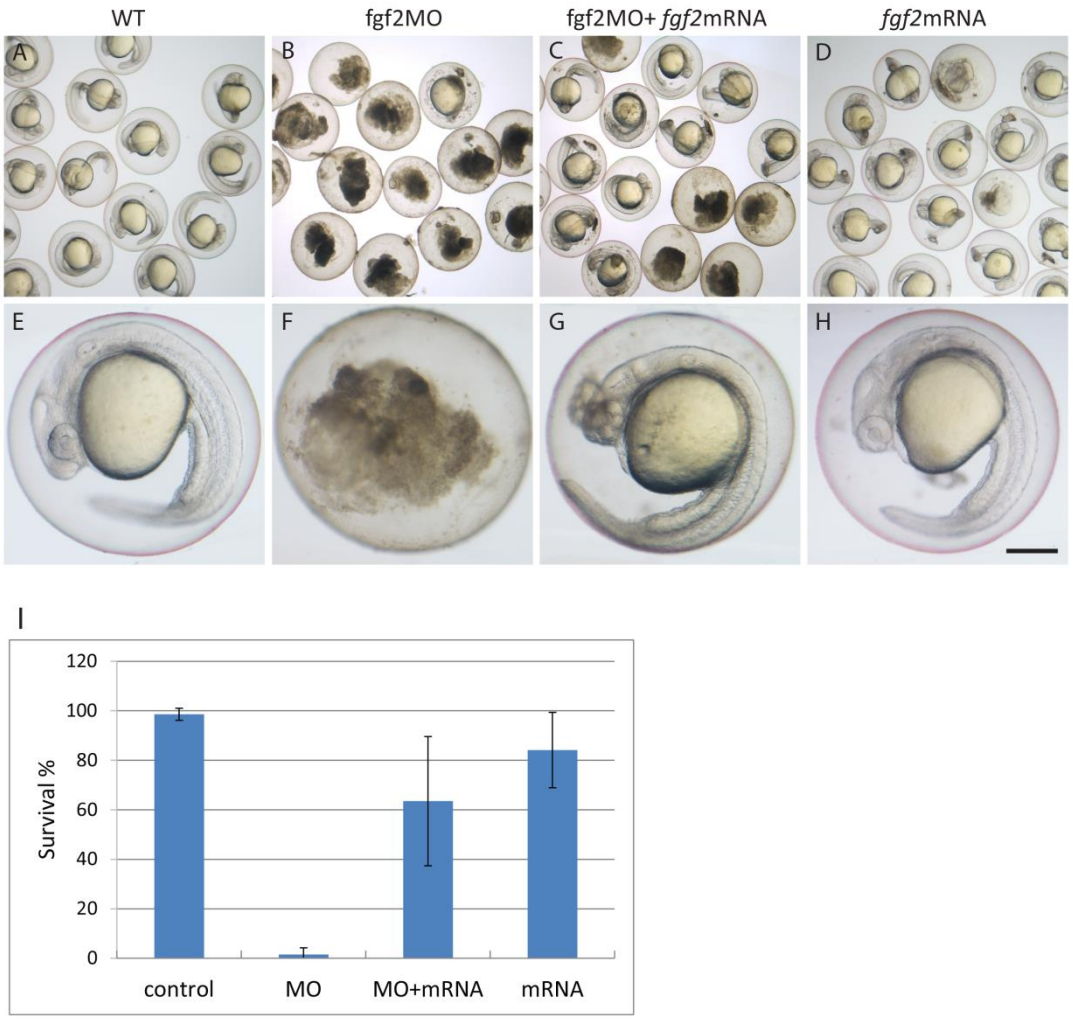

Figure 3. *Fgf2mRNA* rescues the fgf2MO. All embryos are 24hpf stage. A, E. Control embryos. B, F. fgf2MO. C, G. co-injection of *fgf2* mRNA and fgf2MO. D, H. injection of *fgf2* mRNA alone. I. Histogram showing percentage of survival of embryos at 24hpf, replication 3 times. Scale bar is 200µm.

Knockdown of *fgf2* does not affect tissue specific gene expressions in the neural ectoderm, mesoderm and endoderm

It has been known that several *fgf* genes and the receptor *fgfr1* have crucial role in the induction of mesoderm and neural ectoderm (Koshida *et al.,* 1998; Kudoh *et al*., 2004; Yokoi *et al.,* 2007). Therefore we tested the expression of the

genes specific to mesoderm, neural ectoderm and endoderm for comparison. The tested mesoderm genes include *ntl* which is a marker expressed in the germ ring and notochord, *aldhla2* and *spt* in paraxial mesoderm. *Sox3*, *otx2,* and *hoxb1b* probes were used as markers for the neural ectoderm. Data showed no differences between fgf2MO embryos and control (at 90% epiboly stage) (Fig.4, Supp.Table1). Although gene expression was not reduced, the morphology of the expression domain showed several changes, including wider and shorter notochord and the thicker germ ring in the fgf2MO. Positive-staining of cells occurred predominantly on the ventral side (Fig.4, B, D and F), suggesting delay of epiboly and convergent-extension (CE) in the morphant. *Sox17*, a marker for the endoderm and the forerunner cells (Alexander and Stainier, 1999), was also examined, again confirming that the CE movement defect occurred in the endodermal layer (Fig.4H). As a mild epiboly and CE movement defect was observed, potential abnormalities in cell adhesion and actin cytoskeletal organisation was examined using phalloidin staining. However, our data did not detect any abnormality in cell morphology, actin networking and cell-cell connection in the fgf2MO (Fig.5, Supp.Table2), suggesting that FGF2 does not have a significant effect on the cytoskeleton during gastrulation.

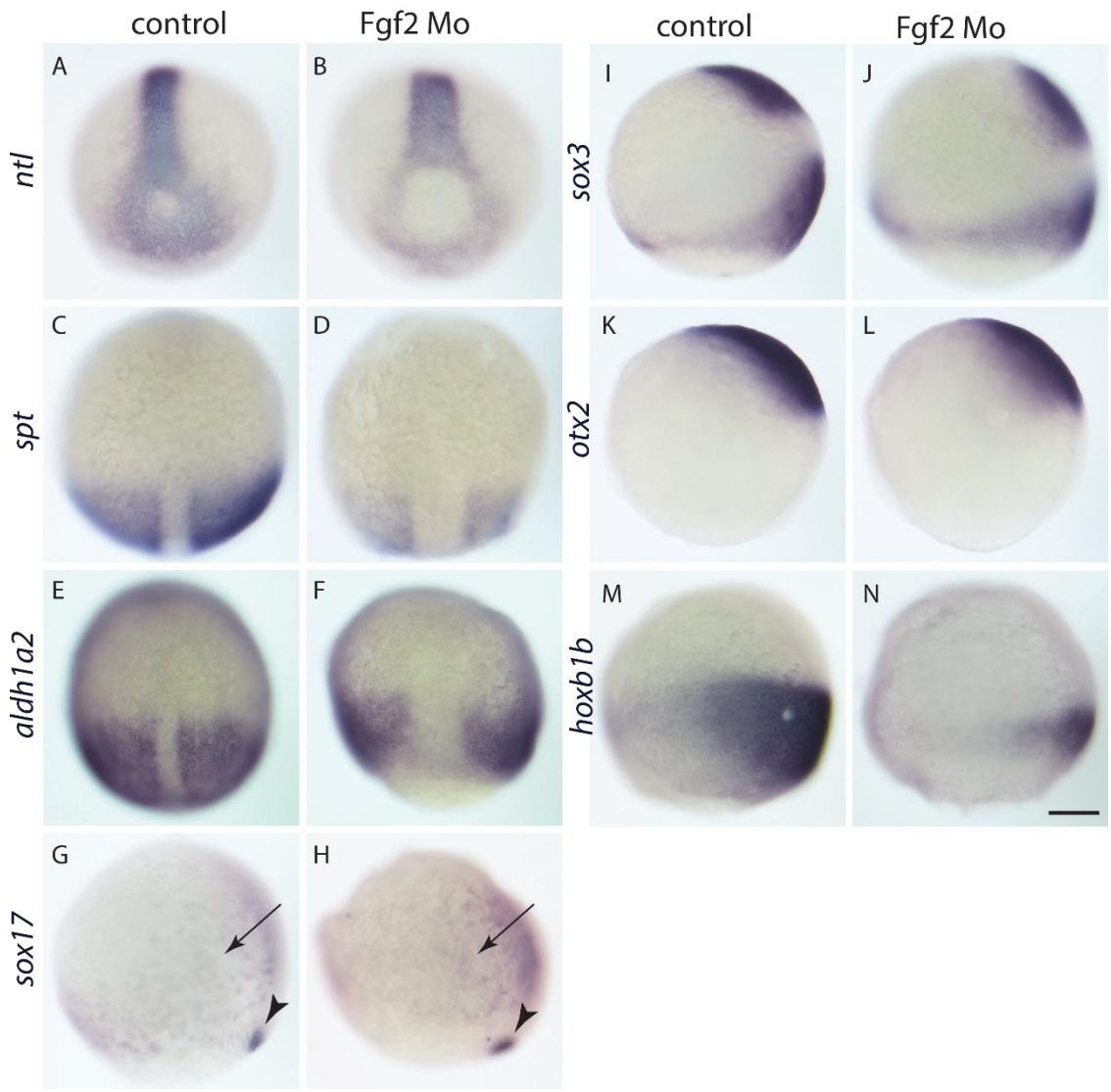

Figure 4. Fgf2MO does not affect cell fate markers for gastrula neural ectoderm, mesoderm and endoderm. Control embryos (A, C, E, G, I, K, M). Fgf2MO injected embryos (B, D, F, H, J, L, N). Late gastrula (90% epiboly) embryos were examined with marker genes, *ntl* (A, B), *spt* (C, D), *aldh1a2* (E, F), *sox17* (G, H), *sox3* (I, J), *otx2* (K, L), *hoxb1b* (M, N). Scale bar is 200µm.

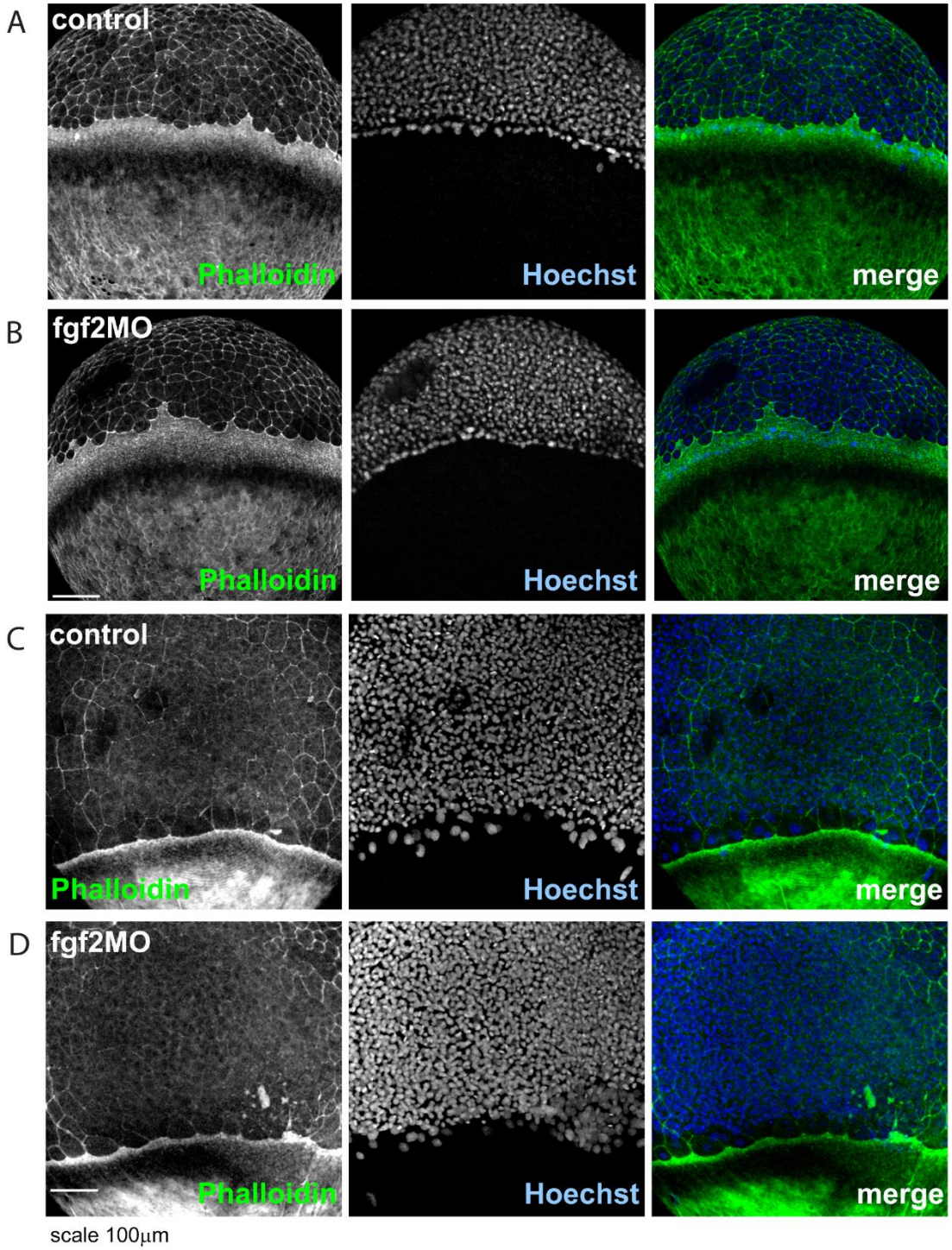

Figure 5. Normal cytoskeletal actin in fgf2MO at gastrula stage. A. control at shield stage. B. fgf2MO at shield stage, C. control at 80% epiboly. D. fgf2MO at 80% epiboly.

Animal cap assay revealed crucial role of *fgf2* in the survival of epidermal primordial cells

In the time lapse analyses, lethality of the embryo seemed to be initiated by dissociation of the animal pole cells from the embryo (Figure 2). The animal pole cells mainly consist of epidermis and neural ectoderm. Therefore we hypothesized that epidermis and/or neural ectoderm may require *fgf2* for differentiation and survival. To test this possibility, the epidermal animal cap and neural animal cap were generated from the zebrafish embryo. To make the epidermal cap, the zebrafish embryo was injected with *bmp2b* mRNA at the one cell stage, followed by fgf2MO injection at the 2-4 cell stage. The animal cap was dissected at high stage, and cultured for 24 hours. To create the neural cap, the animal cap with or without fgf2MO injection was cultured in the presence of a BMP-inhibitor, Dorsomorphin. In the epidermal cap, fgf2MO induced 100% lethality (Fig.6Dii), whereas in the neural cap, fgf2MO did not show strong lethality (Fig.6Bii and Fii). These data suggest that *fgf2* is crucial in the survival of the epidermis/prospective epidermis cells. In the normal animal cap in which both epidermis and neural ectoderm are present 28% (±3) mortality was induced by fgf2MO (Fig.6 Bii) compared to 25% (±7) mortality in controls, again supporting the idea that the tissue containing neural ectoderm can survive in the absence of FGF2.

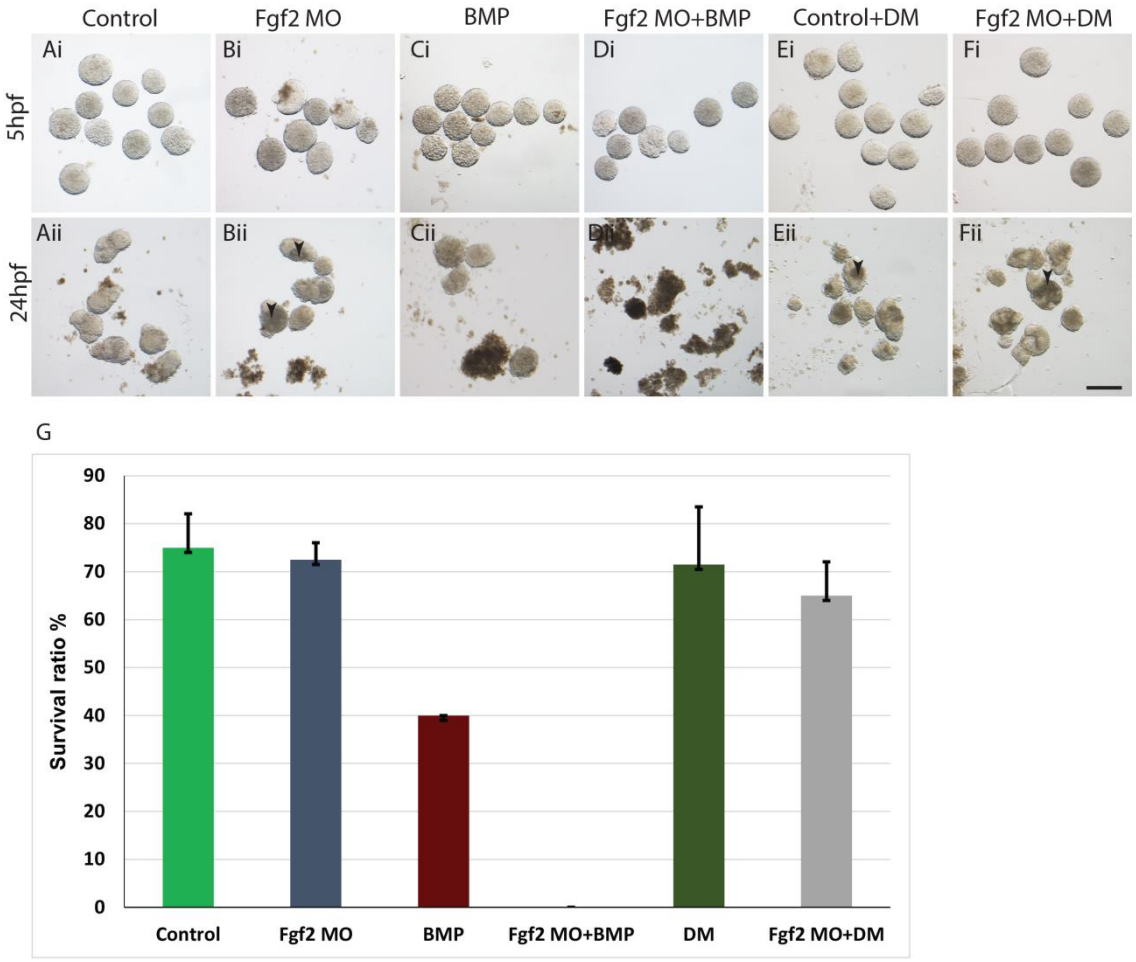

Figure 6. Survival of the epidermis animal cap relies on *fgf2*. Animal caps prepared from embryos of WT (A), injected with fgf2MO (B), *bmp2b* (C), fgf2MO + *bmp2b* (D), embryos treated with Dorsomorphin (E), and embryos injected with fgf2MO and treated with Dorsomorphin (F). The animal cap as photographed at 5hpf (i) and 24hpf (ii). Scale bar is 200μm. Survival of the epidermis animal cap was determined at 24hpf (G). Control 75%(±7), Fgf2MO 72%(±3), BMP 40%(±0), Fgf2MO+BMP 0%(±0), DM 71%(±12), Fgf2MO+DM 70% (±7), (Replication 3 times).

Fgf2 regulates epidermis differentiation

To search for downstream genes that are regulated by *fgf2* during gastrula to early somitogenesis stage, RNA-seq was conducted using the zebrafish epidermal cap with and without fgf2MO at late gastrula stage (90% epiboly).

The data shows that the genes downregulated by the *fgf2* knock-down are highly enriched with the epidermis differentiation markers (Fig.7A). Indeed, *in situ* hybridisation of *p63*, *dlx3* and *tfap2a* showed suppression of gene expression by fgf2*MO* (Fig.7B-I). To further confirm the suppression of epidermis in the *fgf2* knock-down embryo, immunohistochemistry was also conducted using p63 antibody at 3 somite stage. In the control embryos, p63 is specifically expressed in the cell nuclei of the epidermal layer (Fig.7J), but in the *fgf2* knock-down embryos, p63 staining was not visible (Fig.7K), confirming the role of *fgf2* in regulation of a key molecule for epidermis differentiation. Interestingly, at 3 to 7 somite stages, the cell nuclei in the epidermal layer appear highly fragmented and therefore the average diameter of cell nuclei was drastically decreased (Fig.8F-J and Fig.8K). Considering the loss of *p63* mRNA and protein in domain of nuclear fragmentation, we concluded that the epidermal primordial cells, which failed to differentiate to epidermis, probably underwent apoptosis.

A

Gene name	Description	log2FoldChange	P value
dlx3b	distal-less homeobox 3b	-1.923318266	8.27E-05
tp63	tumor protein p63	-1.727216208	2.88E-06
tfap2a	transcription factor AP-2 alpha	-1.726806766	3.21E-07
cyt1	type I cytokeratin, enveloping layer	-1.721752322	7.29E-09
krt5	keratin 5	-1.650304892	7.72E-10
krt17	keratin 17	-1.611256049	1.39E-06
cyt1l	type I cytokeratin, enveloping layer	-1.516534705	8.15E-07

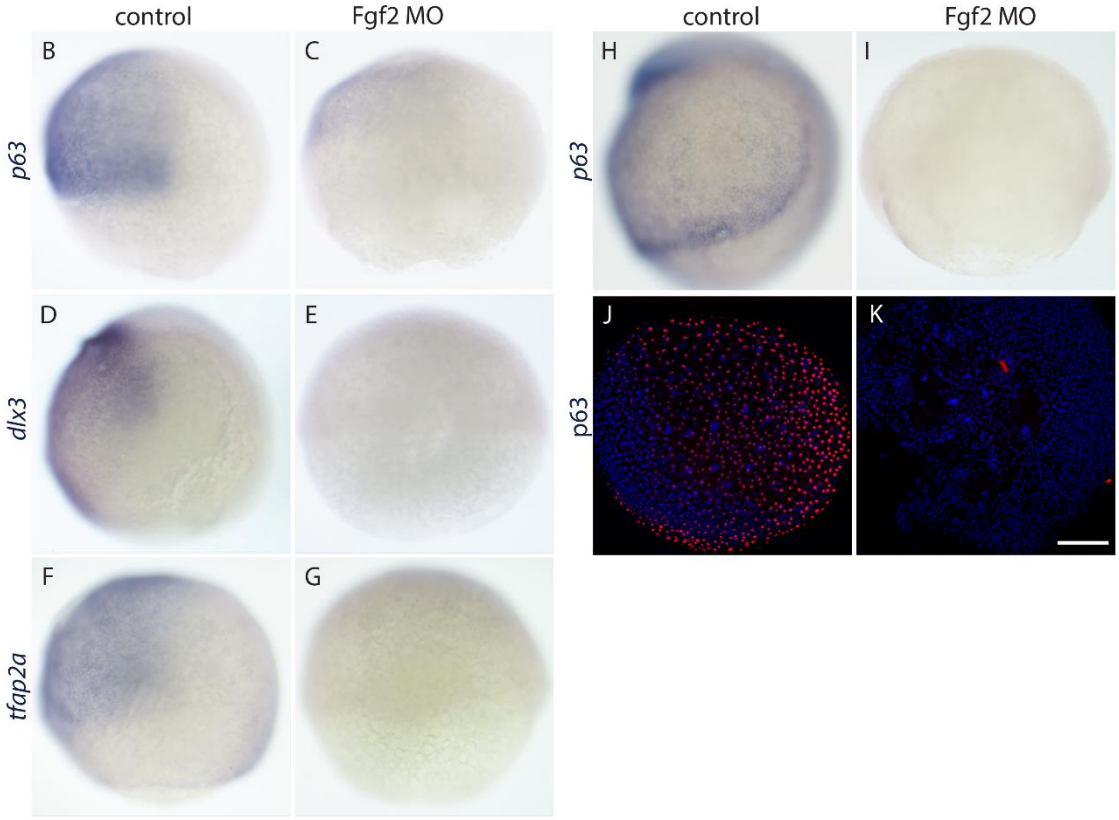

Figure 7. Epidermis gene expressions are reduced by Fgf2MO. A. Differential gene expression was analyzed by RNA-seq between the animal cap samples (8hpf) injected with bmp2b and *bmp2b*+fgf2MO. The table shows skin specific genes found in the top 100 down-regulated genes in the presence of fgf2MO. *In situ* hybridization of these skin specific genes indeed showed suppression of gene expression by fgf2MO: B,D,F,H. control embryo at 90% epiboly (8hpf) stage. C,E,G,I. fgf2MO at the same stage. The embryos were *in situ* stained for *p63* (B, C), *dlx3* (D, E), *tfap2* (F, G). *p63* expression was also examined at 3 somite stage using *in situ* hybridization (H, I) and a specific antibody (J, K). Scale bar is 200µm.

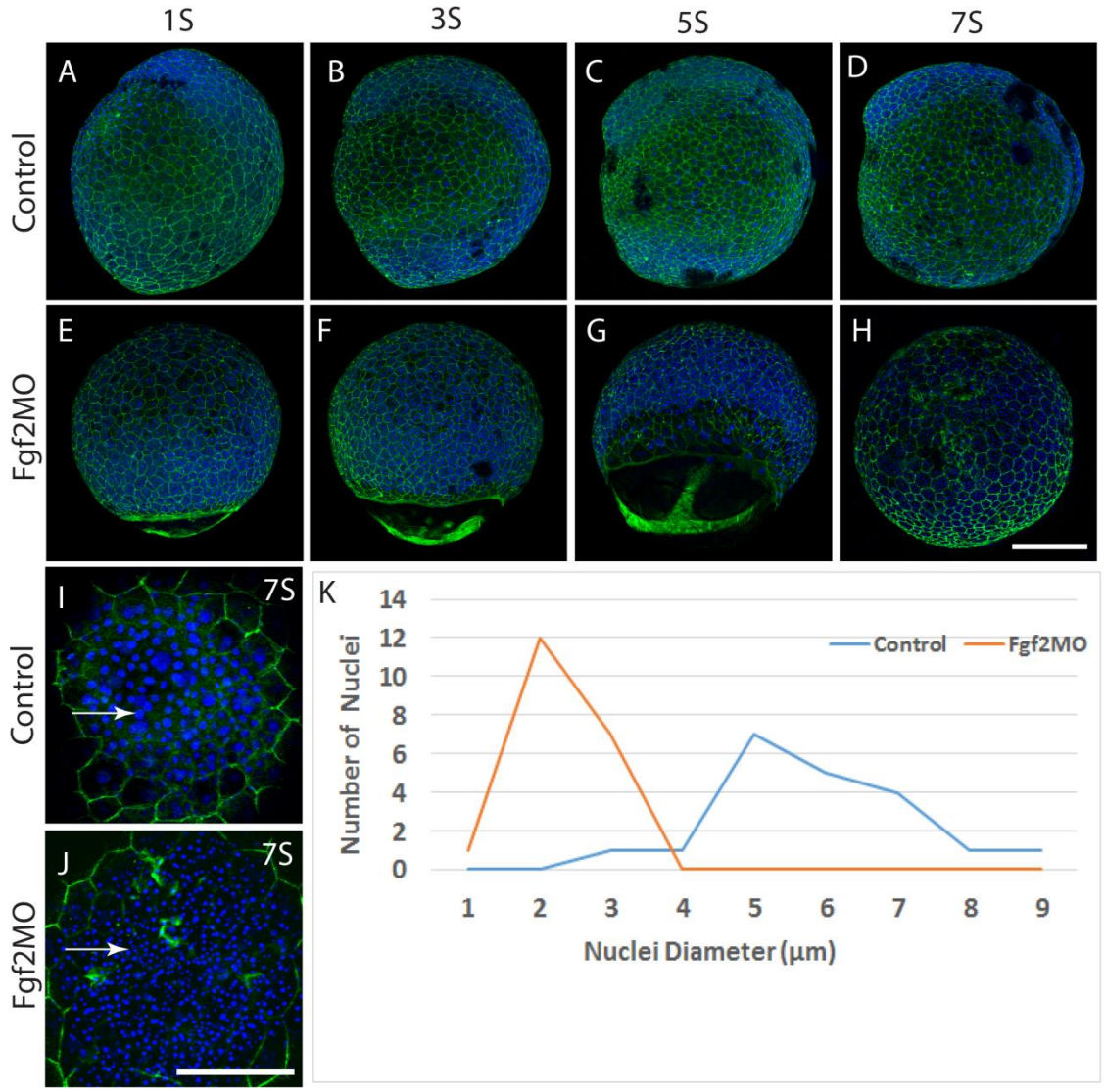

Figure 8. *Fgf2* knock down induces cell degeneration in the epidermis at around 5 to 7 somite stage. Control embryos (A,B,C,D,I) and fgf2MO embryos (E,F,G,H,J) were stained with phalloidin and hoechst at 1 somite (A, E), 3 somite (B, F), 5 somite (C, G) and 7 somite (D, H, I, J) arrow refers to nuclei. Scale bars are 200µm. K. Diameter of nuclei in the control and fgf2MO at 7 somite stage showing an increase in the number of smaller nuclei (possibly fragmented nuclei) and missing larger nuclei (un-fragmented nuclei) in Fgf2MO.

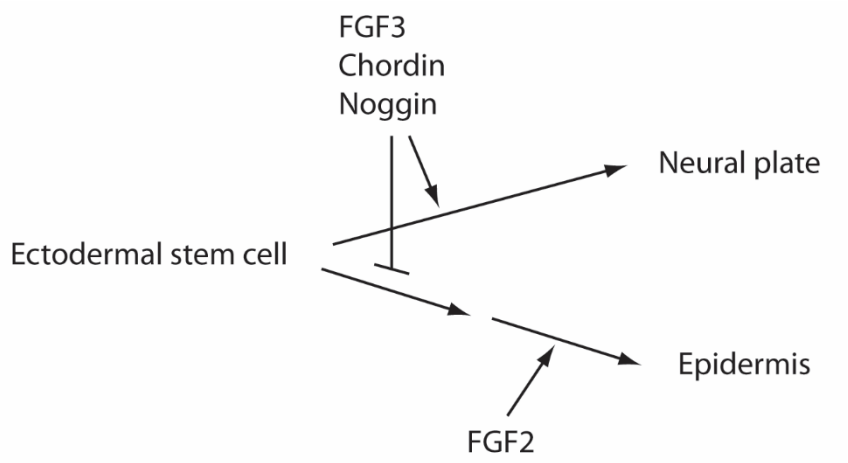

Figure 9. Two step differentiation of the epidermis. In the first step, neural induction signals (e.g. Chordin and FGF3) specify the ectoderm to become neural ectoderm. The area (ventral-animal pole ectoderm) which is away from these signals is specified to become non-neural ectoderm. In the second step, FGF2 induces the non-neural ectoderm to express epidermis genes including *p63*, *dlx3* and *tfap2*.

Discussion

In this research, we found that the role of *fgf2* in zebrafish is critical for early development, but this is not the case in mammalian models such as the mouse: Knockdown of *fgf2* in mouse results in reductions in vascular smooth muscle contractility, thrombocytosis and blood pressure, but no abnormality in morphological phenotype (Zhou *et al.,* 1998). In our study on zebrafish embryos, knockdown of *fgf2* in *fgf2*MO resulted in abnormal phenotypes and high ratio of mortality in embryos at early somite stages, suggesting that the role of *fgf2* is important for cell survival during early embryonic development. A previous study also showed that cell death occurred in *fgf2* morphant zebrafish at early stages of development (before the 14 somite stage) (Lee *et al*., 2010). This study provides a result consistent with our current study, however the

earlier mortality was observed in our study. The *fgf2* function was also investigated in zebrafish by Arington *et al*. (2013), who showed that the expression of *fgf2* is limited to dorsal forerunner cells and Kupffer's vesicle. Furthermore, *fgf2* morphants showed to abnormality of southpaw gene (*spaw*) expression, a member of Nodal family, in the lateral plate mesoderm (there was bilateral expression such that expression was absent in the right side). The differences in severity of morpholinos between these studies are possibly due to differential dose effects and slightly different region and sequence of the fgf2MO used.

These differences in *fgf2* function between organisms may possibly due to different redundancies between FGF family molecules in zebrafish and mice. Therefore, by using zebrafish as a model, we managed to find a potentially novel function of FGF2.

In the current study, at gastrula stage, fgf2MO showed a mild delay of epiboly with suppression of marker genes for epidermal progenitor cells, but did not alter other marker gene expressions for neural ectoderm, axial and paraxial mesoderm and endoderm progenitor cells. In addition, at the gastrula stage, *fgf2* knock down did not show any visible change in the cell size and shape visualised with phalloidin staining, suggesting that FGF2 does not control cell cycle, cytoskeletal organisation nor cell adhesion. *Fgf2* knock down primarily caused an abnormal epidermal phenotype indicating that FGF2 mainly regulates cell differentiation of epidermal progenitor cells FGF2 may have other roles, but due to a possible redundancy to other *fgf* genes no other abnormal phenotypes were conspicuous.

As mentioned above, the loss of function (morpholino) and gain of function (mRNA injection) of *fgf2* revealed interesting contrasts: Although fgf2*MO* suppressed epidermis marker genes, it did not expand non-epidermis genes (e.g. *sox3* in the neural ectoderm) suggesting that the fate for epidermal and non-epidermal (neural) fates were already specified before FGF2 affected the cells. Therefore we propose two steps in epidermal cell fate specification and differentiation (Fig. 9): The first step would be the process of neural induction by the Bmp-antagonists (e.g. Chordin and Noggin) or other FGFs (e.g. FGF3). At this step, dorsal and vegetal ectoderms are induced for neural fates by the Bmp-antagonists and FGF3 respectively, whereas the ventral-animal ectoderm which is devoid of the neural inductive signals is specified to non-neural ectoderm (Kudoh *et al*., 2004). However, here, we showed that absence of the neural inductive signal is not sufficient for the cells to express genes for the epidermal cell lineage. A second step is required by which FGF2 induces the epidermal genes, including *p63*, *tfap2* and *dlx3,* and promotes epidermal cell differentiation and survival (Fig. 9). This model is further supported by the observation of a gain of function of *fgf2*. Overexpression of *fgf2* mRNA did not affect the neural induction (normal morphology of forebrain, midbrain, hindbrain and spinal cord), indicating that FGF2 cannot change the cell fates between neural and epidermal fates, confirming that neural induction is the first step of the neural and non-neural specifications and that the action of FGF2 is required for the following step of epidermal gene expression and differentiation (Fig. 9).

The actin staining at gastrula and early somite stages indicates that the enveloping layer has a relatively normal cell shape and cell adhesion pattern. However, sudden and extensive nuclear fragmentation occurred between 3 to 7 somite stages, leading to embryonic lethality in the following few hours. This

suggests that the epidermal primordial cells which failed to express the key regulators for skin development such as *p63*, *dlx3* and *tfap2*, probably undergo cell death**.** Although *fgf2* is ubiquitously expressed at blastula to gastrula stage, cell death only occurred at mid-somite stage particularly in the epidermis. This suggests that the action of FGF2 is not simply a regulation of cell survival but a specific regulation of cell lineage specific gene expression and cell differentiation.

Though FGF2 can bind to FGFR1, the embryonic phenotype for loss of function of FGFR1 and FGF2 is highly different: FGFR1 inhibitor, SU5402 suppresses neural induction, mesoderm induction with expansion of epidermis (Kudoh *et al*., 2004), whereas FGF2 knockdown suppresses epidermis development, without affecting gene expression in the neural ectoderm and mesoderm. It is known that FGF2 signalling is mediated via its binding to specific transmembrane receptor tyrosine kinases - FGFR1 and FGFR2 that have high affinity to FGF2 (Leali *et al.,* 2010). It was found in mammalian models that *fgf2* is synthesized naturally in the body in five forms, via alternative translation of single mRNA (Prats *et al.,* 1988). Furthermore, it has been suggested that a complex regulatory mechanism may exist in the FGF2 signalling pathway that may be mediated by other FGFRs or by other forms of alternative splicing of mRNA (Dailey *et al.,* 2005).

We believe that our result of fgf2MO is highly reliable as the phenotype is highly specific (sudden death at somite stage) and can be rescued by *fgf2* mRNA injection. However, it is possible to confirm the phenotype using CRISPR/Cas9 mediated gene knock out. As a future research, we should generate mutant fish of *fgf2* using CRISPR/Cas9 to confirm and further characterise the phenotype.

Further research on these receptors and isoforms would be needed to clarify the mechanisms of the signalling pathway in epidermal development of the embryo. Also further clarification of apoptotic processes in epidermal tissue would be beneficial and could involve using specific antibodies for apoptotic events e.g. expression of caspase3.

Supplementary

gene marker	control			Fgf2MO		
	N	-	+	N	-	+
ntl	15	0	15	15	0	15
spt	15	0	15	15	0	15
aldh1a2	15	0	15	15	0	15
sox17	15	0	15	15	0	15
otx2	15	0	15	15	0	15
hoxb1b	15	0	15	15	0	15
P63 90% epiboly	15	0	15	15	15	0
P63 3 somite	15	0	15	15	15	0
dlx3	15	0	15	15	15	0
tfap2a	15	0	15	15	15	0

Supplementary Table 1. Number of embryos showing in situ staining, (N) number of embryos that used in experiment, (-)gene expressions were reduced by Fgf2MO, (+)gene expressions were not reduced by Fgf2MO. Images are shown in Fig. 4 and 7.

phalloidin and hoechst staining	gastrula			1 somite			3 somite			5 somite			7 somite		
	N	-	+	N	-	+	N	-	+	N	-	+	N	-	+
control	20	0	20	20	0	20	18	0	18	16	0	16	16	0	16
Fgf2MO	16	0	16	17	0	17	15	0	15	14	0	14	15	0	15

Supplementary Table 2. Number of embryos showing phalloidin and hoechst staining, (N) number of embryos, (-) negative staining, (+) positive staining. Images are shown in Fig. 5 and 8.

Results Chapter 5

Genetic and molecular mechanisms of embryonic tail development in the self-fertilizing mangrove killifish, *Kryptolebias marmoratus*

Abstract

Among vertebrates, the tail bud acts as the organizer in promoting embryonic tail development. Although many key molecules involved in tail development have been identified and characterized, interactive mechanisms of these factors are still to be understood. Here we demonstrate, for the first time, the use of a novel self-fertilizing vertebrate animal for the identification of both genetic and molecular mechanisms of embryonic development, with a particular focus on tail bud development. Using the self-fertilizing mangrove killifish, *Kryptolebias marmoratus*, we characterized two mutants, *shorttail (stl)* and *balltail (btl)*. *Stl* suppresses tail tissue development, including notochord, somite and spinal cord, whereas *btl* suppresses the tail somite and increases tail notochord development. RNA-Seq and additional morpholino and mRNA injection analyses of these mutants facilitated rapid identification and confirmation of the mutated genes, *noto* and *msgn1* in the *stl* and *btl* mutants respectively. Our data demonstrate a crucial role of *noto* in organizing all three key tissues - notochord, somite and spinal cord, in the tail and also revealed a novel interaction between the two regulatory genes, *noto* and *msgn1*. Our data also reveal an extremely efficient approach for small scale vertebrate mutagenesis and subsequent molecular characterization of specific alleles by utilizing an isogenic self-fertilizing animal model. This novel system of *K. marmoratus* mutagenesis and mutation analysis should become a very powerful and complementary system to existing model animals in identifying genetic

mechanisms of embryonic development beyond tail bud formation presented here.

Introduction

Within vertebrate species, the embryo is organized as a head, trunk and tail along the anterior to posterior axis. Although the trunk and tail consist of a common set of tissues including notochord, somite and neural tube (spinal cord), the timing and location of development of the trunk and tail have fundamental differences. For instance, in zebrafish, the trunk cell fates are specified at gastrula stage around the blastoderm margin where the dorsal-most area gives rise to notochord, lateral side to trunk somite and spinal cord (Kimmel *et al.*, 1990, Woo *et al.*, 1995, Kudoh *et al.*, 2004). At this stage, the cells for tail somite and spinal cord are maintained along the ventral side of the embryo as undifferentiated (Kudoh *et al.*, 2004). At the end of gastrula, axial mesoderm cells from the dorsal side and mesoderm/ectoderm cells from the ventro-lateral side merge to each other and form the tail bud (Kanki & Ho, 1997; Kudoh *et al.,* 2004; Row *et al.,* 2016).The tail bud contains an organizing activity that can promote development of the tail, axial and non-axial mesoderm and neural ectoderm (Row *et al.,* 2016).

In the axial and paraxial mesoderm *noto* and *msgn1* are expressed, respectively. The *noto* gene encodes a homeodomain protein Noto in mammals, and is orthologous to *flh* in zebrafish (Abdelkaleck *et al*., 2004) and *xnot-2* in *Xenopus* (Gont *et al*., 1996). Loss of *noto* function in mouse causes a defect in the posterior trunk and tail notochord, whereas in zebrafish the defect causes loss of the entire notochord (Talbot *et al*., 1995; Abdelkaleck *et al*., 2004). *Noto* is expressed in the organizer, node and prospective notochord

during gastrulation and axis development (Melby *et al*., 1996; McCann *et al*., 2012). Talbot *et al.* (1995) and Halpern *et al.* (1995) cited that in zebrafish floating head (*flh*) mutant (*noto* missing), axial mesoderm developed in to muscle instead of notochord and this fate change occurred at mid gastrulation. *Noto* null mutant mice display segmental reduction of the notochord caudal part leading to tail truncation in adult, suggesting the significant role of *noto* in tail bud morphogenesis (Mitecic *et al.*, 2010). *Noto* works to develop the notochord and repress muscle development in zebrafish (Melby *et al*., 1996), while *spt* acts to promote muscle development genes, indicating the antagonism role of *noto* with *spt* (Amacher and Kimmel, 1998). *Noto* expression is essential for anterior and posterior notochord development (Halpern *et al.*, 1995; Amacher and Kimmel, 1998). Floor plate formation is also required for *noto* function, and *noto* defection in *flh* mutant leading to floor plate disruption (Talbot *et al.*, 1995).

Mesogenin1 (*msgn1*) is involved in vertebrate somitogenesis (Sawada *et al*., 2000). The basic helix-loop-helix (bHLH) domain of *msgn1* is similar among vertebrates: the similarity in amino acid residues between zebrafish and other vertebrates such as mouse, chick and *Xenopus* are 82.4%, 80.4% and 74.5% respectively (Yoo *et al*., 2003). *Msgn1* expression is observed in zebrafish at 60% epiboly in the mesoderm and it is restricted in paraxial mesoderm at 95% epiboly (Yoo *et al*., 2003).

Msgn1 loss of function has been conducted in many vertebrates. In *Msgn1* null mutant mice, the puffed tail bud exhibited cell apoptosis causing acute disruption of posterior paraxial mesoderm and segmentation. However, the axial mesoderm and lateral mesoderm remained normal suggesting the important role of *msgn1* in the trunk paraxial mesoderm and segmentation development

(Yoon and Wold, 2000). Both *msgn1* in mammalian models and *spt* in fish (e.g. zebrafish) are necessary genes for cell movement across the midline and have similar roles in mesoderm development (Chalamalasetty *et al*., 2014). And this role is highly conserved among vertebrates (Yoon and Wold, 2000). *Msgn1* morphants in zebrafish exhibit a mild phenotype, but double morphant or mutant *msgn1*/*spt* generate enlarged tail bud and combined loss of function of *msgn1* and *spt* result in the inability to form trunk and tail muscles (Fior *et al*., 2015).

Msgn1 acts autonomously in cells to facilitate cell migration from the tail bud (Manning and Kimelman, 2015). Transplantation of labelled cells from zebrafish *spt*/*msgn1* morphants into wild type zebrafish resulted in morphant cells remaining undifferentiated in the tail bud. Conversely transplanting wild type cells in a morphant host resulted in their migration out of the tail bud. *Msgn1* and *spt* were shown to be required to form productive lamelipodia enabling the migration of mesoderm cells (Manning and Kimelman, 2015). This suggests the significant role of *masgn1* to drive the cells into paraxial mesoderm. In mouse Nowotschin *et al*. (2012) reported that *msgn1* and *tbx6* mutants have expanded tail buds - due to the accumulation of mesodermal cells. This led the authors to suggest a role for *msgn1* and *tbx6* in facilitating mesoderm cell movement from the tail bud.

Although the fundamental role of the tail bud may be conserved in all vertebrate species, there are substantial differences in embryonic morphology and size, gene duplications and expression patterns. Consequently the mechanisms by which the tail bud regulates tail tissue specification and patterning varies depending on the species observed (Kanki & Ho 1997; Di-Poï-N *et al.,* 2010*;* Finch *et al.,* 2010).

Here we introduce a new model species, the self-fertilizing mangrove killifish, *Kryptolebias marmoratus*, as a tool for studying gene functions in the tail bud. *K. marmoratus* adult fish consist of mainly self-fertilizing hermaphrodites, with smaller numbers of male fish. The hermaphrodites have great potential to increase the throughput of mutant screening as the mutated DNA sequence (allele) induced by mutagenic chemicals is inherited in individual F_1 fish in the ovotestis (ovary and testis located next to each other) (Grageda *et al.*, 2004; Sakakura *et al.*, 2006; Lee *et al.*, 2007). Therefore recessive zygotic mutant phenotypes may be observed in the F_2 embryo derived from the self-fertilizing F_1 parent. This makes the process of mutant screening one generation shorter than sexually reproducing animal models and omits the process of identifying families carrying a mutant allele, leading to quicker mutant screens using smaller numbers of fish in less laboratory space. Using the mangrove killifish, Ring's group conducted a pilot screen for zygotic lethal mutant alleles by using ENU-induced mutagenesis (Moore *et al.,* 2012), followed by a continued F3 screen to confirm zygotic lethal (old and new) and identify sterile mutant lines (Sucar *et al.*, 2016). Among these lines, we selected two mutants, R109/*shorttail (stl)* and R228/*balltail (btl)*, characterized by their unique phenotypes during tail development. In situ analysis revealed that notochord, muscle and spinal cord markers were all missing in in the tail region in the *stl* mutant, whereas in *btl*, only muscle marker was down regulated. Taking advantage of the small number of polymorphisms found in these inbred self-fertilizing animals, we needed to only sequence a small number of mutant fish embryos using one lane of RNA-seq to quickly identify the key mutations that cause the *stl* and *btl* phenotypes in the *noto* and *msgn1* respectively. In the *noto*, a point mutation was found in the C-terminal domain that substitute

conserved Arginine to Cysteine. In the *msgn1* gene, a mutation was identified in the leucine zipper domain in a conserved Isoleucine substituted to Asparagine, suggesting disruption of protein functions in these mutations. Indeed morpholinos for *noto* and *msgn1* in medaka phenocopied, the *stl* and *btl* mutant morphology. mRNAs encoding *Km_noto* or *Km_msgn1* rescued normal morphology of embryos whereas mRNAs encoding mutated form of *Km_noto* or *Km_msgn1* did not rescue the morphant phenotype. From these result we concluded that mutation in *noto* or *msgn1* is responsible for the phenotype of *stl* or *btl* respectively. We further conducted cell lineage tracing analyses by fluorescently labelling tail bud cells using Kaede fluorescent protein and found that *noto* and *msgn1* are responsible for cell movement of tail bud cells into notochord and somite respectively. Our results provide insights of evolutionary diversification of gene function, in addition to redundancy and specification that facilitate establishment of different gene functions and tissue during embryo development. This work also demonstrates the mangrove killifish as a very powerful genetic model to quickly generate mutant lines, characterize novel phenotypes, identify mutated genes, and analyze their role in embryonic development.

Results

Phenotypes of Mutations

To uncover mechanisms of tail development in the self-fertlizing *K. marmoratus*, two ENU-mutated lines, R109 and R228 (Sucar *et al.*, 2016) were analysed. R109/short tail (*stl*) exhibits reduced tail growth with characteristic narrowing at the trunk-tail junction, which can be recognized clearly at development stage 22-23 (Mourabit et al., 2011), with *stl* mutants having a shorter body compared to the wild-type (Fig. 1D,Di). R228/ball tail (*btl*) was characterized by a swollen part at the end of tail resembling a ball shape that appears hollow and, in some embryos filled with blood droplets. *Btl* mutants can be identified earlier at stage 18 (Fig. 1G, Gi). Both mutations show different phenotypes at later stages of development: in *stl* the tail becomes shorter during embryonic development and later the posterior part utterly disappears (Fig.1E, F). In contrast, in the *btl* mutants during later embryonic development the tail forms through an abnormal turn resulting in the irregular tail morphology observed (Fig. 1H, I). Both mutations are not embryonically lethal. However their death occurs within three or four days after hatching due to unknown reasons.

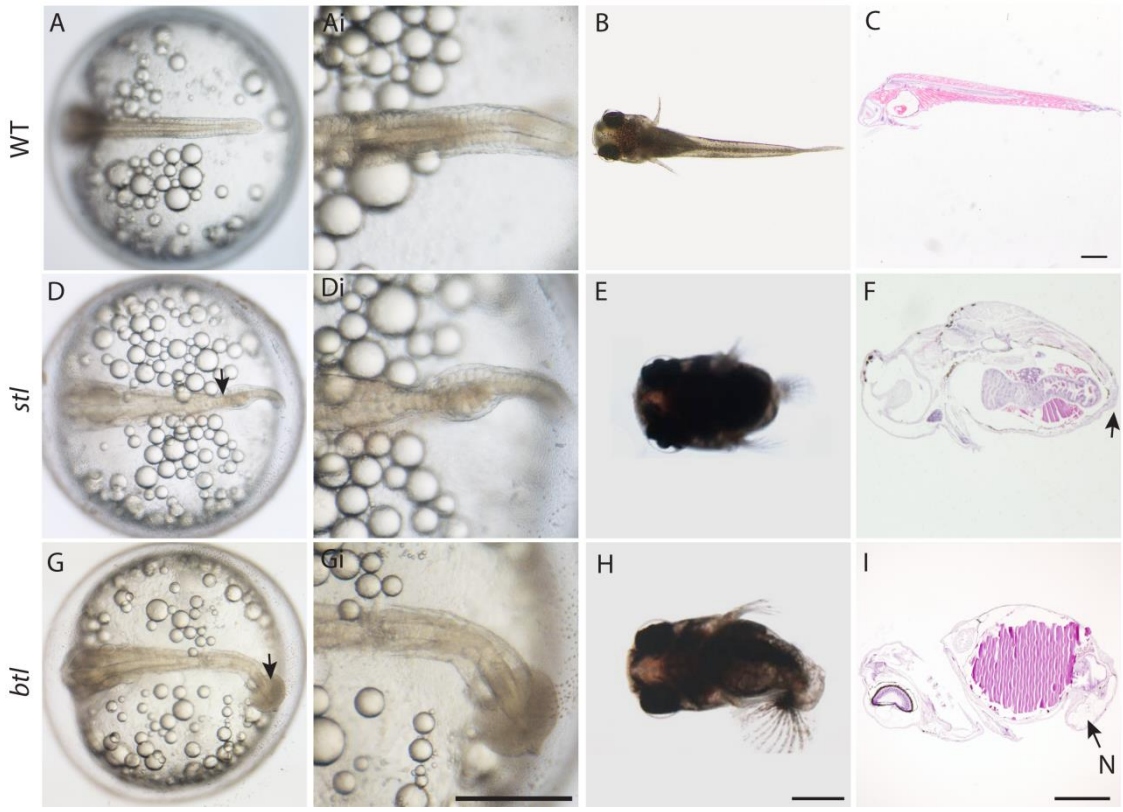

Figure 1. Morphology *of K. marmoratus* mutants, *stl* and *btl*. A-C wild type live embryos and larvae and C sagittal section in wild type larvae; D-F *stl* mutant, arrow indicates narrow region between trunk and tail showing disappearance of notochord along posterior part, F sagittal section represents *stl* mutant exhibiting tail truncation in hatched embryo. G-I *btl* mutant shows the tail malformation, arrow refers to enlarged part and I sagittal section in *btl* mutant showing notochord present (N) and disappearance of muscles in the tail. Scale bars in all images are 200µm. The scale bar for A, B, D, E, F, G is seen in H, and Ai, Di is seen in Gi. A, D, G embryos at St.23; B, C, E, F, H, I at 1day post hatching.

In situ hybridization of gene markers in tail tissues at early stages of *K. marmoratus* embryonic development

To examine the molecular mechanisms of tail developmental defects in the *stl* and *btl* mutants, four molecular markers expressed in different domains of the

tail tissue were visualized using *in situ* hybridisation (Fig. 2). In the *stl* mutant, markers for notochord (*col9a1b*), somite (*hsp90*) and spinal cord (*sox3*) were all downregulated in the tail region, but not in the trunk (Fig. 2B,E,H) suggesting a crucial role of the *stl* gene involved in the development of the major tissues in the tail. On the other hand, in the *btl* mutant, somite marker, *hsp90aa* was mainly suppressed in the tail (Fig.2F) whereas *col9a1b* was rather slightly upregulated (Fig.2C). In the *btl*, spinal cord marker, *sox3* was not downregulated (Fig. 2I). These data suggest that *btl* gene is primarily involved in cell fate specification and development of the somite. *Spt* is expressed in the tail bud especially in the paraxial domain and undifferentiated marginal area in the tail bud (Fig.2J). *Spt* expression in both *stl* and *btl* was not clearly affected (Fig. 2K, L).

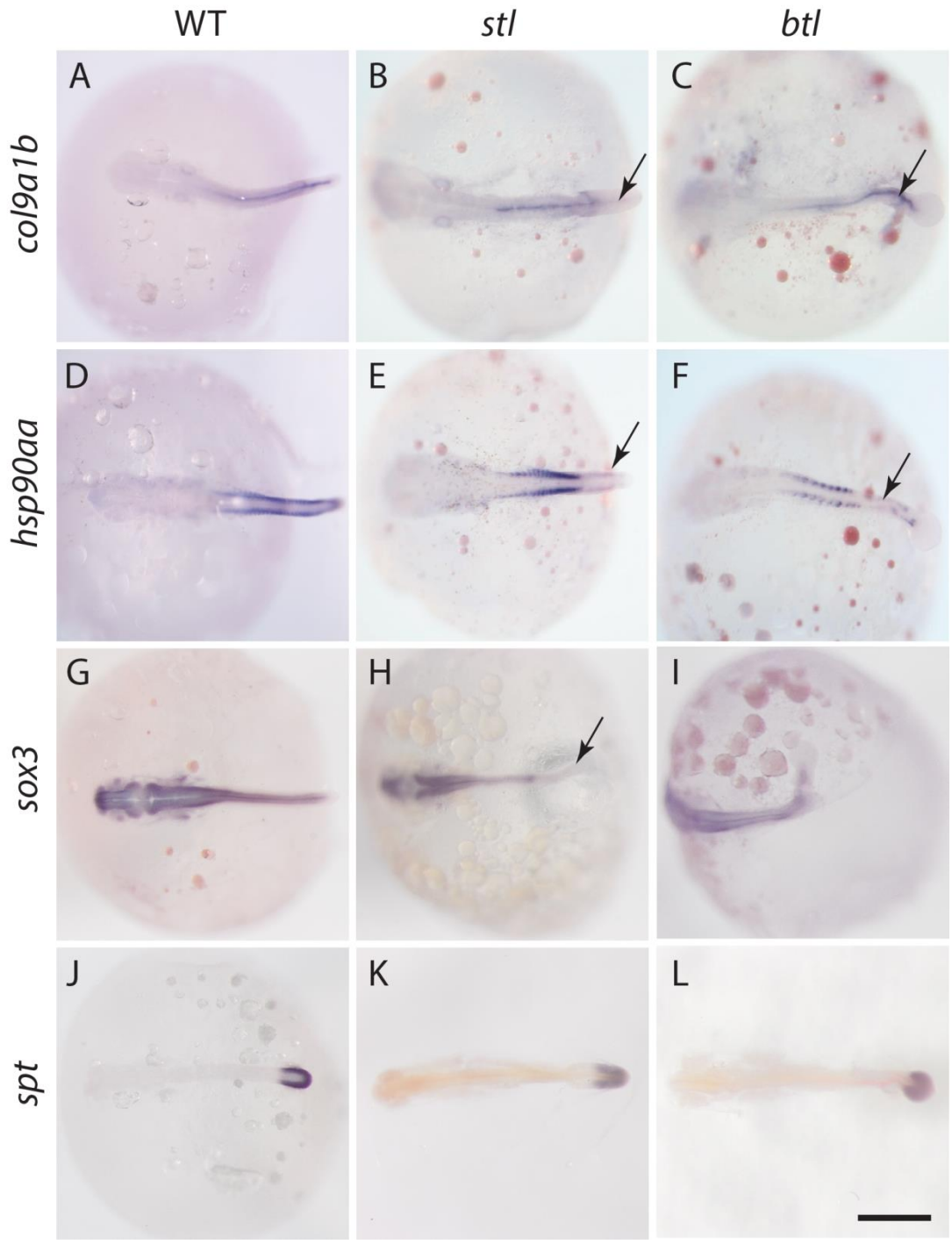

Figure 2. In situ hybridization in *K. marmoratus*. A-C, a notochord marker, *col9a1b*, D-F, a somite marker, *hsp90aa* and G-I, a spinal cord marker, *sox3*. J-L, *spt* show widely expressed in the tail bud both *stl* and *btl*. A, D, G, J, wild type, B, E, H, K *stl* mutant, and C, F, I, L, *btl* mutant. *Stl* decreases *col9a1b*, *hsp90aa* and *sox3* expression (B, E, H, arrow). *Btl* slightly expands the *col9a1b* expression domain (C arrow) whereas it reduces *hsp90aa* expression (F, arrow). Scale bar is 200μm.

Identification of the key genetic mutations underlying *stl* and *btl* mutant phenotypes

To search for the key mutations that caused the *stl* or *btl* phenotype, the protein coding sequence of the embryonically expressed genes were analysed in the mutant and sibling groups using RNA-Seq. Naturally spawned eggs were collected from the tank of the wild type, *Hon9* strain, *stl* or *btl* mutant strains. The eggs were developed to mid somite stage (st.19) when the *stl* or *btl* phenotype is obvious, and were separated into mutant or non-mutant (sibling) groups. Twenty embryos were pooled from each group (5 groups: WT, *stl*, *stl*-sibling, *btl* and *btl*-sibling). Total RNA was prepared from each pool and analysed on one lane of RNA-Seq using Illumina HiSeq2500 100bp paired end reading. According to RNA analysing data, the number of homozygous variants between the WT and mutants were 4544 for the R109/*stl* and 884 for the R228/*btl*. Among these variants, the ones which showed 0% enrichment in the WT and 100% enrichment in the *stl* and *btl* mutants were 91 and 77 respectively (in *stl* mutant, there were 4544 variants and only 91 existed in mutant embryos in 100% of cases, whereas none of these 91 variants were found in the WT; a similar approach was taken for studying the *btl* mutant). However, most of these variants show some unnatural patterns such as small number of reads from particular samples (e.g. Sibling sample or WT sample) (Table 1), suggesting these variants are most likely due to sequencing errors. To remove these unreliable variants, the variants having less than 10 reads from Sibling or WT with WT form of variant reads were eliminated, leaving only 2 and 5 variants for R109/*stl* and R228/*btl* respectively. We used a *de novo* transcriptome assembly to identify the transcripts associated with these variations and subsequently annotated them through BLASTn searches to the NCBI-nr database. Upon

annotation, we analysed the type of variations from these 2 and 5 variants and searched for the one showing a specific change in amino acid(s) sequence in a highly conserved amino acid sequence between species (e.g. zebrafish and human). Under these conditions, we identified only one variant each from R109/*stl* and R228/*btl*, *noto* and *msgn1* respectively. Fig. 3A shows the pattern of reads from the WT, R109/*stl* and R109 siblings showing the mutation in *noto* is 100% enriched in the mutant group, 19% in the sibling and 0% in the WT. Mutation in *msgn1* is 100 % enriched in the mutants, 33% in the sibling and 0% in the WT (Fig. 4A).

Noto gene in R109/*stl* shows a point mutation in the C-terminal region leading to a missense base pair transition from Cytosine to Thymine resulting in an Arginine to Cysteine amino acid change (Fig.3B). R228/*btl* also has a single missense point mutation in *msgn1* changing the amino acid from Isoleucine to Asparagine resulting from a Thymine to Adenine transversion (Fig.4B). This Isoleucine is located in a periodical Leucine/Isoleucine position of a Leucine zipper structure of the protein and therefore is expected to have a functional role in protein folding. In both *stl* and *btl* mutations, the mutated amino acid is conserved between the fish species and mammals (Fig. 3C and 4C), suggesting an indispensable role of this amino acid for the protein function. Protein analysis of lesion position in mutated *noto* showed that the lesion is located outside of the homeodomain (Fig.3D), whereas the lesion position of mutated *msgn1* is located inside the homeodomain of this gene in the Leucine zipper region (Fig.4D). We concluded that *noto* and *msgn1* were very strong candidates for mutated alleles causing the *stl* or *blt* mutant phenotypes.

A

Strain	R109	R228
Total variant (Mu vs WT, homozygous)	4544	884
100% Mu, 0% WT	91	77
At least 10 reads in Sib-WT and WT-WT	2	5
Sib-WT > Sib-Mu	2	4

B

Identity No. (bcc)	R109-WT	R109-Mu	Sib-WT	Sib-Mu	WT-WT	WT-Mu	Annotation
54721	0	20	29	7	19	0	*Kryptolebias marmoratus* homeobox protein not2-like (LOC108246077), transcript variant X2, mRNA
19900	0	3	12	4	12	0	*Kryptolebias marmoratus* transmembrane protein 110 (tmem110), mRNA

C

Identity No. (bcc)	R228-WT	R228-Mu	Sib-WT	Sib-Mu	WT-WT	WT-Mu	Annotation
12272	0	1468	59	30	82	0	*Kryptolebias marmoratus* mesogenin1 (*msgn1*), mRNA
32117	0	24	20	15	21	0	No annotation
45753	0	2	15	9	19	0	*Kryptolebias marmoratus* neuroblast differentiation-associated protein AHNAK-like (LOC108245323), mRNA
26487	0	2	12	5	20	0	No annotation

Table 1. Filtering candidate gene variants responsible for the *stl* and *btl* phenotypes.

A. From the RNA-seq total homozygous variants between the mutant and WT were selected (4544 and 884 variants for *stl* and *btl* respectively). Subsequently, 91 and 77 of variants from *stl* and *btl* were selected depending on their existence exclusively in 100% of the respective mutants. The candidates were filtered selecting the variants that have read not less than 10 in the sibling WT or WT that narrowed down to 2 and 4 variants respectively.

B. The two gene variants matched to the filtering condition from the *stl* mutant are displayed. Among these two, *noto* was identified as the key mutation for the *stl* phenotype.(i.e. mutated *noto* showed the following reads: 20 in mutated homozygous , 7 in heterozygous sibling and 0 in WT, while normal *noto* presented 19 in WT, 29 WT homozygous sibling and 0 in mutated homozygous).

C. The four variants matched to the condition from the *btl* mutant are displayed including the *msgn1* gene. Candidates in *btl* were filtered in the same way as described above.

A

	R109_Mu	R109_Sib	WT
*Noto*_WT variant	0	29	19
*Noto*_Mu variant	20	7	0
% of the mutant variant	100%	19%	0%

B

```
Km_noto(WT) 571  TGG TTC CAG AAC CGA CGC ATC AAG TGG CGC 600
                  W   F   Q   N   R   R   I   K   W   R

Km_noto(Mu) 571  TGG TTC CAG AAC CGA TGC ATC AAG TGG CGC 600
                  W   F   Q   N   R   C   I   K   W   R
```

C

```
Km_Noto 168 LASALQLTEAQVKVWFQNRRIKWRKQ 193
            LA+ L+LTE QV+VWFQNRR+K++KQ
Hs_Noto 189 LAARLKLTENQVRVWFQNRRVKYQKQ 214
```

D

Figure 3. *Stl* mutant has 100% enrichment of a mutated form of *noto*. A. frequency of the wild type and mutated form of *noto* in the wildtype *Hon9*, mutants and siblings. B. cDNA and protein sequence of *Km_noto* from the *Hon9* and *stl* mutant showing amino acid substitution from R (Arginine) 187 to C (Cysteine) (R187C). C. This Arginine is highly conserved in other vertebrate orthologues including human. D. The position of mutation located just outside of Homeodomain (HD) region in Noto protein.

A

	R228_Mu	R228_Sib	WT
*Msgn1*_WT variant	0	59	82
*Msgn1*_Mu variant	1468	30	0
% of the mutant variant	100%	33%	0%

B

```
Km_msgn1(WT)361 ACC ATT GAA TAC ATC AAC AAG CTT GCG GAC 390
                  T   I   E   Y   I   N   K   L   A   D
Km_msgn1(Mu)361 ACC ATT GAA TAC AAC AAC AAG CTT GCG GAC 390
                  T   I   E   Y   N   N   K   L   A   D
```

C

```
Km_Msgn1   75 EKMRMRSIAEALHQLRDYLPPDYSKKGQPLTKIQTLKYTIEYINKLADMLSRA 127
              EK+RMR++A+ALH LR+YLPP YS++GQPLTKIQTLKYTI+YI +L D+L+R
Hs_Msgn1  133 EKLRMRTLADALHTLRNYLPPVYSQRGQPLTKIQTLKYTIKYIGELTDLLNRG 185
```

D

Figure 4. *Btl* mutant has 100% enrichment of a mutated form of *msgn1*. A. frequency of the wild type and mutated form of *msgn1* in the wildtype Hon9, mutants and siblings. B. cDNA and protein sequence of *Km_msgn1* from the Hon9 and *btl* mutant showing amino acid substitution from I (Isoleucine) 117 to N (Asparagine). C. This Isoleucine is highly conserved in other vertebrate orthologues including human. D. The position of mutation inside of Helix loop Helix (HLH) domain in Msgn1 protein.

Blocking *noto* or *msgn1* in medaka phenocopy *stl* or *btl* respectively

To confirm that the mutation phenotypes of *K. marmoratus* resulted from missense mutant alleles of *msgn1* and *noto* in *btl* and *stl*, we planned to inject morpholinos of these genes in 1 cell stage embryos to phenocopy the mutant phenotype. However, *K. marmoratus* often hold fertilized eggs within the body and randomly release eggs to the water at varying stages of development. Therefore, it is difficult to obtain many one-cell stage embryos for morpholino

injections. To overcome this problem, we designed *msgn1* and *noto* morpholino orthologues to another killifish, medaka (*Oryzias latipes*) and injected the morpholinos into medaka embryos to phenocopy the *K. marmoratus stl and btl* mutant phenotypes. Indeed, results of morpholino injections produced morphants presenting a typical phenotype of *stl* (short tail with narrowing of the trunk-tail junction) and *btl* (ball-shaped enlarged tip of tail) (Fig. 5B, E). In addition, co-injection of mRNAs encoding *Km_msgn1* or *Km_noto* with morpholinos rescued the phenocopy (Fig. 5 C, F, H, I). To test if the mutant alleles identified in the *noto* and *msgn1* genes in the *stl* and *btl* mutants are non-functional, mRNAs containing the point mutations of *Km_noto* or *Km_msgn1* were synthesized using mMACHINE SP6 Transcription Kit (method section 8) and co-injected with their corresponding morpholinos. The mutant phenotype was not rescued in resulting embryos (Fig. 5D, G), indicating that these mutations are responsible for the *K. marmoratus stl* and *btl* mutant phenotypes.

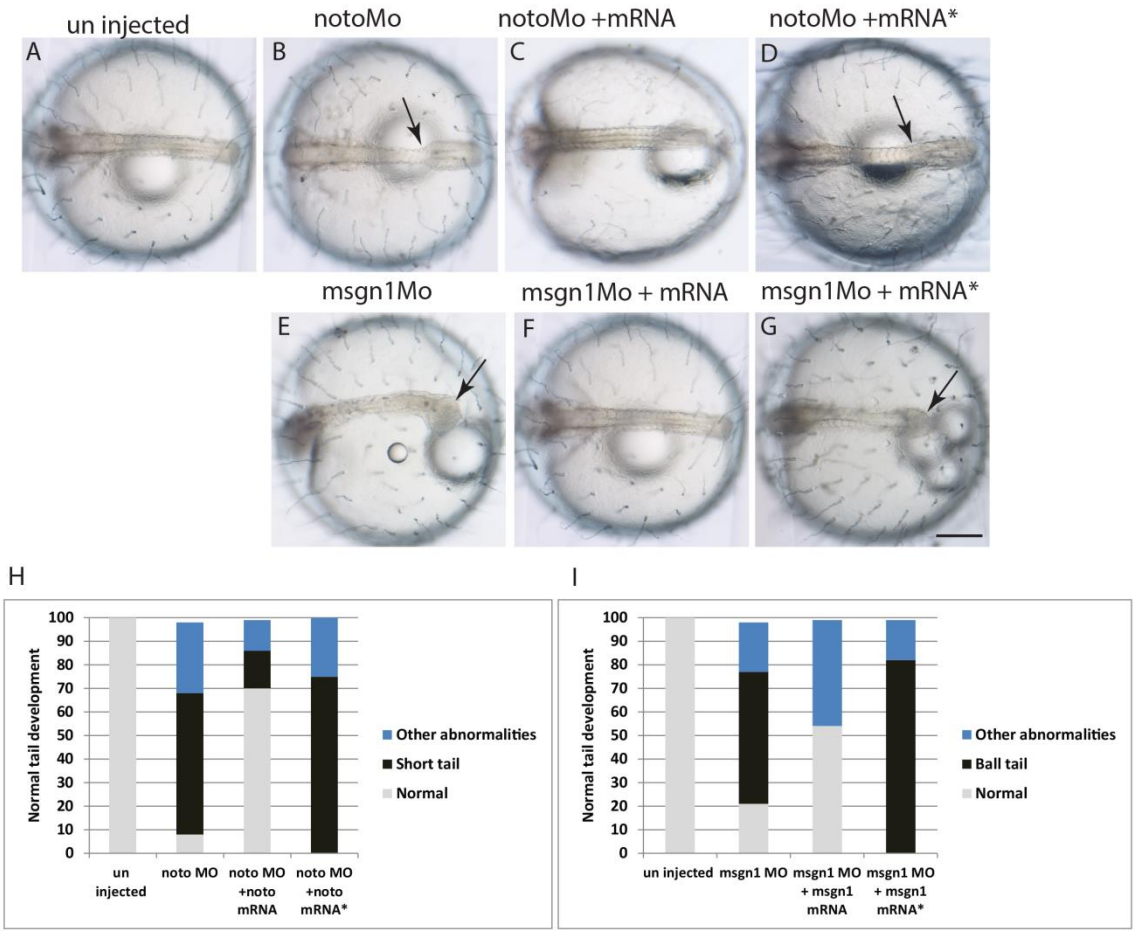

Figure 5. Medaka morphants of *noto* and *msgn1* phenocopy the mangrove killifish *stl* and *btl* mutants respectively. A. wild type medaka embryo (St.23). Medaka *noto*MO phenocopies the *stl* mutant (B) (arrow indicates the typical narrowing of the trunk-tail junction). The morphant phenotype is rescued by co-injection of the wild type *Km_noto* mRNA (C), but is not rescued by co-injection of mutated form of *Km_noto* R187C mRNA. Similarly, medaka *msgn1*MO phenocopies *bt*l mutant (E), rescued by wild type *Km_msgn1* mRNA (F) but not by a mutant form of *Km_msgn1* I117N mRNA (G). H, I, The histograms represent the ratio of rescued morphant embryos using mRNA injection. Scale bar is 200µm.

Km_Noto and *Km_msgn1* are expressed in the tail bud and reciprocally interact with each other

To examine the expression pattern of *noto* and *msgn1* in *K. marmoratus*, whole mount *in situ* hybridisation was conducted. *K. marmoratus noto* is expressed in the central part of the tail bud including newly synthesised notochord cells whereas *msgn1* is expressed in the paraxial part of the tail bud (Fig. 6A and 6D respectively). *In situ* hybridisation of *noto* in the *stl* mutant exhibited suppression of the gene, (Fig. 6B) whereas the *noto* expression was enhanced in the *btl* embryo (Fig. 6C). Similar patterns were observed for *msgn1* in situ; *msgn1* presented reduced expression in the *stl* and ectopic expression in *btl* (Fig. 6E, F respectively).

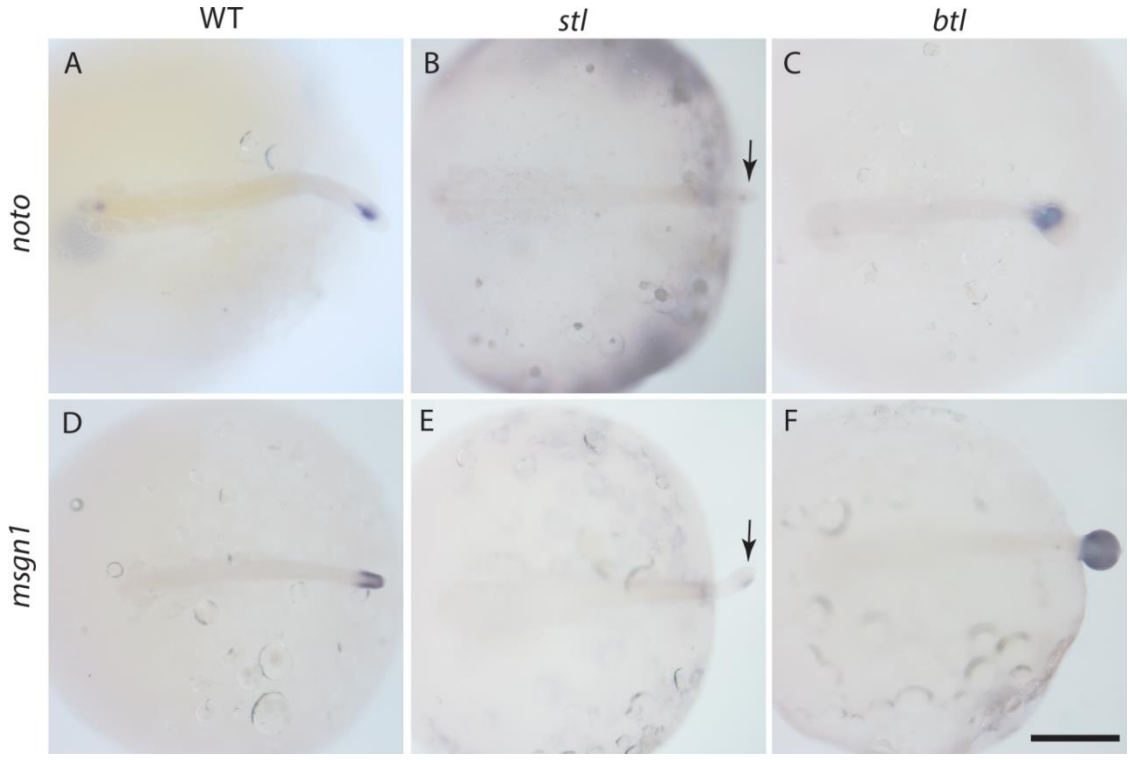

Figure 6. In situ hybridization of *noto* and *msgn1* in *K. marmoratus*. A-C, *noto* expression at St.20. D-F *msgn1* expression at St.20. A, D wild type, B, E *stl* mutant, C, F *btl* mutant embryos. Both *noto* and *msgn1* expression are suppressed in the *stl* mutant (B, E arrow). Scale bar is 200µm.

Progenitor cells of tail bud behaviour in *btl* and *stl* mutants

The mutant phenotype and gene expression data for the *stl* and *btl* mutants suggest that *noto* and *msgn1* play a crucial role in tail bud development to form axial mesoderm (notochord) and paraxial mesoderm (somite), respectively. To examine cell behaviour of the axial and paraxial part of the tail bud, we used medaka embryos and traced tail bud cell fate in the wild type and morpholino injected embryos. For labelling tail bud cells, Kaede mRNA was injected at the 1 cell stage, which made the embryo fluorescent green. At the tail bud stage, the tail bud was exposed to UV, which photo-converted these cells to become fluorescent red. As a result, the red cells in the tail bud of wild type medaka embryos gave rise to notochord and somite over the next two days (Fig. 7, A-C). In contrast, in the *noto* morphant medaka embryos, the tail bud cells failed to develop notochord and mainly distributed to the paraxial region (Fig. 7, D-F). Conversely, in the *msgn1* morphant, the tail bud cells gathered in the midline and failed to migrate to the paraxial region (Fig. 7, G-I). The *noto*/*msgn1* double MO induced ball tail similar to tail bud as seen in *msgn1* morphant but with severe failure of the tail bud cell deposition into the axial and paraxial part of the tail (Fig. 8Ai-Ci). Collectively, these data indicate that both *noto* and *msgn1* have crucial roles in cell movement and deposition in the tail bud, and therefore reciprocal interaction between these two genes determines a balanced patterning of tail containing axial and paraxial components of the tail tissues.

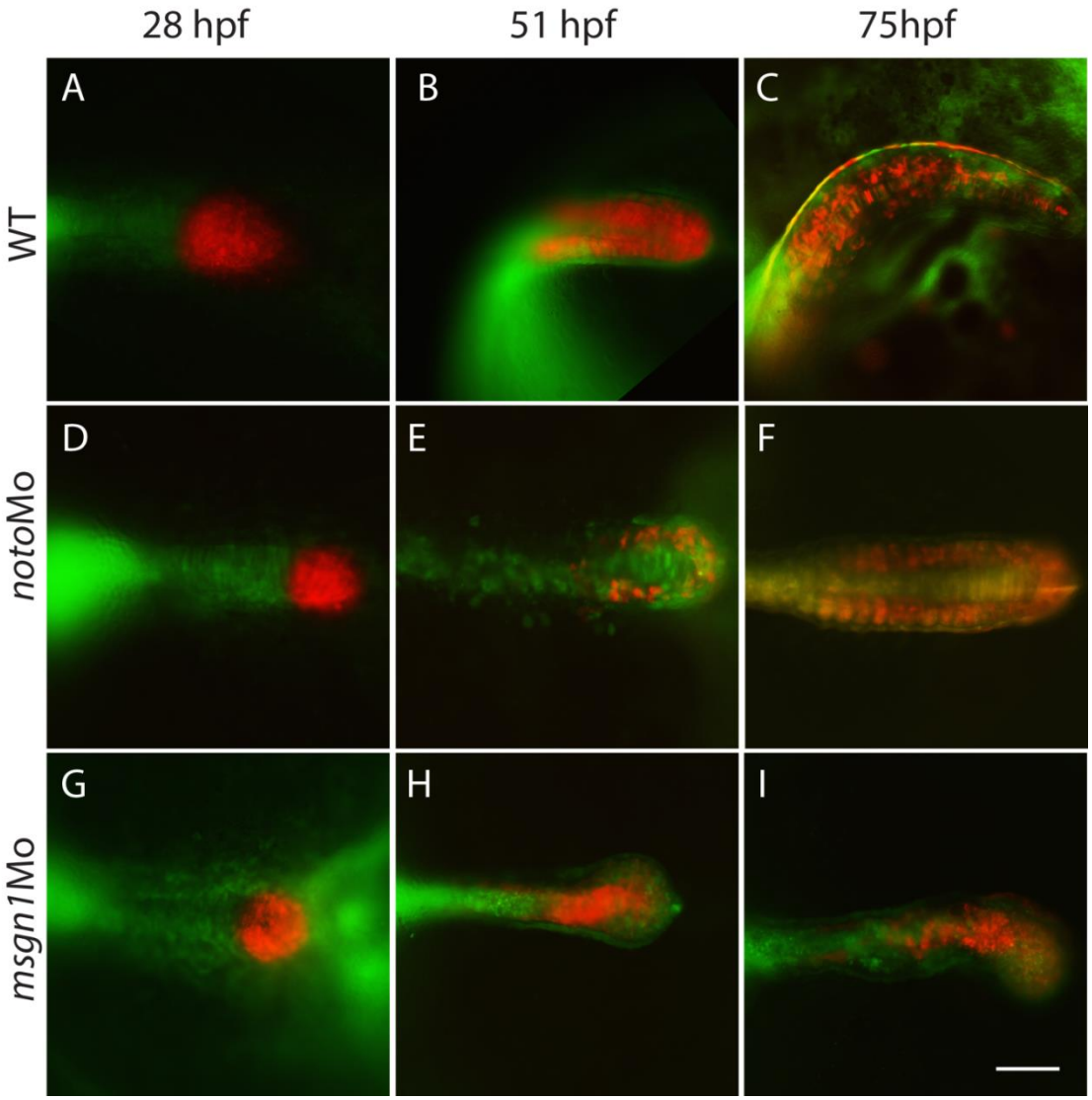

Figure 7. *Noto* and *msgn1 morphants* show specific cell migration defects in the tail bud. Medaka embryos were injected with Kaede mRNA at 1-cell stage. At 28hpf (St.19), tail bud cells were exposed with UV to activate the red-fluorescence. The cell fate of red-fluorescent cells were examined in the following stages. A-C, wild type embryo, D-F, *noto* morphant embryo, G-I, *msgn1* morphant embryo. Scale bar is 200μm.

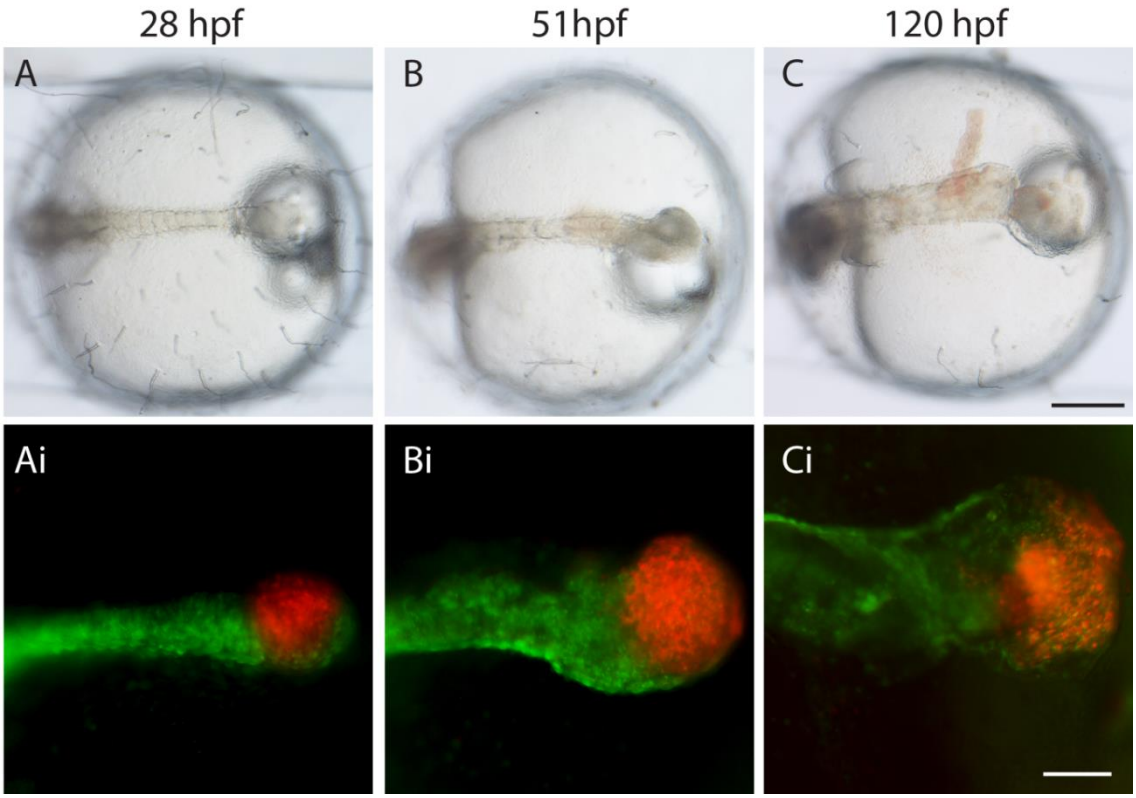

Figure 8. *Noto* and *msgn1* double morphants show loss of tail elongation. Medaka embryos were injected with Kaede mRNA at 1-cell stage. At 28hpf (St.19), tail bud cells were exposed with UV to activate the red-fluorescence. The cell fates of red-fluorescent cells were examined in the following stages. A-C, live image of the embryos. Ai-Ci: Fluorescent image of the same embryo. Scale bars are 200μm.

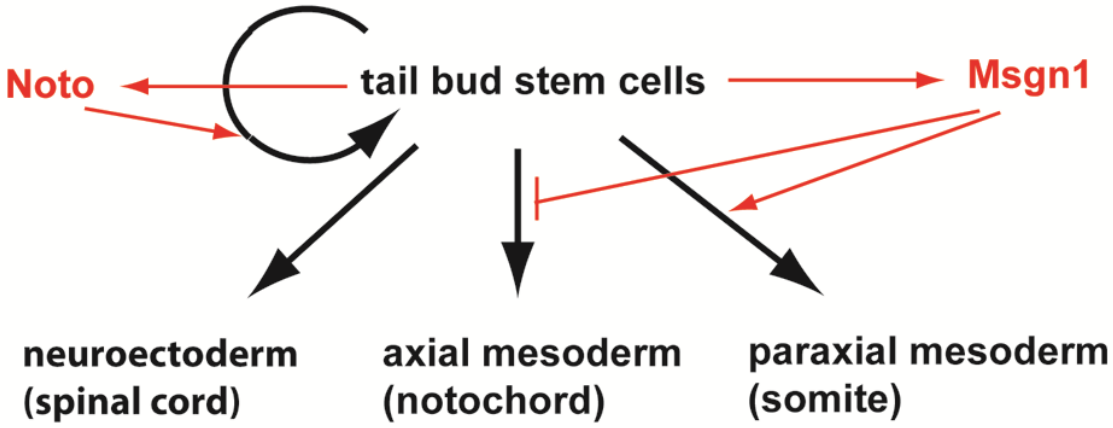

Figure 9: Proposed Model: *Noto* regulates maintenance of the tail organizer therefore a mutation in *noto* (*stl*) causes suppression of development of key tail tissues including notochord, somite and spinal cord. *Msgn1* is crucial in somite cell fate specification. There is a transition between the somite and notochord cell fate in the tail bud and therefore a mutation in *msgn1* (*btl*) causes loss of tail somites with an expansion of the tail notochord.

Discussion

Noto maintains the tail organiser activity

We demonstrate here that *stl* mutants lose gene expression for tail cell lineage specific marker genes including: *col9a1b* (notochord), *hsp90aa* (somite) and *sox3* (spinal cord). These data lead us to make two important observations: firstly, although notochord, somite and spinal cord are continuous structures from the trunk to tail, these marker gene expression patterns were primarily suppressed in the tail. This suggests that molecular and cellular mechanisms of tissue development and associated gene regulation are different between the trunk and tail. For example in zebrafish in the trunk mesoderm, both *spt* and *ntl* are express independently and both genes regulate *tbx6* which is co-expressed

with *spt* and regulates trunk mesoderm genes, but in tail mesoderm both *spt* and *tbx6* that regulate tail mesoderm genes become dependent on *ntl* function (Griffin *et al*., 1998). Secondly, the data indicate that *Noto* is the key regulator for inducing and/or maintaining the tail organiser activity that promotes tail notochord, somite and spinal cord development. The role of *noto* homologues has been investigated in several model animals including mice, *Xenopus* and zebrafish, to demonstrate *noto* plays a crucial role in both trunk and tail notochord development. (Talbot *et al.*, 1995; Halpern *et al.*, 1995; Gont *et al.*, 1996; Yamanaka *et al*., 2007; Beckers *et al.*, 2007). In zebrafish *noto* is required for notochord development along the entire body axis, while mutation in the mouse *noto* gene causes truncation disturbing caudal notochord formation (Abdelkhalek *et al*., 2004). However, from these studies, the role of *noto* in inducing other cell lineages such as somite and spinal cord was not observed. Therefore our *K. marmoratus* mutant data showed for the first time, the role of *noto* as the master gene regulating all three major tissues in the tail bud. The differences among loss of function of *noto* phenotypes between the killifish species (*K. marmoratus* and *O. latipe*s) and other model animals may be due to variations in functional redundancies between *noto* and other key regulators for notochord and other tail tissue development including *brachyury, spt, tbx6* and *msgn1*. Although *msgn1* and *spt* are both expressed in the paraxial part of the *K. marmoratus* tail bud, regulatory mechanisms of the gene expression by the *noto*-mediated tail organising activity is different: in the *stl* mutant, only the *msgn1* was suppressed (Fig. 6E) but *spt* was not (Fig. 2K). This indicates that the link between *noto* and *msgn1* is a crucial mechanism in the tail bud to develop and organise the tail paraxial mesoderm while neither effect *spt* expression posteriorly.

Msgn1 primarily regulates tail paraxial mesoderm organisation and development

The function of *msgn1* has also been studied in other model animals including *Xenopus* (Yoon *et al.*, 2000), mice (Chalamalasetti *et al.*, 2014) and zebrafish (Yabe and Takada, 2012; Fior *et al.*, 2012; Row *et al.*, 2016): These data showed its crucial role in somite (muscle) development. Null mutation in the mouse *msgn1* gene results in failure of somitogenesis, leading to absence of all tail and trunk muscles (Yoon and Wold, 2000). In the case of zebrafish, *msgn1* and *spt* are redundant in paraxial mesoderm (Yabe and Takada, 2012). Failure of somitogenesis in the absence *spt* and *msgn1* is interpreted as an inability of the cell to perform the epithelial to mesenchymal transition that is necessary for cells to reach into paraxial mesoderm (Manning and Kimelman, 2015). However, the above authors did not show a differential role of *msgn1* between the trunk and tail. Our *in situ* data from the *K. marmoratus btl* mutant showed a crucial role for *msgn1* in inducing the somite gene expression (*hsp90aa*) in the tail whereas the *hsp90aa* expression was not clearly suppressed in the trunk, consistent with our observation that *msgn1* is not expressed in the trunk. Likewise, in the *btl* mutant, expression of notochord marker (*col9a1b)* was expanded only in the tail, but not in trunk (Fig. 2B, C). These data suggest that the role of the *msgn1* is particularly important in the tail bud region for specifying paraxial mesoderm cell fate, but may have a more redundant role in the trunk paraxial mesoderm in *K. marmoratus*. It is also worth noting that *msgn1* gene knock down does not show a ball tail phenotype in the zebrafish. The phenotype of *msgn1* loss of function is very mild in zebrafish compared with the one in the mangrove killifish and medaka. As discussed in the *noto* section above, the differential phenotypes observed in tail regulatory (loss of function)

genes may be due to different variations of redundancies to other regulatory genes. For example, in tail paraxial mesoderm development, functional synergism and redundancy between *msgn1*, *txb16* and *spt* are possibly crucial (Yabe and Takada, 2012; Fior *et al.*, 2012). Therefore, the differential balance and level of redundancies between these factors may change the relative contribution of each factor during tail paraxial mesoderm development.

Noto **and** ***msgn1*** **are crucial in the migration and deposition of the tail bud cells to form somite and notochord respectively**

Although there is an apparent epistatic relationship between the *noto* and *msgn1* genes, they may have independent and primary roles to regulate cell migration and localisation of the notochord and somite cells, respectively (Chalamalasetti *et al.*, 2014; Yamanaka *et al.*, 2007). We labelled the tail bud cells at the tail bud stage using Kaede fluorescent protein and traced the tail bud cell fates in the control, *noto*MO, *msgn*MO and double MO morphants. The data show specific loss of migratory cells toward notochord or muscle in the *noto*MO and *msgn1*MO, respectively, indicating a crucial role of *noto* and *msgn1* in cell movement and localisation. *Msgn1* role for cell migration into paraxial mesoderm in the mangrove killifish consistent with the function of *msgn1* and *spt* together in zebrafish in grant the progenitor cells to migrate anteriorly from tail. Although *noto*MO cells can still migrate to the somite position, the gene expression for the tail somite was suppressed (Fig. 2E) suggesting *noto* has dual roles in the tail bud, maintaining the tail bud organiser activity to induce key tissues in the tail and at the same time, promoting the tail bud cells to migrate toward and/or along the midline of the tail.

Our proposed model - Function of *noto* and *msgn1* in the tail bud

We propose a model of action of *noto and msgn1* in the tail bud (Fig. 9). Our data from the *stl* mutant indicates that *noto* is crucial in maintaining the tail organising activity: Without the activity, notochord, somite and neural tube (spinal cord) are lost specifically in the tail (Fig. 2). This activity might involve maintaining undifferentiated stem cell state and/or renewing these cells with enhancing cell proliferation. *Msgn1* expression is also under the control of this tail organising activity of *noto* therefore *msgn1* expression is suppressed in the *stl* mutant as demonstrated (Fig. 6E). In turn, *msgn1* positively regulates paraxial mesoderm development via regulation of cell movement and lineage specific gene expression. At the same time, *msgn1* suppresses notochord cell fates in some tail bud cells therefore; the *btl* mutant has expanded notochord marker expression in the posterior part (Fig. 2C).

***K. marmoratus* as a model for mutagenesis and associated gene analyses**

This is the first report using *K. marmoratus* as a model for mutant and associated gene analyses. *K. marmoratus* is a self-fertilizing fish. Since mutagenized hermaphrodites give rise to both oocyte and sperm within the same body, the generation of homozygous mutants from single hermaphroditic lineages does not require large amounts of labour, facilitating quick generational screening and simple maintenance of the mutant fish lines in limited space compared with zebrafish and medaka. Here, we applied a single lane of RNA-Seq, including wild type, homozygous *stl*, *btl* mutants and heterozygous siblings, using a simple bioinformatics pipeline for narrowing down the mutations to identify the mutated gene(s) for these two mutants (Fig. 3, 4). The success of such a simple sequencing strategy to identify the key mutation(s) is

largely due to the character of the inbred mangrove killifish genome (isogeny). For example, the highly isogenic *Hon9* strain, from over 20 years of inbreeding in the laboratory, exhibits 99.97% homozygosity of single nucleotide polymorphisms by next generation rad-tag sequencing (Ring, unpublished data). Consequently we only identified a small handful of variants as the candidate causes of mutations (2 and 5 for *stl* and *btl,* respectively, as mentioned above). Therefore the method that we applied here for identifying mutations would be highly applicable for future research into other mutants generated in this vertebrate model. In particular, forward genetics in this species would become powerful when it's applied toward identifying parental effect genes. In sexually reproducing fish, parental-effect mutant screens require four generations of screening, and maintenance of large numbers of fish until the completion of the screening process, making it difficult to screen for mutants at saturation levels (Pelegri and Mullins, 2011). However, by using this self-fertilizing fish, the screening process can be reduced by one generation and therefore large scale screening is possible (Sucar *et al.*, 2016). Although it is difficult to obtain many 1-cell stages *K. marmoratus* embryos due to internal self-fertilization, we showed here that it is possible to use another killifish (medaka) to confirm mutants by morpholino and mRNA injection analyses. Therefore the novel approach demonstrated here for identifying and analysing mutants and mutated genes would open an interesting possibility of further gene discovery and analyses in developmental biology.

Chapter 6: General Discussion

General discussion

From the results of the three chapters, I have widely investigated the mechanisms of early embryonic development using some key model fish species including zebrafish, medaka and the mangrove killifish.

I show that null mutation of the same gene in different fish species can show different effects, which might be due to different gene duplications, different levels of redundancy in gene functions, different body size, shape and timing of embryo development. I used several methods to investigate gene functions including mutant analyses, morpholino, mRNA over expression, and application of chemical inhibitors. My results indicate that it is important to use several different model species to investigate a gene function in embryo development.

In this project, I have used the most appropriate model species for each aspect of development studied and applied a variety of different experimental methods to investigate gene function in early development focusing in particular on the blastula, gastrula to the early somitogenesis stages when the basic cell lineages are determined by a combination of key gene functions.

1- Early stage of teleost development

The development of teleost embryos occurs from the cleavage stage followed by the blastula, gastrula, somitogenesis and organogenesis stages to form the head, trunk and tail. The initial steps of development are regulated by maternally supplied molecules from the cleavage to early blastula stage. At mid blastula stage, zygotic gene expression occurs (MBT/MZT) when the embryonic transcription starts and generates mRNAs. Before the MBT/MZT, embryonic development is regulated by the maternally supplied factors such as maternal

mRNAs and proteins. Therefore to learn the gene functions regulating embryonic development, it is important to learn the function of both maternally supplied signalling molecules and zygotically synthesised molecules. Although the functions of zygotically expressed signalling molecules have been studied extensively, the studies on the maternal contribution of the signalling molecules are still limited. In the first and second result chapters, I analysed both maternal and zygotic function of signalling molecules, focusing on the FGF signalling pathway and examined the stage-specific roles of this signalling in early body patterning and cell fate specification.

2- FGF signalling is required at pre-MZT stage to give competence for cells specification post-MZT

I found an important role of the FGF pathway at the pre-MZT stage, which may be explained by the induction of competence for neural cell fate specification, effected globally through chromatin modification via histone methylation. Methylation of H3K36 or H3K4 histone turns on genes through activation of transcriptional sites (Barski *et al.,* 2007; Morris *et al.,* 2007). I found that blocking FGF by the chemical inhibitor SU5402 at the pre-MZT stage caused gene silencing in a large number of genes at early post-MZT stage.

Embryo development and patterning start from the cleavage stage. At this stage, zygotic transcription is silent. However, I discovered that maternal signalling via FGF already regulates development and patterning. I propose that FGF signalling is a vital activity in the development of the embryo that initiates at the pre-MZT stage and continues at the zygotic stage.

I found a novel role for FGF signalling (pre-MZT) in regulating histone methylation. My data suggest that this action is required for cell competency

and subsequent acquisition of the inductive signals post MZT that induce neural tissue subsequently (Chapter 3, Figure 5). Competence is required for the stem cells to be able to receive tissue inductive signals. For example, Pre-MZT FGF signalling is required for zygotic FGF or Chordin to stimulate neural gene expression subsequently (Stern, 2005).

Our understanding is that FGF is important for H3K4 and H3K36 tri-methylation before or around MZT, but it is still unknown if this occurs at pre-MZT or post-MZT or in both. This significant role of pre-MZT FGF in regulating post-MZT gene expression at late blastula stage (dome stage) and during neural induction (gastrula stage) has been proved since these stages of development were inhibited by pre-MZT SU5402 treatment. There is a time gap (0-3hpf) between active pre-MZT FGF signalling possibly started at the early embryo stage (one cell stage) and the onset of the downstream gene expression at post-MZT stages around sphere to dome stage.

In future studies, it will be important to elucidate the molecular link between FGF and Histone modification. It is likely that FGF activates MapK to trigger this epigenetic regulation. It can be proven that MapK is a key downstream molecule of maternal FGF through loss and gain of function of MapK (Erk). Loss of function of MapK can be achieved by using Erk inhibitor (see Nissan *et al.*, 2013) or Erk morpholino. Gain of function of MapK (Erk) can also be achieved by overexpressing an activated mutant form of the Erk (Dailey *et al.*, 2005). By testing the gain and loss of function of MapK on histone methylation, it can be examined if MapK is involved in the histone methylation. Subsequently, the change in the histone methylation could open the chromatin and enable the recruitment of transcription factors (TFs) (e.g. Pou5f3, Nanog, Klf5 and Sox2) to

the gene regulatory domains. Chromatin immunoprecipitation sequencing (Chip-seq) is one of the more accurate technologies for measuring TF-DNA binding sites of genes (Ouyang *et al*., 2009). Nanog, Pou5f3 and Sox2 are major transcription factors that are involved in maintaining pluripotency during MZT (Lee *et al*., 2013). In zebrafish, as in mammalian models, Pou5f3, SoxB1 and Nanog are ubiquitously expressed during maternal zygotic transition (MZT). Chip-seq has been performed to investigate Pou5f3 and Sox2 chromatin binding in zebrafish, and more than 100 genes have been shown to be activated by Pou5f3 and Sox2, with co-occupancy of Nanog, indicating a significant role for Pou5f3 and Sox2 in embryonic regulatory pathways (Leichsenring *et al*., 2013).

To test these factors associated with stem cell regulation and histone modification, we could analyse the correlation of TFs and histone methylation using chromatin immunoprecipitation sequencing (ChIP-seq) with specific antibodies for the TFs and methylated histone (Leichsenring *et al*., 2013, Vastenhouw *et al.*, 2010). This method can detect the H3K4me3 and/or TFs binding to DNA in a stage specific manner around MZT, enabling us to confirm their role in adding a competency to the cells for neural induction. It would be possible to test the Chip-seq of H3K4me3 and TFs in the normal development with time series and with SU5402 treated embryos.

Although I discovered that maternal FGF pathway is linked to the histone modification, the mechanism by which the pathway alters the histone is still not known. The histone methylation is mediated by many methylases and demethylases (Shi *et al*., 2004). In general, histone methylation of H3K4 and H3K36 link to promoter/enhancer activity and gene expression respectively,

whereas methylation of H3K9 and H3K27 is associated with gene silencing (Peterson and Laniel, 2004). Histone methylation is performed through nuclear receptor binding SET domain (NSD) proteins that comprise of members belonging to NSD families such as NSD1, NSD2, NSD3, SETD1 and SETD2 (Morishita *et al*., 2014). H3K36me3, for instance, is methylated by the specific chromatin activator SETD2 that is encoded by the *setd2* gene (Kouzarides, 2007). Therefore, it would be interesting to examine the potential contribution of different methylase and demethylase enzymes in mediating the FGF pathway. To test this possibility, we could knock down genes encoding these enzymes, such as *setd2,* and examine the competence for neural induction using the *in situ* markers that we used in this project.

3- FGF2 signalling is vital for the gastrula to somite stage embryo

In the Chapter 4, the study has addressed the function of *fgf2* at gastrula to early somite stages of development in zebrafish. Here, *fgf2* has been studied in different aspects from many other studies previously reported: Many of these investigations have focussed on the role of *fgf2* in wound healing and angiogenesis in the mouse and cell culture systems (Pintucci *et al.,* 2002). However, limited investigations have been carried out on fish concerning *fgf2* function at early stages of development, except Arrington *et al* (2013) who studied the role of *fgf2* in the forerunner cell that is important for asymmetries in the orientation of organs during development in zebrafish. In Chapter 4 I discovered a novel function of *fgf2* in epidermis differentiation that is different from other members of the FGF gene family being involved in neural induction or mesoderm induction (Maroon *et al*., 2002; Rogers *et al*., 2011). From previous studies our understanding is that FGFR1 is a receptor for many FGF

gene family members such as *fgf2, fgf3*, *fgf8* and *fgf24*. Among these, *fgf3*, *fgf8* and *fgf24* are involved in neural-ectoderm and mesoderm induction: for example these *fgfs* are expressed in the germ ring and in the embryonic shield, and can induce posterior neural tissue in the adjacent vegetal ectoderm (Koshida *et al.,* 1998, Kudoh *et al*., 2004). In addition, *fgf8* and *fgf24* are co-expressed in the early mesoderm and are required for posterior mesoderm development (Draper *et al.,* 2003).

My results in the chapter 3 and 4 revealed a complexity of the FGF/FGFR signalling pathway. In Chapter 3, I showed that blocking FGFR1 via the chemical inhibitor SU5402 suppressed neural induction by concealing neural gene expression (e.g. *sox3* and *hoxb1b*), conversely FGFR1 inhibition induced epidermis induction (e.g. *p63*). However in Chapter 4, an involvement of *fgf2* in epidermis development was discovered via the *fgf2*MO (morpholino) experiment. If FGF2 signalling is mediated by FGFR1, the FGFR1 inhibitor SU5402 would be expected to suppress FGF2 function. But in the SU-treaded embryos, epidermis marker *p63* was not suppressed but rather over-expressed. In contrast, in the *fgf2*MO injected embryos, *p63* and other epidermis marker genes were suppressed. Therefore it is still unclear if *fgf2* was repressed when FGFR1 was blocked. These data suggest that there are different signalling pathways including different receptors (e.g. FGFR2, R3 and R4) involved in FGF2 signalling for epidermis development.

At the gastrula stage, many different signals specify cell fate and body patterning. *Fgf2* blocking showed that epidermal cell specification was changed and caused embryonic lethality at the somite stage. It is reported by other authors that *fgf2* is a pleiotropic gene, affecting cell growth, differentiation and

migration, through binding to receptors (FGFR1, FGFR2 and FGFR3) on the cell surface (Bailly *et al.*, 2000; Bansal *et al*., 2003; Quarto *et al.*, 2005). In zebrafish Arrington *et al*., (2013) cited the role of *fgf2* for left-right pattering during early embryogenesis. In other animal models such as the mouse for instance *fgf2* has important functions in cartilage and bone differentiation (Montero *et al.*, 2000) and limb bud development (Webb *et al*., 1997). These data together illustrate the multifunction of *fgf2* at different stages of embryonic development. A gene function can be changed according the stage of development or condition of cells. Substitutional splicing in FGFR also creates variance in receptor binding activation (Dailey *et al.,* 2005). This can be one of many reasons that lead to contrasting FGFR gene function in different cells. Further studies are required to discover the sophisticated signalling pathways of FGF during the different stages of embryonic development.

Future research can be directed by ATAC-seq using the *fgf2*MO embryos. This technique would provide a list of potential cis elements regulated by FGF2. Particularly the cis elements located in the epidermis genes, *p63, AP2* and *dlx3* are of interest. It would be interesting to check the three major pathways; Map kinase pathway, IP3 pathway and PI3kinase pathway, to examine which pathways mediate FGF2 signalling and epidermis development. Future research can be targeted on enzymes located downstream of FGF pathways, using antagonist protein for example by inhibition of phosphatidylinositol 3-kinase (PI3k)-AKT using LY294002 (Bondar *et al*., 2002) or by inhibition the catalytic activity of p21-activated kinase (PAK) using inhibitors like CEP-1343 (Crawford *et al*., 2012). Further work is also required to understand which receptor mediates the novel function of *fgf2*. This can be tested through

Knockout or knockdown of the FGFRs (*fgfr1*, *fgfr2*, *fgfr3* and *fgfr4*) as a single or double knockout/knockdown.

4- Self-fertilising mangrove killifish as a novel genetic model species

I further extended my research on early embryonic patterning using a novel model fish species, *K. marmoratus*, because of the ability of this species for self-fertilising that facilitates the creation of mutants in a relatively short time. I obtained very interesting mutants from Ring's lab in Valdosta state University showing abnormality in early patterning of the tail bud development. To investigate the tail bud function, I analysed these tail mutants using *K. marmoratus*. *K. marmoratus* is a novel and powerful tool that may allow us to discover new gene functions which have not been discernible in other animals. We suspected the mutated genes in these mutants act downstream of FGF signalling, which is the key factor for the tail bud formation. FGF signalling is important for tail and trunk development involving formation of axial and paraxial mesoderm (Amaya *et al.,* 1993; Dorey and Amaya, 2010). FGF signalling contributes to maintenance of the genes that express in tail bud and are induced through undifferentiated mesoderm in the germ ring induction (Griffien *et al.,* 1995). Using RNA-seq and bioinformatics analysis, we have discovered that the null mutants: *ball tail* and *short tail* have specific mutations in the *msgn1* and *noto* gene respectively. These genes encode transcription factors being involved in the mesoderm development (Yabe and Takada, 2012; Halpern *et al*., 1995). My study discovered differences in the function of these genes in *K. marmoratus* compared with what has been described in zebrafish, possibly because of different levels of gene duplication and redundancy between these animal models. Through this finding, I conclude that more studies on new

models are required to investigate diversities of a gene function more deeply and comprehensively. RNA-seq has previously been used to identify mutations in zebrafish. This approach (e.g. Mutation Mapping Analysis Pipeline for Pooled RNA-seq (MMAPPR)) is highly applicable organisms that have comprehensive annotation of their transcriptome, such as zebrafish. However, it is important to recognise that RNA-seq methods may be inappropriate if there are incorrectly annotated or missing genes in the reference transcriptome for a given developmental time point. In such cases these methods will be unable to identify mutated genes in pooled samples collected after or before their expression time (Hill *et al*., 2013). In current study, due to a lack of polymorphisms in the highly inbred mangrove killifish, identification of mutated DNA sequence was extremely straight forward, and therefore the mapping strategy using MMAPPR was not needed.

Medaka has been used in phenocopying the *btl* and *stl* mutation phenotypes using morpholinos and can successfully produce *btl* and *stl* phenotypes similar to those found in K. marmoratus. Furthermore, the rescue of the morphant phenotypes using mRNA injection was also effective in recovery of the wild type morphology. My data show that these genes are greatly conserved between *K. marmoratus* and medaka.

Using Kaede mRNA injection, cell motility of tail-progenitor cells has been examined to analyse the role of genes in driving stem cells to migrate to the domain of differentiation. Our result showed that *msgn1* and *noto* have significant roles in regulating cell movement in the tail bud of the *K. marmoratus*. This is revealed by cell labelling with Kaede in the tail bud, which indicated the inability of stem cells to translocate in tail paraxial mesoderm to

create somites in embryos lacking *msgn1* (*btl*). Embryos lacking *noto* (*stl*) stem cells in the tail bud failed to translocate into axial mesoderm to differentiate the notochord.

5- Advantages and limitations of pharmacological agents

Gene knock down using morpholinos may have side effects, for instance loss of gene function can have off-target effects by blocking other genes or causing partial inhibition and resulting in non-specific phenotypes (Eisen and Smith, 2008). Therefore successful use of mopholinos requires the use of multiple MOs (including control morpholinos), and the rescue of abnormal phenotypes by supplying WT product and/or by examining protein expression.

Recently Staininer's group reported that mutated gene/mRNA can activate expression of redundant gene(s) and compensate/weaken a mutant phenotype (Rossi *et al*., 2015). Considering these findings, it would be ideal to conduct both MO and mutant analyses and compare the resulting phenotypes, in order to specify gene function.

In our case, we confirmed that the effect of morpholinos in both zebrafish *fgf2* and medaka *noto* and *msgn1* are specific, via phenotypic rescue by mRNA injection. In zebrafish injection of *fgf2* mRNA achieved statistically significant rescue. And in medaka knock down of *noto* and *msgn1* were identical to *stl* and *btl* mangrove killifish respectively. Currently more specific gene knock out such as CRISPR Cas9 must be considered for making CRISPR mutants in FGF2 zebrafish and *stl* and *btl* medaka. Control morpholinos also should be used in morpholino experiments under standardised conditions. Despite pharmacological agents (e.g. specific chemical inhibitors) is being designed to have specific molecular targets (e.g. proteins, receptors, enzymes etc.), these

agents may also have off-target effects. For example SU5402 can be used for *fgfr1* receptor specific tyrosine kinase, but it is also has effect on *fgfr3* phosphorylation and also inhibits vascular endothelial growth factor (VEGF) and PDGR (Mohamadi *et al*., 1997, Fong *et al*., 1999). In addition the result of treatment can be varying depending on the concentration of inhibitor and the time of exposure. In this research, to confirm crucial role of the FGF signalling pathway, result of SU5402 was repeated through another FGFR1 specific inhibitor PD173074 and confirmed morphological and gene expression changes. In addition, dominant negative FGFR1, XFD was overexpressed which also showed consistent abnormalities in morphology and marker gene expression (Fig.1 and 2 chapter 3).

6- Advantages and disadvantages of different fish models in studying gene functions

Fish in genetic experiments have contributed to the diagnosis and understanding of many human diseases. Most human genes have orthologous genes in fishes (e.g. zebrafish) and these genes are mostly expressed in similar ways (Lardelli, 2014). Large scale mutation screening in different animal models has enabled mechanistic understanding of a variety of genetic diseases in humans (Lieschke and Currie, 2007). Three fish models (zebrafish, mangrove killifish and medaka) were used in my research to study gene function. Some advantages and disadvantages surrounding these models lead me to use a certain model in specific experiments in preference to the others.

Zebrafish is an excellent model in developmental biology study (Veldman and Lin, 2008). It is small in size, easy to maintain in laboratory condition, spawns daily producing many one cell stage eggs, larvae begin to hatch two days post

fertilization which enables time to conduct some experiment post hatching (before external feeding), many transgenic fish and mutants, its genome is fully annotated and several large scale genetic screening studies have been carried out in zebrafish. Negative points in this model also are included such as the large genome size (1.421GB) and genome duplication, leading to a high level of gene redundancy. This presents some difficulties in effectively identifying phenotypes from the loss of function of genes. For example, mild phenotype can be obtained through a gene mutation, versus other models that represent severe phenotypes (i.e. *msgn1* loss of function in mouse or in mangrove killifish generates much severer phenotypes than the one in zebrafish (Yabe and Takada, 2012).

Medaka also possesses significant features that enable scientists to use it in genetic studies. It has a small body size like zebrafish and requires a low cost for maintaining in a laboratory condition. It has a smaller genome size (800MB) and a short generation time. These are all advantageous as a model for mutant and morphant analyses. Medaka shows a severe phenotype in *msgn1* mutant mimicking mangrove killifish *msgn1* mutant (*btl*). However, some shortcomings include: a rigid chorion, which confronts the dechorionation process that is required specific methods of treatment. In addition, the presence of hair surrounding their chorion and many yolk droplets reduce the visibility of embryo becoming an obstacle for fluorescent imaging.

Mangrove killifish has a relatively smaller genome size as a vertebrate model (680MB) (Rhee *et al*., 2017). Using animal models with smaller genome size and gene numbers like mangrove killifish, it is possible to see more enhanced mutant phenotype and to learn gene function in development. It is also possible

that gene function and redundancy changes in each evolutionary lineage due to differences in life history, morphology, size and other physiological features. Therefore applying mutagenesis and mutant analyses to other animal species is required for us to understand gene function in embryo development. Nevertheless, there are some disadvantages. For instance, unlike zebrafish, mangrove killifish produces low amount of broods and the majority of eggs are laid at different stages of development. This difficulty stands as an obstacle in gene knockdown or rescue experiments that are applied on embryos at early stages of development. In spite of these shortcomings, mangrove killifish has achieved great success in mutation screening and understanding the relationship between the genes its function.

Mangrove killifish has been reported as a potential new model for molecular and developmental studies (i.e. Lee *et al.,* 2008; Tatarenkov *et al.,* 2010; Mourabit *et al.,* 2011; Kelley *et al.,* 2012). The most important characteristic of this model is self-fertilization. Generation of genetic mutants is normally a time consuming processes involving mutagenesis, raising generations and testing phenotypes. However, the self-fertilising ability allows quick and small space mutant screening and maintenance: In sexually reproducing animals such as zebrafish and medaka, to generate genetic mutants using a chemical mutagen (e.g. ENU), the adult fish is mutagenized (founder/F0). The offspring (F1) are carriers of the mutation as a heterozygous form. All F2 siblings from the same F1 parent need to be raised as a group in an individual tank. When The F2 fish grow up to adult, the fish are in-crossed (within the siblings) to generate homozygous mutant embryos (F3). In contrast, in the self-fertilising mangrove killifish, the individual F1 fish has the same mutation in the ovary and testis and can lay homozygous mutant embryo at F2 generation (one generation earlier than two-

sex animal models) without laborious pair-wise crossing of sibling fishes, making the process of mutant generation and isolation quicker with smaller space and labour requirements (Moore *et al*., 2012).

In future research, it would be interesting to screen for maternal effect mutants. Screening of these mutants requires one generation longer (i.e. to the F3 generation in zebrafish and medaka), making it costly to do this work in these species. Because of the difficulty, the maternal effect mutants have not been screened on a large scale yet (Pelegri and Mullins, 2011). By using the mangrove killifish, large scale maternal effect mutant screening would be feasible. These mutants are mainly the mutants of genes involved in the early development at pre-MZT to early post-MZT stage. Therefore it is possible that these maternal effect mutants may include some gene mutations involved in the maternal FGF signalling pathway and chromatin modification. Maternal effects may also include the key molecular machinery that directly regulates the MBT/MZT. Therefore future research on such maternal effect mutant screening using the mangrove killifish would be a very important project as an extension of the current project.

In addition to easing the generation of mutants, there is another crucial character of the mangrove killifish. It is also easy to identify genetic mutations from the isolated mutant fish. Many generations kept in the lab from self-fertilizing individuals, which are highly inbred, provide a low level of polymorphisms in progeny. This feature that is unparalleled in other vertebrates has made mangrove killifish more fitting in mutation studies making identification of sequences variations and the identification of mutated genes quick and easy. For instance, in the zebrafish, genetic variation in individual fish

and complementary chromosomes are substantial. Because of this, identification of a mutation from these variations is a time consuming process requiring many pair-wise crossings and mappings. However, in my project, we obtained only 20 embryos each from the mutants, siblings and wild types, isolated their mRNA, and ran them in one lane of an Illumina sequencing run and instantly identified a mutation. This is also a remarkable feature of *K. marmoratus*, allowing identification of mutations in a very short time, labour and cost.

Therefore, the *K. marmoratus* has a large potential to become an alternative genetic model, complementary to the existing models.

References

Abdelkhalek, H. Ben, Beckers, A., Schuster-gossler, K., Pavlova, M. N., Burkhardt, H., Lickert, H. & Gossler, A. (2004). The mouse homeobox gene Not is required for caudal notochord development and affected by the truncate mutation. *Genes & Development*, 1725–1736.

Acevedo-Arozena, A., Wells, S., Potter, P., Kelly, M., Cox, R. D., & Brown, S. D. M. (2008). ENU mutagenesis, a way forward to understand gene function. *Annual Review of Genomics and Human Genetics*, *9*, 49–69.

Agathon, A., Thisse, C., & Thisse, B. (2003). The molecular nature of the zebrafish tail organizer. *Nature*, *424*(July), 448–452.

Alexander, J., & Stainier, D. Y. (1999). A molecular pathway leading to endoderm formation in zebrafish. *Current Biology 9*(20), 1147–57.

Altschul, S. F., Gish, W., Miller, W., Myers, E. W., & Lipman, D. J. (1990). Basic local alignment search tool. *Journal of Molecular Biology*, *215*(3), 403–10.

Amacher, S. L. and Kimmel, C. B. (1998). Promoting notochord fate and repressing muscle development in zebrafish axial mesoderm. *Development 125*, 1397-1406.

Amaya, E., Stein, P. a, Musci, T. J., & Kirschner, M. W. (1993). FGF signalling in the early specification of mesoderm in Xenopus. *Development 118*(2), 477–487.

Anders, S., Pyl, P. T., & Huber, W. (2015). HTSeq-a Python framework to work with high-throughput sequencing data. *Bioinformatics, 31*(2), 166-169.

Andersen, I. S., Reiner, A. H., Aanes, H., Aleström, P., & Collas, P. (2012). Developmental features of DNA methylation during activation of the embryonic zebrafish genome. *Genome Biology*, *13*(7), R65.

Anderson, R. M., Lawrence, A. R., Stottmann, R. W., Bachiller, D., & Klingensmith, J. (2002). Chordin and noggin promote organizing centers of forebrain development in the mouse. *Development*, *129*(21), 4975–4987.

Aronesty,E. (2011). *ea-utils* : "Command-line tools for processing biological sequencing data"; https://github.com/ExpressionAnalysis/ea-utils

Arrington, C. B., Peterson, A. G., & Yost, H. J. (2013). Sdc2 and Tbx16 regulate Fgf2-dependent epithelial cell morphogenesis in the ciliated organ of asymmetry. *Development*, *140*(19), 4102–9.

Avise, G. (2008). *Genetic , Ecology and evolution of sexual abstinence*. (Trudy Nicholson, Ed.) (Oxford Uni).

Bailly, K., Soulet, F., Leroy, D., Amalric, F., & Bouche, G. (2000). Uncoupling of cell proliferation and differentiation activities of basic fibroblast growth factor. *Faseb J*, *14*(2), 333–344.

Bansal, R., Magge, S., & Winkler, S. (2003). Specific Inhibitor of FGF receptor signaling-FGF2 mediated effects on proliferation-differentiation and MAPK activation are inhibited by PD173074 in oligodendrocyte lineage cells, *Journal of Neuroscience Research*, *74*(4), 1–8.

Baroux, C., Autran, D., Gillmor, C. S., Grimanelli, D., & Grossniklaus, U. (2008). The maternal to zygotic transition in animals and plants. *Cold Spring Harbor Symposia on Quantitative Biology*, *73*, 89–100.

Barski, A., Cuddapah, S., Cui, K., Roh, T. Y., Schones, D. E., Wang, Z., … Zhao, K. (2007). High-Resolution Profiling of Histone Methylations in the Human Genome. *Cell*, *129*(4), 823–837.

Basilico, C., & Moscatelli, D. (1992). The FGF family of growth factors and oncogenes. *Adv Cancer Res*, *59*, 115–65.

Beckers, A., Alten, L., Viebahn, C., Andre, P., & Gossler, A. (2007). The mouse homeobox gene Noto regulates node morphogenesis, notochordal ciliogenesis, and left right patterning. *PNAS*, *104*(40), 15765–70.

Belting, H. G., Wendik, B., Lunde, K., Leichsenring, M., Mössner, R., Driever, W., & Onichtchouk, D. (2011). Pou5f3 contributes to dorsoventral patterning by positive regulation of vox and modulation of fgf8a expression. *Developmental Biology, 356(2)*, 323–336.

Bondar, V. M., Sweeney-Gotsch, B., Andreeff, M., Mills, G. B., & McCey, D. J. (2002). Inhibition of the phosphatidylinositol 3 ’-kinase-AKT pathway induces apoptosis in pancreatic carcinoma cells in vitro and in vivo. *Mol Cancer Ther*, *1*(12), 989–997.

Bottcher, R. T., & Niehrs, C. (2005). Fibroblast growth factor signaling during early vertebrate development. *Endocrine Reviews*, *26*(1), 63–77.

Bruce, A. E. E., Howley, C., Zhou, Y., Vickers, S. L., Silver, L. M., King, M. Lou, & Ho, R. K. (2003). The maternally expressed zebrafish T-box gene eomesodermin regulates organizer formation. *Development*, *130*, 5503–5517.

Buenrostro, J. D., Wu, B., Chang, H. Y., & Greenleaf, W. J. (2015). ATAC-seq: A method for assaying chromatin accessibility genome-wide. *Current Protocols in Molecular Biology*, *109*(21*)*, 21-29.

Carballada, R., Yasuo, H., & Lemaire, P. (2001). Phosphatidylinositol-3 kinase acts in parallel to the ERK MAP kinase in the FGF pathway during Xenopus mesoderm induction. *Development*, *128*, 35–44.

Chalamalasetty, R. B., Garriock, R. J., Dunty, W. C., Kennedy, M. W., Jailwala, P., Si, H., & Yamaguchi, T. P. (2014). Mesogenin 1 is a master regulator of paraxial presomitic mesoderm differentiation. *Development, 141*(22), 4285–4297.

Chang, W. J., & Hwang, P. P. (2011). Development of zebrafish epidermis. *Birth Defects Research, 93*(3), 205–214.

Chen, Y., & Schier, A. (2001). The zebrafish Nodal signal Squint functions as a morphogen. *Nature*, *411*, 607–610.

Cole, K. S., & Noakes, D. L. G. (1997). Gonadal development and sexual allocation in mangrove killifish, Rivulus marmoratus (Pisces: Atherinomorpha). *Copeia*, *1997*(3), 596–600.

Coumoul, X., & Deng, C. (2003). Roles of FGF receptors in mammalian development and congenital diseases. *Birth Defects Research Part C: Embryo*, *69*, 286–304.

Crawford, J. J., Hoeflich, K. P., & Rudolph, J. (2012). p21-Activated kinase inhibitors: a patent review. *Expert Opinion on Therapeutic Patents*, *22*(3), 293–310.

Crocetta, F., Marino, R., Cirino, P., Macina, A., Staiano, L., Esposito, R., … Sordino, P. (2015). Mutation Studies in Ascidians :A Review. *Genesis*, *53*(1), 160–169.

Cruz, C., Maegawa, S., Weinberg, E. S., Wilson, S. W., Dawid, I. B., & Kudoh, T. (2010). Induction and patterning of trunk and tail neural ectoderm by the homeobox gene eve1 in zebrafish embryos. *PNAS*, *107*(8), 3564–3569.

Dailey, L., Ambrosetti, D., Mansukhani, A., & Basilico, C. (2005). Mechanisms underlying differential responses to FGF signaling. *Cytokine & Growth Factor Reviews*, *16*(2), 233–47.

Dawid, I. B. (2004). Organizing the vertebrate embryo - A balance of induction and competence. *PLoS Biology*, *2*(5), 579–582.

Dee, C.T., Gibson, A., Rengifo, A., Sun, S-K., Patient, R.K. and Scotting, P. J. (2007). A change in response to BMP signalling precedes ectodermal fate choice. In *Dev. Biol.* (51st ed., pp. 79 – 84).

Delaune, E., Lemaire, P., & Kodjabachian, L. (2005). Neural induction in Xenopus requires early FGF signalling in addition to BMP inhibition. *Development*, *132*(2), 299–310.

Dick, A., Hild, M., Bauer, H., Imai, Y., Maifeld, H., Schier,A., Talbot, W., Bouwmeester ,T.,& Hammerschmidt, M. (2000). Essential role of Bmp7 (snailhouse) and its prodomain in dorsoventral patterning of the zebrafish embryo. *Development*, *127*(2), 343–354.

Di-Poï, N., Montoya-Burgos, J. I., Miller, H., Pourquié, O., Milinkovitch, M. C., & Duboule, D. (2010). Changes in Hox genes' structure and function during the evolution of the squamate body plan. *Nature*, *464*(7285), 99–103.

Dooley, K. & Zon, L. (2000). Zebrafish: a model system for the study of human disease. *Current Opinion in Genetics & Development*, *10*(3), 252–256.

Dorey, K., & Amaya, E. (2010). FGF signalling: diverse roles during early vertebrate embryogenesis. *Development*, *137*(22), 3731–42.

Draizen, E. J., Shaytan, A. K., Mariño-Ramírez, L., Talbert, P. B., Landsman, D., & Panchenko, A. R. (2016). HistoneDB 2.0: A histone database with variants - An integrated resource to explore histones and their variants. *Database, 2016*, 1–10.

Draper, B. W., Morcos, P. a., & Kimmel, C. B. (2001). Inhibition of zebrafish fgf8 pre-mRNA splicing with morpholino oligos: A quantifiable method for gene knockdown. *Genesis*, *30*(3), 154–156.

Draper, B. W., Stock, D. W., & Kimmel, C. B. (2003). Zebrafish fgf24 functions with fgf8 to promote posterior mesodermal development. *Development*, *130*(19), 4639–4654.

Driever, W., Stemple, D., Schier, A., & Solnica-Krezel, L. (1994). Zebrafish: genetic tools for studying vertebrate development. *Trends in Genetics*, *10*(5), 152–159.

Egger, G., Liang, G., Aparicio, A., & Jones, P. a. (2004). Epigenetics in human disease and prospects for epigenetic therapy. *Nature, 429*(6990), 457–63.

Eisen, J. S., & Smith, J. C. (2008). Controlling morpholino experiments: don't stop making antisense. *Development, 135*(10), 1735–1743.

Ellison, A., Wright, P., Taylor, D. S., Cooper, C., Regan, K., Currie, S., & Consuegra, S. (2012). Environmental diel variation, parasite loads, and local population structuring of a mixed-mating mangrove fish. *Ecology and Evolution*, *2*(7), 1682–1695.

Fallon, J., Lopez, A., Ros, A., Savage, M., Olwin, B., & Simandl, B. (1994). FGF-2: apical ectodermal ridge growth signal for chick limb development. *Science, 264*(5155), 104–107.

Finch, E., Cruz, C., & Sloman, K. A. (2010). Heterochrony in the germ ring closure and tail bud formation in embryonic development of rainbow trout (Oncorhynchus mykiss). *Molecular and Developmental Evolution*, *314B*(3), 187–195.

Fior, R., Maxwell, A., Ma, T. P., Vezzaro, A., Moens, C. B., Amacher, S. L., Lewis, J.,& Saúde, L. (2012). The differentiation and movement of presomitic mesoderm progenitor cells are controlled by Mesogenin 1. *Development*, *139*, 4656–65.

Fischer, S., Draper, B. W., & Neumann, C. J. (2003). The zebrafish fgf24 mutant identifies an additional level of Fgf signaling involved in vertebrate forelimb initiation. *Development*, *130*, 3515–3524.

Fiset, P., & Gounni, A. (2001). Antisense oligonucleotides: problems with use and solutions. *Rev Biol Biotech*, *1*(2), 27–33.

Fong, T. A. T., Shawver, L. K., Sun, L., Tang, C., App, H., Powell, T. J., … McMahon, G. (1999). SU5416 Is a Potent and Selective Inhibitor of the Vascular Endothelial Growth Factor Receptor (Flk-1 / KDR) That Inhibits Tyrosine Kinase Catalysis , Tumor Vascularization , and Growth of Multiple Tumor Types SU5416 Is a Potent and Selective Inhibitor o. *Cancer Research*, *59*(37), 99–106.

Furutani-Seiki, M., Sasado, T., Morinaga, C., Suwa, H., Niwa, K., Yoda, H., … Kondoh, H. (2004). A systematic genome-wide screen for mutations affecting organogenesis in Medaka, *Oryzias latipes*. *Mechanisms of Development*, *121*(7-8), 647–658.

Furutani-Seiki, M., & Wittbrodt, J. (2004). Medaka and zebrafish, an evolutionary twin study. *Mechanisms of Development*, *121*(7-8), 629–637.

Gibran, N. S., Isik, F. F., Heimbach, D., & Gordon, D. (1994). Basic Fibroblast Growth Factor in the Early Human Burn Wound. *Journal of Surgical Research, 56*(3), 226–234.

Gont, L. K., Fainsod, a, Kim, S. H., & De Robertis, E. M. (1996). Overexpression of the homeobox gene Xnot-2 leads to notochord formation in Xenopus. *Developmental Biology*, *174*(1), 174–178.

Gouti, M., Delile, J., Stamataki, D., Wymeersch, F. J., Huang, Y., Kleinjung, J., … Briscoe, J. (2017). A Gene Regulatory Network Balances Neural and Mesoderm Specification during Vertebrate Trunk Development. *Developmental Cell, 41*(3), 243–261.

Gouti, M., Metzis, V., and Briscoe, J. (2015). The route to spinal cord cell types: a tale of signals and switches. *Trends Genet. 31*, 282–28.

Grageda, M. V. C., Sakakura, Y., & Hagiwara, A. (2004). Early development of the self-fertilizing mangrove killifish Rivulus marmoratus reared in the laboratory. *Ichthyological Research*, *51*, 309–315.

Grageda, M., Sakakura, Y., Minamimoto, M.&Hagiwara, A.(2005). Differences in life-history traits in two clonal strains of the self-fertilizing fish, Rivulus marmoratus. *Environ Biol Fish*, *73*(4), 427–436.

Griffin, K. J., Amacher, S. L., Kimmel, C. B., & Kimelman, D. (1998). Molecular identification of spadetail: regulation of zebrafish trunk and tail mesoderm formation by T-box genes. *Development*, *125*(17), 3379–3388.

Griffin, K. J. P., & Kimelman, D. (2003). Interplay between FGF, one-eyed pinhead, and T-box transcription factors during zebrafish posterior development. *Developmental Biology, 264*(2), 456–466.

Griffin, K., Patient, R., & Holder, N. (1995). Analysis of FGF function in normal and no tail zebrafish embryos reveals separate mechanisms for formation of the trunk and the tail. *Development*, *121*(9), 2983–2994.

Gupta, S., Kim, S. Y., Artis, S., Molfese, D. L., Schumacher, A., Sweatt, J. D., pylor,E. & Lubin, F. D. (2010). Histone Methylation Regulates Memory Formation. *Journal of Neuroscience, 30*(10), 3589–3599.

Gurdon, J. B. (1987). Embryonic induction--molecular prospects. *Development*, *99*(3), 285–306.

Haas, B. J., Papanicolaou, A., Yassour, M., Grabherr, M., Blood, P. D., Bowden, J., … Regev, A. (2013). De novo transcript sequence reconstruction from RNA-seq using the Trinity platform for reference generation and analysis. *Nature Protocols*, *8*(8), 1494–1512.

Hall, H., Williams, E. J., Moore, S. E., Walsh, F. S., Prochiantz, a, & Doherty, P. (1996). Inhibition of FGF-stimulated phosphatidylinositol hydrolysis and neurite outgrowth by a cell-membrane permeable phosphopeptide. *Curr Biol*, *6*(5), 580–587.

Halpern, M. E., Ho, R. K., Walker, C., & Kimmel, C. B. (1993). Induction of muscle pioneers and floor plate is distinguished by the zebrafish no tail mutation. *Cell*, *75*, 99–111.

Halpern, M. E., Thisse, C., Ho, R. K., Thisse, B., Riggleman, B., Trevarrow, B.& Kimmel, C. B. (1995). Cell-autonomous shift from axial to paraxial mesodermal development in zebrafish floating head mutants. *Development*, *121*(12), 4257–64.

Hammerschmidt, M., Pelegri, F., Mullins, M. C., Kane, D. a, Brand, M., van Eeden, F. J. & Nüsslein-Volhard, C. (1996). Mutations affecting morphogenesis during gastrulation and tail formation in the zebrafish, Danio rerio. *Development*, *123*, 143–151.

Harland, R., & Gerhart, J. (1997). Formation and function of Spemann's organizer. *Annual Review of Cell and Developmental Biology*, *13*, 611–667.

Harrington W. and Rivas Jr. (1958). The Discovery in Florida of the Cyprinodont Fish, Rivulus marmoratus, with a Redescription and Ecological Notes. *American Society of Ichthyologists and Herpetologists*, *2*, 125–130.

Harrington, R. (1967). Environmentally controlled induction of primary male gonochorists from eggs of the selffertilizing hermaphroditic fish, Rivulus marmoratus Poey. *The Biological Bulletin*, *132*, 174–199.

Harris, M. P., Rohner, N., Schwarz, H., Perathoner, S., Konstantinidis, P., & Nüsslein-Volhard, C. (2008). Zebrafish eda and edar mutants reveal conserved and ancestral roles of ectodysplasin signaling in vertebrates. *PLoS Genetics*, *4*(10).

Hill, J. T., Demarest, B. L., Bisgrove, B. W., Gorsi, B., Su, Y., & Yost, H. J. (2013). MMAPPR : Mutation Mapping Analysis Pipeline for Pooled RNA-seq MMAPPR : Mutation Mapping Analysis Pipeline for Pooled RNA-seq. *Genome Research, (23)*, 687–697.

Hiller, M., Agarwal, S., Notwell, J. H., Parikh, R., Guturu, H., Wenger, A. M., & Bejerano, G. (2013). Computational methods to detect conserved non-genic elements in phylogenetically isolated genomes: Application to zebrafish. *Nucleic Acids Research*, *41*(15) e151.

Howe, K., Clark, M. D., Torroja, C. F., Torrance, J., Berthelot, C., Muffato, M., … Stemple, D. L. (2013). The zebrafish reference genome sequence and its relationship to the human genome. *Nature*, *496*(7446), 498–503.

Hublitz, P., Albert, M., & Peters, A. H. F. M. (2009). Mechanisms of transcriptional repression by histone lysine methylation. *International Journal of Developmental Biology, 53*(2–3), 335–354.

Inoue, K., & Takei, Y. (2003). Asian medaka fishes offer new models for studying mechanisms of seawater adaptation. *Comparative Biochemistry and Physiology Part B: Biochemistry and Molecular Biology*, *136*(4), 635–645.

Ishikawa, Y. (2000). Medakafish as a model system for vertebrate developmental genetics. *BioEssays*, *22*, 487–495.

Iwamatsu, T. (2004). Stages of normal development in the medaka Oryzias latipes. *Mechanisms of Development*, *121*(7-8), 605–618.

Jahangiri, L., Nelson, A. C., & Wardle, F. C. (2012). A cis-regulatory module upstream of deltaC regulated by Ntla and Tbx16 drives expression in the tailbud, presomitic mesoderm and somites. *Developmental Biology, 371*(1), 110–120

Jia, S., Wu, D., Xing, C., & Meng, A. (2009). Smad2/3 activities are required for induction and patterning of the neuroectoderm in zebrafish. *Developmental Biology*, *333*(2), 273–284.

Jiang, X. Y., Sun, C. F., Zhang, Q. G., & Zou, S. M. (2011). ENU-induced mutagenesis in grass carp (Ctenopharyngodon idellus) by treating mature sperm. *PLoS ONE*, *6*(10), 1–8.

Joseph, E. M., & Cassetta, L. A. (1999). Mespo: A novel basic helix-loop-helix gene expressed in the presomitic mesoderm and posterior tailbud of Xenopus embryos. *Mechanisms of Development*, *82*(1–2), 191–194.

Justice, M. J., Noveroske, J. K., Weber, J. S., Zheng, B., & Bradley, A. (1999). Mouse ENU mutagenesis. *Human Molecular Genetics*, *8*(10), 1955–1963.

Kanamori, A., Sugita, Y., Yuasa, Y., Suzuki, T., Kawamura, K., Uno, Y., … Sakakura, Y. (2016). A Genetic Map for the Only Self-Fertilizing Vertebrate. *Genes|Genomes|Genetics, 6*(4), 1095–1106.

Kanamori, A., Yamamura, A., Koshiba, S., Lee, J. S., Orlando, E. F., & Hori, H. (2006). Methyltestosterone efficiently induces male development in the self-fertilizing hermaphrodite fish, Kryptolebias marmoratus. *Genesis*, *44*, 495–503.

Kang, C. K., Tsai, S. C., Lee, T. H., & Hwang, P. P. (2008). Differential expression of branchial Na+/K+-ATPase of two medaka species, Oryzias latipes and Oryzias dancena, with different salinity tolerances acclimated to fresh water, brackish water and seawater. *Comparative Biochemistry and Physiology - A Molecular and Integrative Physiology*, *151*(4), 566–575

Kanki, J. P., & Ho, R. K. (1997). The development of the posterior body in zebrafish. *Development*, *124*(4), 881–93.

Kelley, J. L., Yee, M. C., Lee, C., Levandowsky, E., Shah, M., Harkins, T., … Bustamante, C. D. (2012). The possibility of de novo assembly of the genome and population genomics of the mangrove rivulus, *kryptolebias marmoratus*. *Integrative and Comparative Biology*, *52*, 737–742.

Kelly, C., Chin, A. J., Leatherman, J. L., Kozlowski, D. J., & Weinberg, E. S. (2000). Maternally controlled (beta)-catenin-mediated signaling is required for organizer formation in the zebrafish. *Development (Cambridge, England)*, *127*, 3899–3911.

Kim, D., Landmead, B., & Salzberg, S. L. (2015). HISAT: a fast spliced aligner with low memory requirements. *Nature Methods, 12*(4), 357-362.

Kimmel, C. B. (1989). Genetics and early development of zebrafish. *Trends in Genetics*, *5*(8), 283–288.

Kimmel, C. B., Warga, R. M., & Schilling, T. F. (1990). Origin and organization of the zebrafish fate map. *Development*, *108*(4), 581–594.

Kimmel, C., Ballard, W., Kimmel, S., Ullmann, B., & Schilling, T. (1995). Stages of embryonic development of the zebrafish. *Developmental Dynamics*, *203*(3), 253–310.

Kimura, Y., Hisano, Y., Kawahara, A., & Higashijima, S. (2014). Efficient generation of knock-in transgenic zebrafish carrying reporter/driver genes by CRISPR/Cas9-mediated genome engineering. *Scientific Reports*, *4*, 6545.

King, J.A.C., Abel, D.C. & DiBona, D. R. (1989). Effects of salinity on chloride cells in the euryhaline cyprinodontid fish Rivulus marmoratus. *Cell Tissue Res.*, *257*(2), 367–377.

Kishimoto, Y., Lee, K. H., Zon, L., Hammerschmidt, M., & Schulte-Merker, S. (1997). The molecular nature of zebrafish swirl: BMP2 function is essential during early dorsoventral patterning. *Development*, *124*(22), 4457–4466.

Koshida, S., Shinya, M., Mizuno, T., Kuroiwa, a, & Takeda, H. (1998). Initial anteroposterior pattern of the zebrafish central nervous system is determined by differential competence of the epiblast. *Development*, *125*(10), 1957–1966.

Kouzarides, T. (2007). Chromatin Modifications and Their Function. *Cell, 128*(4), 693–705.

Krens, S. F. G., He, S., Lamers, G. E. M., Meijer, A. H., Bakkers, J., Schmidt, T.& Snaar-Jagalska, B. E. (2008). Distinct functions for ERK1 and ERK2 in cell migration processes during zebrafish gastrulation. *Developmental Biology*, *319*(2), 370–383.

Kudoh, T., Concha, M. L., Houart, C., Dawid, I. B., & Wilson, S. W. (2004). Combinatorial Fgf and Bmp signalling patterns the gastrula ectoderm into prospective neural and epidermal domains, *Development, 131*(15) 3581–3592.

Kunath, T., Saba-El-Leil, M. K., Almousailleakh, M., Wray, J., Meloche, S., & Smith, A. (2007). FGF stimulation of the Erk1/2 signalling cascade triggers transition of pluripotent embryonic stem cells from self-renewal to lineage commitment. *Development*, *134*(16), 2895–902.

Kwon, H. J., Bhat, N., Sweet, E. M., Cornell, R. A., & Riley, B. B. (2010). Identification of early requirements for preplacodal ectoderm and sensory organ development. *PLoS Genetics, 6*(9)1-14.

Lachnit, M., Kur, E., & Driever, W. (2008). Alterations of the cytoskeleton in all three embryonic lineages contribute to the epiboly defect of Pou5f3/Pou5f3 deficient MZspg zebrafish embryos. *Developmental Biology, 315*(1), 1–17.

Lardelli, M. (2014). Using zebrafish in human disease research: some advantages, disadvantages and ethical considerations. *PloS One*, *9*(11), 23–28.

Lawrence, C. (2007). The husbandry of zebrafish (*Danio rerio*): A review. *Aquaculture*, *269*(1-4), 1–20.

Leali, D., Bianchi, R., Bugatti, A., Nicoli, S., Mitola, S., Ragona, L., … Presta, M. (2010). Fibroblast growth factor 2-antagonist activity of a long-pentraxin 3-derived anti-angiogenic pentapeptide. *Journal of Cellular and Molecular Medicine, 14*(8), 2109–2121.

Lee, H., & Kimelman, D. (2002). A dominant-negative form of p63 is required for epidermal proliferation in zebrafish. *Developmental Cell, 2*(5), 607–616.

Lee, H. O., Choe, H., Seo, K., Lee, H., Lee, J. and Kim, J. (2010). Fgfbp1 is essential for the cellular survival during zebrafish embryogenesis. *Mol. Cells 29*, 501-507.

Lee, J. S., Raisuddin, S., & Schlenk, D. (2008). *Kryptolebias marmoratus* (Poey, 1880): A potential model species for molecular carcinogenesis and ecotoxicogenomics. *Journal of Fish Biology*, *72*, 1871–1889.

Lee, M. T., Bonneau, A. R., Takacs, C. M., Bazzini, A. A., DiVito, K. R., Fleming, E. S., & Giraldez, A. J. (2013). Nanog, Pou5f3 and SoxB1 activate zygotic gene expression during the maternal-to-zygotic transition. *Nature*, *503*, 360–364.

Lee, M. T., Bonneau, A. R., & Giraldez, A. J. (2014). Zygotic genome activation during the maternal-to-zygotic transition. *Annu Rev Cell Dev Biol*, *30*(1), 581–613.

Lee, Y. M., Rhee, J.-S., Hwang, D.-S., Kim, I.-C., Raisuddin, S., & Lee, J.-S. (2007). Mining of biomarker genes from expressed sequence tags and differential display reverse transcriptase-polymerase chain reaction in the self-fertilizing fish, Kryptolebias marmoratus and their expression patterns in response to exposure to an endocrine-dis. *Molecules and Cells*, *23*(3), 287–303.

Leichsenring, M., Maes, J., Mössner, R., Driever, W., & Onichtchouk, D. (2013). Pou5f3 Transcription Factor Controls Zygotic Gene Activation In Vertebrates. *Science*, *341*(6149), 1005–1009.

Lieschke, G. J., & Currie, P. D. (2007). Animal models of human disease: zebrafish swim into view. *Nature Reviews Genetics*, *8*(5), 353–367.

Lindeman, L. C., Andersen, I. S., Reiner, A. H., Li, N., Aanes, H., Østrup, O., Collas, P. (2011). Prepatterning of Developmental Gene Expression by Modified Histones before Zygotic Genome Activation. *Developmental Cell*, *21*(6), 993–1004.

Lister Hill National Center for Biomedical Communications, U.S. National Library of Medicine, N. I. of H., & Department of Health & Human Services, U. go. (2015). *Genetics Home Reference Your Guide to Understanding Genetic Conditions*.

Litwiller, S. L., O'Donnell, M. J., & Wright, P. A. (2006). Rapid increase in the partial pressure of NH3 on the cutaneous surface of air-exposed mangrove killifish, *Rivulus marmoratus*. *The Journal of Experimental Biology*, *209*, 1737–1745.

Londin, E. R., Niemiec, J., & Sirotkin, H. I. (2005). Chordin, FGF signaling, and mesodermal factors cooperate in zebrafish neural induction. *Developmental Biology*, *279*(1), 1–19.

Loosli, F., Köster, R. W., Carl, M., Kühnlein, R., Henrich, T., Mücke, M., … Wittbrodt, J. (2000). A genetic screen for mutations affecting embryonic development in medaka fish (Oryzias latipes). *Mechanisms of Development*, *97*(1-2), 133–9.

Lopez-Maestre, H., Brinza, L., Marchet, C., Kielbassa, J., Bastien, S., Boutigny, M., … Lacroix, V. (2016). SNP calling from RNA-seq data without a reference genome: Identification, quantification, differential analysis and impact on the protein sequence. *Nucleic Acids Research*, *44*(19), 1–13.

Love, M. I., Huber, W., & Anders, S. (2014). Moderated estimation of fold change and dispersion for RNA-seq data with DESeq2. *Genome Biology, 15*(12),550P.

Mackiewicz, M., Tatarenkov, A., Perry, A., Martin, J. R., Elder, J. F., Bechler, D. L., & Avise, J. C. (2006a). Microsatellite documentation of male-mediated outcrossing between inbred laboratory strains of the self-fertilizing mangrove killifish (Kryptolebias Marmoratus). *Journal of Heredity*, *97*(5), 508–513.

Mackiewicz, M., Tatarenkov, A., Taylor, D. S., Turner, B. J., & Avise, J. C. (2006b). Extensive outcrossing and androdioecy in a vertebrate species that otherwise reproduces as a self-fertilizing hermaphrodite. *PNAS*, *103*(26), 9924–9928.

Manning, A. J., & Kimelman, D. (2015). Tbx16 and Msgn1 are required to establish directional cell migration of zebrafish mesodermal progenitors. *Developmental Biology, 406*(2), 172–185.

Maroon, H., Walshe, J., Mahmood, R., Kiefer, P., Dickson, C., & Mason, I. (2002). Fgf3 and Fgf8 are required together for formation of the otic placode and vesicle. *Development*, *129*, 2099–2108.

Martin, B. L., & Kimelman, D. (2010). Brachyury establishes the embryonic mesodermal progenitor niche. *Genes and Development, 24*(24), 2778–2783.

McCann, M. R., Tamplin, O. J., Rossant, J., & Seguin, C. A. (2012). Tracing notochord-derived cells using a Noto-cre mouse: implications for intervertebral disc development. *Disease Models & Mechanisms, 5*(1), 73–82.

Melby, A. E., Kimelman, D., & Kimmel, C. B. (1997). Spatial regulation of floating head expression in the developing notoehord. *Developmental Dynamics, 209*(2), 156–165.

Mendieta-Serrano, M. A., Schnabel, D., Lomelí, H., & Salas-Vidal, E. (2013). Cell Proliferation Patterns in Early Zebrafish Development. *The Anatomical Record*, *296*(5), 759–773.

Mitrecic, M., Mitrecic, D., Pochet, R., Kostovic-Knezevic, L., & Gajovic, S. (2010). The mouse gene noto is expressed in the tail bud and essential for its morphogenesis. *Cells Tissues Organs, 192*(2), 85–92.

Mohammadi, M., Mcmahon, G., Sun, L., Tang, C., Hirth, P., Yeh, B. K., … Schlessinger, J. (1997). Structures of the Tyrosine Kinase Domain of Fibroblast Growth Factor Receptor in Complex with Inhibitors. *Science, 276*, 955–960.

Montero, A., Okada, Y., Tomita, M., Ito, M., Tsurukami, H., Nakamura, T., … Hurley, M. M. (2000). Disruption of the fibroblast growth factor-2 gene results in decreased bone mass and bone formation. *The Journal of Clinical Investigation*, *105*(8), 1085–93.

Moore, G. L., Sucar, S., Newsome, J. M., Ard, M. E., Bernhardt, L., Bland, M. J., & Ring, B. C. (2012). Establishing developmental genetics in a self-fertilizing fish (Krytolebias marmoratus). *Integrative and Comparative Biology*, *52*(6), 781–791.

Mork, L. & Crump, G. (2015). Zebrafish Craniofacial Development: A Window into Early Patterning. *Curr Top Dev Biol*, (115), 235–269.

Morishita, M., Mevius, D., & Luccio, E. (2014). In vitro histone lysine methylation by NSD1, NSD2/MMSET/WHSC1 and NSD3/WHSC1L. *BMC Structural Biology, 12*(25), 1–13.

Morris, S. A., Rao, B., Garcia, B. A., Hake, S. B., Diaz, R. L., Shabanowitz, J.& Strahl, B. D. (2007). Identification of histone H3 lysine 36 acetylation as a highly conserved histone modification. *Journal of Biological Chemistry*, *282*(10), 7632–7640.

Mourabit, S., Edenbrow, M., Croft, D. P., & Kudoh, T. (2011). Embryonic development of the self-fertilizing mangrove killifish Kryptolebias marmoratus. *Developmental Dynamics*, *240*, 1694–1704.

Mourabit, S., & Kudoh, T. (2012). Manipulation and imaging of kryptolebias marmoratus embryos. *Integrative and Comparative Biology*, *52*(6), 761–768.

Mourabit, S., Moles, M. W., Smith, E., Van Aerle, R., & Kudoh, T. (2014). Bmp suppression in mangrove killifish embryos causes a split in the body axis. *PLoS ONE*, *9*(1), 1–8.

Nugent, M., & Iozzo,R. (2000). Fibroblast growth factor-2. *The International Journal of Biochemistry & Cell Biology, 32*(2), 115–120.

Mullins, M. C., Hammerschmidt, M., Haffter, P., & Nüsslein-Volhard, C. (1994). Large-scale mutagenesis in the zebrafish: in search of genes controlling development in a vertebrate. *Current Biology*, *4*(3), 189–202.

Naruse, K., Hori, H., Shimizu, N., Kohara, Y., & Takeda, H. (2004). Medaka genomics: A bridge between mutant phenotype and gene function. *Mechanisms of Development*, *121*(7-8), 619–628.

Nicoli, S., De Sena, G., & Presta, M. (2009). Fibroblast growth factor 2-induced angiogenesis in zebrafish: The zebrafish yolk membrane (ZFYM) angiogenesis assay. *Journal of Cellular and Molecular Medicine, 13(8 B)*, 2061–2068.

Nissan, M. H., Rosen, N., & Solit, D. B. (2013). ERK pathway inhibitors: How low should we go? *Cancer Discovery*, *3*(7), 719–721.

Nordlie, F. G. (2006). Physicochemical environments and tolerances of cyprinodontoid fishes found in estuaries and salt marshes of eastern North America. *Reviews in Fish Biology and Fisheries*, *16*(1), 51–106.

Nowotschin, S., Ferrer-Vaquer, A., Concepcion, D., Papaioannou, V. E., & Hadjantonakis, A. K. (2012). Interaction of Wnt3a, Msgn1 and Tbx6 in neural versus paraxial mesoderm lineage commitment and paraxial mesoderm differentiation in the mouse embryo. *Developmental Biology*, *367*(1), 1–14.

Nusslein-Volhard, C. (2012). The zebrafish issue of Development. *Development*, *139*(22), 4099–4103.

Nusslein-Volhard, C., Glimour, D., & Dahm, R. (2002). *Zebarfish A practical Approach*. (C. Nusslein-Volhard & R. Dahm, Eds.). *Oxford University Press, USA.*

Odenthal, J., Haffter, P., Vogelsang, E., Brand, M., van Eeden, F. J., Furutani-Seiki, M., … Nüsslein-Volhard, C. (1996). Mutations affecting the formation of the notochord in the zebrafish, Danio rerio. *Development*, *123*, 103–115.

Okuda, Y., Ogura, E., Kondoh, H., & Kamachi, Y. (2010). B1 SOX coordinate cell specification with patterning and morphogenesis in the early zebrafish embryo. *PLoS Genetics, 6*(5), 1-18.

Ortega, S., Ittmann, M., Tsang, S. H., Ehrlich, M., & Basilico, C. (1998). Neuronal defects and delayed wound healing in mice lacking fibroblast growth factor 2. *PNAS, 95*(10), 5672–7.

Østrup, O., Andersen, I. S., & Collas, P. (2013). Chromatin-linked determinants of zygotic genome activation. *Cellular and Molecular Life Sciences, 70*(8), 1425–1437.

Ota, S., Hisano, Y., Ikawa, Y., & Kawahara, A. (2014). Multiple genome modifications by the CRISPR/Cas9 system in zebrafish. *Genes to Cells*, *19*(7), 555–564.

Ouyang, Z., Zhou, Q., & Wong, W. H. (2009). ChIP-Seq of transcription factors predicts absolute and differential gene expression in embryonic stem cells. *PNAS*, *106*(51), 21521–6.

Ozato, K., & Wakamatsu, Y. (1994). Developmental Genetics of Medaka. *Development Growth and Differentiation*, *36*(5), 437–443.

Pelegri, F., & C.Mullins, M. (2004). Genetic screens for maternal-effect mutations. *Methods Cell Biol*, *77*, 21–51.

Pelegri, F., & Mullins, M. C. (2011). Genetic Screens for Mutations Affecting Adult Traits and Parental-effect Genes. *Methods in Cell Biology*, *104*, 83–120.

Peterson, C. L., & Laniel, M.-A. (2004). Histones and histone modifications. *Current Biology, 14*(14), 546–551.

Pintucci, G., Moscatelli, D., Saponara, F., Biernacki, P. R., Baumann, F. G., Bizekis, C.& Mignatti, P. (2002). Lack of ERK activation and cell migration in FGF-2-deficient endothelial cells. *FASEB Journal : Official Publication of the Federation of American Societies for Experimental Biology*, *16*(6), 598–600.

Powers, C., McLeskey, S., & Wellstein, A. (2000). Fibroblast growth factors, their receptors and signaling. *Endocrine-Related Cancer*, *7*, 165–197.

Prats, A., De, B., Wang, P., & Darlix, J. (1989). CUG initiation codon used for the synthesis of a cell surface antigen coded by the murine leukemia virus. *J Mol Biol, 205*(2), 363–72.

Quarto, N., Fong, K. D., & Longaker, M. T. (2005). Gene profiling of cells expressing different FGF-2 forms. *Gene*, *356*(1-2), 49–68.

Raballo, R., Rhee, J., Lyn-Cook, R., Leckman, J. F., Schwartz, M. L., & Vaccarino, F. M. (2000). Basic fibroblast growth factor (Fgf2) is necessary for cell proliferation and neurogenesis in the developing cerebral cortex. The Journal of Neuroscience : *The Official Journal of the Society for Neuroscience, 20*(13), 5012–5023.

Ramel, M. C., Buckles, G. R., Baker, K. D., & Lekven, A. C. (2005). WNT8 and BMP2B co-regulate non-axial mesoderm patterning during zebrafish gastrulation. *Developmental Biology*, *287*(2), 237–248.

Rentzsch, F., Bakkers, J., Kramer, C. and Hammerschmidt, M. (2004). FGF signaling induces posterior neuroectoderm independently of BMP signaling inhibition. In *Dev. Dyn.* (231st ed., pp. 750–757).

Rhee, J. S., & Lee, J. S. (2014). Whole genome data for omics-based research on the self-fertilizing fish *Kryptolebias marmoratus*. *Marine Pollution Bulletin*, *85*(2), 532–541.

Rhee, J., Choi, B., Kim, J., Kim, B., Lee, Y., Kim, C., … Lee, J. (2017). Diversity, distribution, and significance of transposable elements in the genome of the only selfing hermaphroditic vertebrate Kryptolebias marmoratus. *Scientific Reports*, *40121*(*7*), 1-10.

Rogers, C. D., Ferzli, G. S., & Casey, E. S. (2011). The response of early neural genes to FGF signaling or inhibition of BMP indicate the absence of a conserved neural induction module. *BMC Developmental Biology*,*11*(1), 74.

Rossi, A., Kontarakis, Z., Gerri, C., Nolte, H., Hölper, S., Krüger, M., & Stainier, D. Y. R. (2015). Genetic compensation induced by deleterious mutations but not gene knockdowns. *Nature*, (524), 230–233.

Row, R. H., Maître, J. L., Martin, B. L., Stockinger, P., Heisenberg, C. P., & Kimelman, D. (2011). Completion of the epithelial to mesenchymal transition in zebrafish mesoderm requires Spadetail. *Developmental Biology*, *354*(1), 102–110.

Sabel, J. L., d'Alençon, C., O'Brien, E. K., Otterloo, E. Van, Lutz, K., Cuykendall, T. N.& Cornell, R. A. (2009). Maternal Interferon Regulatory Factor 6 is required for the differentiation of primary superficial epithelia in Danio and Xenopus embryos. *Developmental Biology, 325*(1), 249–262.

Saera-Vila, A., Kish, P. E., & Kahana, A. (2016). Fgf regulates dedifferentiation during skeletal muscle regeneration in adult zebrafish. *Cellular Signalling*, *28*(9), 1196–1204.

Sakakura, Y., & Noakes, D. L. G. (2000). Age, growth, and sexual development in the self-fertilizing hermaphroditic fish Rivulus marmoratus. *Environmental Biology of Fishes*, *59*, 309–317.

Sakakura, Y., Soyano, K., Noakes, D. L. G., & Hagiwara, A. (2006). Gonadal morphology in the self-fertilizing mangrove killifish, Kryptolebias marmoratus. *Ichthyological Research*, *53*, 427–430.

Sasaki, S., Ohta, H., Nakayama, Y., Konishi, M., Miyake, A., & Itoh, N. (2011). The FGF Family in Humans, Mice, and Zebrafish: Development, Physiology, and Pathophysiology. In *Human Genetic Diseases* (pp. 38–56).

Saúde, L., Woolley, K., Martin, P., Driever, W., & Stemple, D. L. (2000). Axis-inducing activities and cell fates of the zebrafish organizer. *Development*, *127*, 3407–3417.

Sawada, a, Fritz, a, Jiang, Y. J., Yamamoto, a, Yamasu, K., Kuroiwa, a, … Takeda, H. (2000). Zebrafish Mesp family genes, mesp-a and mesp-b are segmentally expressed in the presomitic mesoderm, and Mesp-b confers the anterior identity to the developing somites. *Development (Cambridge)*, *127*, 1691–1702.

Scheel, J. J. (1972). Rivuline Karyotypes and their Evolution (Rivulinae, Cyprinodontidae, Pisces). *Journal of Zoological Systematics and Evolutionary Research*, *10*(1), 180–209.

Schier, A. F. (2007). The Maternal-Zygotic Transition: Death and Birth of RNAs. *Science*, *316*, 406–407.

Scholpp, S., Groth, C., Lohs, C., Lardelli, M., & Brand, M. (2004). Zebrafish fgfr1 is a member of the fgf8 synexpression group and is required for fgf8 signalling at the midbrain-hindbrain boundary. *Development Genes and Evolution, 214*(6), 285–295.

Schulte-Merker, S., Ho, R. K., Herrmann, B. G., & Nüsslein-Volhard, C. (1992). The protein product of the zebrafish homologue of the mouse T gene is expressed in nuclei of the germ ring and the notochord of the early embryo. *Development*, *116*(4), 1021–1032.

Schulte-Merker, S., van Eeden, F. J., Halpern, M. E., Kimmel, C. B., & Nüsslein-Volhard, C. (1994). no tail (ntl) is the zebrafish homologue of the mouse T (Brachyury) gene. *Development , 120*, 1009–1015.

Schultz, J. E. J., Witt, S. A., Nieman, M. L., Reiser, P. J., Engle, S. J., Zhou, M., … Doetschman, T. (1999). Fibroblast growth factor-2 mediates pressure-induced hypertrophic response. *Journal of Clinical Investigation, 104*(6), 709–719.

Shi, Y., Lan, F., Matson, C., Mulligan, P., Whetstine, J. R., Cole, P. A., … Shi, Y. (2004). Histone demethylation mediated by the nuclear amine oxidase homolog LSD1. *Cell*, *119*(7), 941–953.

Shimada, A., Yabusaki, M., Niwa, H., Yokoi, H., Hatta, K., Kobayashi, D., & Takeda, H. (2008). Maternal-zygotic medaka mutants for fgfr1 reveal its essential role in the migration of the axial mesoderm but not the lateral mesoderm. *Development*, *135*, 281–290.

Shimizu, T., Yamanaka, Y., Nojima, H., Yabe, T., Hibi, M., & Hirano, T. (2002). A novel repressor-type homeobox gene, ved, is involved in dharma/bozozok-mediated dorsal organizer formation in zebrafish. *Mechanisms of Development*, *118*(1-2), 125–138.

Shimomura, A., & Hashino, E. (2103). Epigenetic Regulation of Neural Differentiation from Embryonic Stem Cells. *In Trends in Cell Signaling Pathways in Neuronal Fate Decision* (p. 325).

Shinya, M., Koshida, S., Sawada, a, Kuroiwa, a, & Takeda, H. (2001). Fgf signalling through MAPK cascade is required for development of the subpallial telencephalon in zebrafish embryos. *Development*, *128*, 4153–4164.

Stainier, D. Y. R., Kontarakis, Z., & Rossi, A. (2015). Making sense of anti-sense data. *Developmental Cell, 32*(1), 7–8.

Stainier, D. Y. R., Raz, E., Lawson, N. D., Ekker, S. C., Burdine, R. D., Eisen, J. S.& Moens, C. B. (2017). Guidelines for morpholino use in zebrafish. *PLoS Genetics, 13*(10), 6–10.Stern, C. D. (2005). Neural induction: old problem, new findings, yet more questions. *Development*, *132*(9), 2007–21.

Stern, C. D. (2006). Neural induction: 10 years on since the “default model.” *Current Opinion in Cell Biology*, *18*(6), 692–697.

Streit, A., Berliner, A. J., Papanayotou, C., Sirulnik, A. and Stern, C. D. (2000). Initiation of neural induction by FGF signalling before gastrulation. In *Nature* (406th ed., pp. 74–78).

Sucar, S., Moore, G. L., Ard, M. E., & Ring, B. C. (2016). A Simultaneous Genetic Screen for Zygotic and Sterile Mutants in a Hermaphroditic Vertebrate (Kryptolebias marmoratus). *Genes|Genomes|Genetics*, *6*, 1107–1119.

Tadros, W., & Lipshitz, H. D. (2009). The maternal-to-zygotic transition: a play in two acts. *Development*, *136*(18), 3033–3042.

Talbot, W. S., Trevarrow, B., Halpern, M. E., Melby, E., Farr, G., Postlethwait, J. H., Jowett,T., Kimmel, C., & Kimelman, D. (1995). A homeobox gene essential for zebrafish notochord development. *Nature,378,*150-157.

Tanaka, T., Saika, S., Ohnishi, Y., Ooshima, A., McAvoy,J., Liu, C., Azhar,M., Doetschman, T., & Yang Kao, W. (2004). Fibroblast growth factor 2: roles of regulation of lens cell proliferation and epithelial-mesenchymal transition in response to injury. *Molecular Vision, 10*, 462–467

Tatarenkov, A., Ring, B. C., Elder, J. F., Bechler, D. L., & Avise, J. C. (2010). Genetic composition of laboratory stocks of the self-fertilizing fish Kryptolebias marmoratus: A valuable resource for experimental research. *PLoS ONE*, *5*(9), 1–9.

Taylor, S., Davis, W., & Bruce, T. (1995). Rivulus-Marmoratus - Ecology of Distributional Patterns in Florida and the Central Indian River Lagoon. *Bulletin of Marine Science*, *57*(1), 202–207.

Taylor, D.S., Fisher, M.T. & Turner, B. . (2001). Homozygosity and Heterozygosity in three Populations of *Rivulus marmoratus*. *Environmental Biology of Fishes*, *61*(4), 455–459.

Taylor, D. S. (2012). Twenty-four years in the mud: What have we learned about the natural history and ecology of the mangrove rivulus, kryptolebias marmoratus? *Integrative and Comparative Biology*, *52*(Costa 2011), 724–736.

Thisse, B., & Thisse, C. (2005). Functions and regulations of fibroblast growth factor signaling during embryonic development. *Developmental Biology*, *287*(2), 390–402.

Thisse, B., Thisse, C., & Weston, J. A. (1995). Novel FGF receptor (Z-FGFR4) is dynamically expressed in mesoderm and neurectoderm during early zebrafish embryogenesis. *Developmental Dynamics : An Official Publication of the American Association of Anatomists*, *203*(3), 377–391.

Varga, M., Maegawa, S., Bellipanni, G., & Weinberg, E. S. (2007). Chordin expression, mediated by Nodal and FGF signaling, is restricted by redundant function of two β-catenins in the zebrafish embryo. *Mechanisms of Development*, *124*(9-10), 775–791.

Varga, M., Maegawa, S., & Weinberg, E. S. (2011). Correct anteroposterior patterning of the zebrafish neurectoderm in the absence of the early dorsal organizer. *BMC Developmental Biology*, *11*(1), 26.

Vastenhouw, N. L., Zhang, Y., Woods, I. G., Imam, F., Regev, A., Liu, X. S., Rinn, j., & Schier, A. F. (2010). Chromatin signature of embryonic pluripotency is established during genome activation. *Nature*, *464*(7290), 922–926.

Veldman, M., & Lin, S. (2008). Zebrafish as a Developmental Model Organism for Pediatric Research. *Developmental Biology*, *64*(5), 470–476.

Vinuela, P. F. (2008). *The role of Fibroblast Growth Factor Signalling on the Regulation of Embryonic Stem cells*. A thesis of Doctor of Philosopy at the University of Edinburgh,297.

Wardle, F. C., & Tan, H. (2017). A ChIP on the shoulder? Chromatin immunoprecipitation and validation strategies for ChIP antibodies. *F1000Research, 235*, 1–10.

Webb, S. E., Lee, K. K. H., Tang, M. K., & Ede, D. A. (1997). Fibroblast growth factors 2 and 4 stimulate migration of mouse embryonic limb myogenic cells. *Developmental Dynamics*, *209*(2), 206–216.

Wilson, S. I., Graziano, E., Harland, R., Jessell, T. M. and Edlund, T. (2000). An early requirement for FGF signalling in the acquisition of neural cell fate in the chick embryo. In *Curr. Biol.* (10th ed., pp. 421–429).

Wittbrodt, J., Shima, A., & Schartl, M. (2002). Medaka — a model organism from the far east. *Nature Reviews Genetics*, *3*, 53–64.

Wolpert, L., Tickle, C., Jessel, T., Lawrence, P., Meyerowitz, E., Roberston, E., & Smith, J. (2011). *Principles of Development*. (L. Wolpert & C. Tickle, Eds.) (Forth). Oxford University Press, USA.

Wong, T., & Collodi, P. (2013). Biochemical and Biophysical Research Communications Effects of specific and prolonged expression of zebrafish growth factors , Fgf2 and Lif in primordial germ cells in vivo. *Biochemical & Biophysical Research Communications, 430*(1), 347–351.

Woo, K., Shih, J., & Fraser, S. E. (1995). Fate maps of the zebrafish embryo. *Current Opinion in Genetics and Development*, *5*(4), 439–443.

Wright, P. A. (2012). Environmental physiology of the mangrove rivulus, kryptolebias marmoratus, a cutaneously breathing fish that survives for weeks out of water. *Integrative and Comparative Biology*, *52*(6), 792–800.

Xu, C., Fan, Z. P., Müller, P., Fogley, R., DiBiase, A., Trompouki, E.& Zon, L. I. (2012). Nanog-like Regulates Endoderm Formation through the Mxtx2-Nodal Pathway. *Developmental Cell, 22*(3), 625–638.

Yabe, T., & Takada, S. (2012). Mesogenin causes embryonic mesoderm progenitors to differentiate during development of zebrafish tail somites. *Developmental Biology*, *370*(2), 213–222.

Yamanaka, Y., Tamplin, O. J., Beckers, A., Gossler, A., & Rossant, J. (2007). Live Imaging and Genetic Analysis of Mouse Notochord Formation Reveals Regional Morphogenetic Mechanisms. *Developmental Cell*, *13*(6), 884–896.

Yokoi, H., Shimada, A., Carl, M., Takashima, S., Kobayashi, D., Narita, T. & Takeda, H. (2007). Mutant analyses reveal different functions of fgfr1 in medaka and zebrafish despite conserved ligand-receptor relationships. *Developmental Biology*, *304*, 326–337.

Yoo, K.-W., Kim, C.-H., Park, H.-C., Kim, S.-H., Kim, H.-S., Hong, S.-K. & Huh, T. L. (2003). Characterization and expression of a presomitic mesoderm-specific mespo gene in zebrafish. *Development Genes and Evolution*, *213*(4), 203–206.

Yoon, J. K., & Wold, B. (2000). The bHLH regulator pMesogenin1 is required for maturation and segmentation of paraxial mesoderm. *Genes & Development*, *14*, 3204–3214.

Yu, P.B., Hong, C.C., Sachidanandan, C., Babitt, J.L., Deng, D.Y., Hoyng, S.A., L., & H.Y., Bloch, K.D. & Peterson, R. T. (2007). The small molecule dorsomorphin inhibits BMP signals required for embryogenesis and iron metabolism. In *Nat Chem. Biol.* (4th ed., pp. 33– 41).

Zhang, Y., & Reinberg, D. (2001). Transcription regulation by histone methylation: Interplay between different covalent modifications of the core histone tails. *Genes and Development, 15*(18), 2343–2360.

Zhou, M., Sutliff, RL., Paul, RJ., Lorenz, JN., Hoying, JB., Haudenschild, CC., Yin M., Cof fin, JD., Kong, L., Kranias, EG., Luo, W., Boivin, GP., Duffy, JJ., Pawlowski, S.A.&Doetschman, T. (1998) Fibroblast growth factor 2 control of vascular tone. *Nat Med 4*:201–207.

Appendix

Material and method

Animal cap dissection and culture

Prior to dissection, embryos were dechorinated with Pronase (1mg/ml, Sigma-Aldrich) in 1x Ringer's solution (zebrafish book) on an agarose bed. Subsequent to Pronase treatment, embryos were washed four times with 1x Ringer's solution and then put in fish water (treated or untreated), still on agarose. Control (untreated/uninjected) embryos, embryos which were injected only and embryos whose caps were exposed from the MBT were dechorinated at the eight cell stage. For exposures from the 1 cell stage embryos were exposed either to SU5402, PD173074, DM, or to both. All embryos were allowed to develop at 28°C until the 256/512 cell stage when the animal caps were dissected (prior to the MBT). Except where treatment was from the 1 cell stage to fixation, all dissection was done in 0.5% methyl cellulose/1xRinger with great care being taken to avoid cells close to the margin. For treatments from the 1 cell stage to fixation, dissection took place in the treated fish water. The caps were then transferred to a different dish with the same concentration of chemical prepared together with that of the first dish. For treatments from the 1 cell stage to the MBT, embryos were first washed four times with fish water prior to dissection. For treatments from the MBT, the animal caps were first dissected then placed in treated water. All caps were transferred to 24 well plates (in treated or untreated fish water) after a ten minute recovery period, with a maximum of 20 caps per well, and allowed to develop to fixation.

SU5402 (Sigma-Aldrich SML0443) was added to the embryo medium at a final concentration of 20 µM when embryos were at 2 cells stage. When they

reached 1K cells stage, the treatment was washed off with fresh medium. Control embryos were incubated with the same volume of DMSO (dimethyl sulfoxide, Sigma-Aldrich D8418, SU5402 carrier) during the same period. Embryos were raised until dome stage, when RNA-seq and ATAC-seq experiments were performed.

For both techniques, RNA-seq and ATAC-seq, two biological replicates of each condition were performed, with unexposed embryos and embryos treated with SU5402.

RNA-seq

Total RNA was isolated at the dome stage from the unexposed and SU5402 (80uM) treated embryos (duplicated). cDNA was synthesised and analysed with RNA-seq in one lane of the next generation sequencer Illumina HiSeq2500 with 100bp paired end reading.

The sequencing data were first trimmed to remove sequencing adaptors, low quality terminal ends (<Q20) and short sequences using fastq-mcf v1.1.2-537 (Aronesty, 2011). *De-novo* transcriptome assembly was performed for each of the groups using Trinity v v2.2.0 (Haas *et al*., 2013).

For expression levels analysis:

HISAT2 (Kim *et al*., 2015) was used to align the filtered reads against the *Danio rerio* genome Zv9._assembly (Ensembl) obtained from iGenomes (Illumina). Gene expression levels were quantified using HTSeq (Anders *et al*., 2015) and differential expression analysis between the two groups was performed using DESeq2 (Love *et al.*, 2014).

For mutation analysis:

Variants between the groups (mutants, siblings and wild type) were identified and quantified using KisSplice v2.4.0-p1 (Lopez-Maestre *et al*., 2016) with a k-mer size of 53. The variants identified by KisSplice were mapped to the *de novo* transcriptomes with BLASTn v2.5.0 (Altschul *et al*., 1990) to obtain the associated transcript. The transcripts containing variants were then annotated with BLASTn to NCBI-nr (downloaded Nov 11, 2016) with an e-value threshold of 1e-4, keeping only the best hit. To identify candidate mutation related variations we filtered the list of variations produced by KisSplice with custom scripts, applying the following criteria: 0 % of reads in the WT group compared to 100 % of reads in mutant group, with the sibling group being intermediate. RNA sequencing analysis for zebrafish animal cap and mangrove killifish were done by Paul A. O'Neill (University of Exeter).

ATAC-seq

ATAC-seq experiments were performed as previously described (Buenrostro et al., 2015), with minor modifications. Briefly, 100 embryos were dechorionated and disrupted in 500 µl of Ginzburg Fish Ringers (55 mM NaCl, 1.8 mM KCl, 1.25 mM NaHCO3). Cells were lysed (lysis buffer: 10 µM Tris pH7.4, 10 µM NaCl, 3 µM MgCl2, 0.1% IGEPAL) and incubated for 30 min at 37ºC with the TDE1 enzyme. The sample was then purified with Qiagen Minelute kit, and a PCR was performed with 13 cycles using Ad1F and Ad2.1R primers and KAPA HiFi hotstart enzyme (Kapa Biosystems). The resulting library was sequenced in aIllumina Hiseq 2000 pair-end lane. Reads were aligned with Bowtie2 software (Langmead B, Salzberg S. *Nature Methods*. 2012, 9:357-359), using zebrafish assembly danRer7 (July 2010) as reference genome. Duplicated pairs or those separated by more than 2Kb were removed. The enzyme cleavage site

was determined as the position -4 (minus strand) or +5 (plus strand) from each read start, and this position was extended 5 bp in both directions.

ATAC-seq experiments in unexposed embryos and embryos treated with SU5402 yielded, when concatenated and merged, a total number of peaks of 680422, using MACS2 with the parameters --nomodel --shift 50 --extsize 100. Then we calculated the number of ATAC peaks from each sample (two replicates of wild type and two replicates of SU5402 treated embryos) that overlapped each of these peaks. This produced a 4x680422 matrix that was analyzed for differential accesibility using the program *Cuffdiff*, from *Cufflinks* software package (Trapnell et al., *Nature Biotechnology*, 2010).

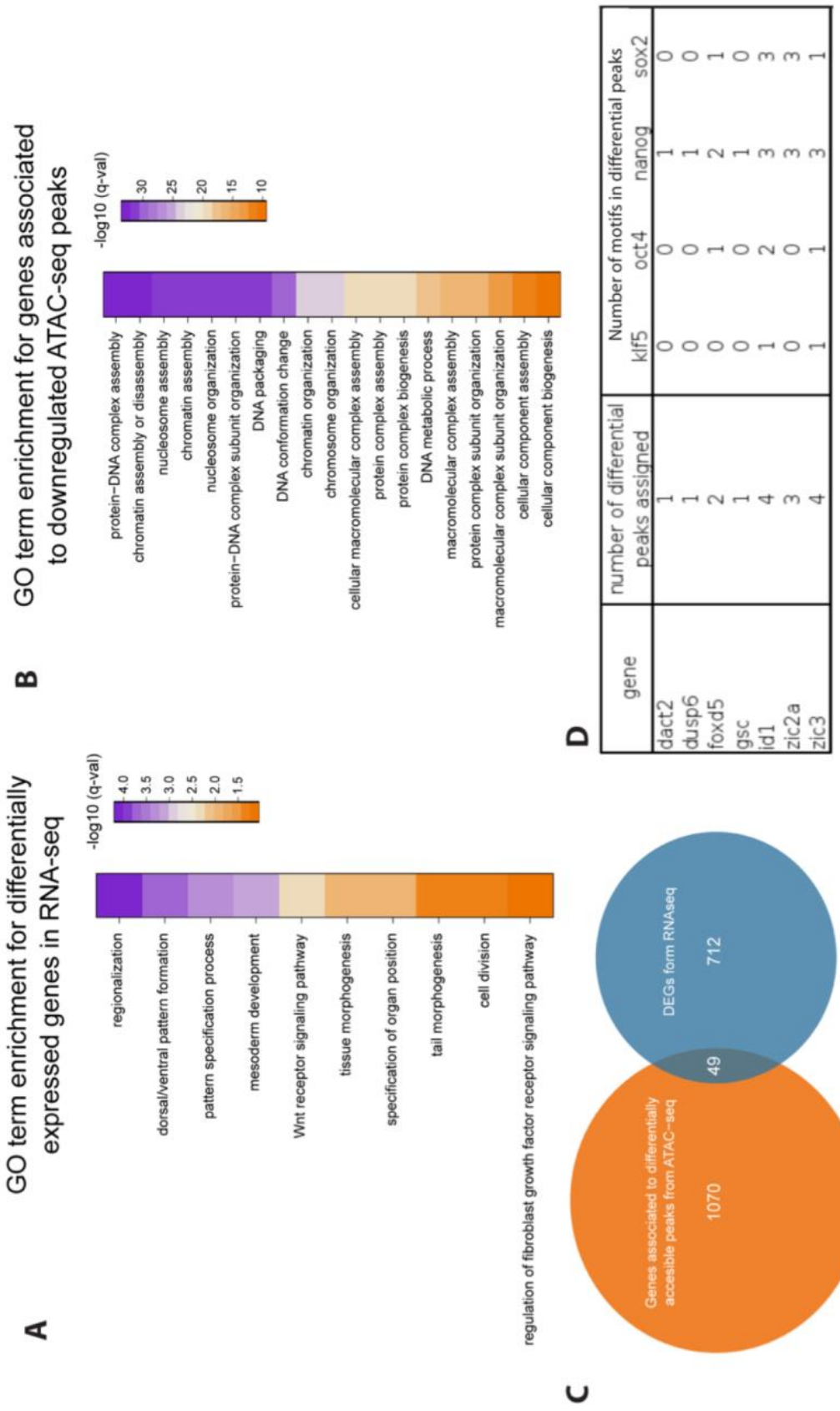

gene	number of differential peaks assigned	Number of motifs in differential peaks			
		klf5	oct4	nanog	sox2
dact2	1	0	0	1	0
dusp6	1	0	0	1	0
foxd5	2	0	1	2	1
gsc	1	0	0	1	0
id1	4	1	2	3	3
zic2a	3	0	0	3	3
zic3	4	1	1	3	1

Figure 1. RNA-seq and ATACseq identify genes affected by pre-MZT FGFR signalling. A. Gene ontology (GO) enrichment analysis of the downregulated genes by

pre-MZT SU5402 treatment with RNA-seq showed enrichment terms related to early development processes such as regionalization, pattern formation, pattern specification and mesoderm development. B. Embryos treated with or without SU5402 from one cell stage onward were analysed using ATAC-seq to determine the genomic regions that showed differences in ATAC signal between the control and the SU5402 treated embryos. The genes associated with the downregulated ATAC peaks showed strong enrichment for GO terms related to chromatin assembly and nuclear organization. C. Number of differentially expressed genes from the RNA-seq and genes associated to ATAC peaks downregulated after SU5402 treatment. There are 49 common genes identified from the both lists. D. Some representatives of the 49 genes in C: Many of these genes showed multiple ATAC peak and associated cis elements for pluripotent stem cell factors (Nanog, Sox2, Klf5 and Pou5f3) in their vicinity affected by the reduction of the FGF signalling.

Table 1. List of genes downregulated by SU5402 with downregulated ATAC-seq peaks

Gene_id	Gene name	Locus	Control	SU5402	log2 (fold change)	p_value
XLOC_033433	zic2a	9:32307415-32347632	8.85475	0.250185	-5.14539	0.00185
XLOC_005517	dact2	13:44029502-44036259	11.5228	1.06819	-3.43125	5.00E-05
XLOC_003611	id1	11:19124534-19125635	204.415	30.3986	-2.74942	5.00E-05
XLOC_028819	atp1b1a	6:28931187-28941283	38.27	10.2558	-1.89977	5.00E-05
XLOC_023038	si:dkey-56d12.4 (beta-parvin?)	3:15047005-15048990	4.42132	1.26702	-1.80304	0.002
XLOC_029956	zgc:114037 (histon H2a)	7:7234272-7236228	6.55817	2.26687	-1.53259	0.0035
XLOC_025149	prickle1b	4:12957296-13060290	25.4358	9.62106	-1.40259	0.00365
XLOC_026283	zgc:173702 (zinc finger protein 568)	4:54126518-54136531	2.88646	1.16954	-1.30337	0.0061
XLOC_027864	gas1b	5:33997953-34000987	5.39918	2.22144	-1.28124	0.0006
XLOC_001826	prkab1a	10:17966646-17976383	4.93359	2.27243	-1.1184	0.01405
XLOC_013764	stard3nl (endosomal choresterol transport)	2:31556297-31571329	22.5614	11.876	-0.925804	0.00035
XLOC_017283	mat2b (methionine adenosyltransferase 2B)	21:30832204-30849421	16.9406	9.03773	-0.906451	0.0022
XLOC_004634	cyp26a1	12:9708962-9712555	41.2974	22.6864	-0.864221	5.00E-05
XLOC_015706	znf770	20:10244835-10252216	20.0784	11.1915	-0.843244	0.0001
XLOC_001460	si:ch211-286b5.5	1:55803827-55810769	36.047	20.3017	-0.828283	0.0034
XLOC_014179	prkacbb	2:2617660-2642068	6.59621	3.72501	-0.824393	0.0145
XLOC_000897	actb1	1:7725182-7728816	282.208	188.656	-0.581001	0.00075
XLOC_006666	pcdh1b	14:38820051-39059088	42.6204	30.3674	-0.489023	0.00915

XLOC_023039	spns1	3:15059912-15079761	94.2287	68.0684	-0.469182	0.01325
XLOC_022531	fscn1a	3:40571228-40584271	103.648	76.5267	-0.43766	0.013
XLOC_017837	klf2a	22:16044380-16047079	31.7609	45.9664	0.533327	0.00835
XLOC_013813	ing5b	2:36326363-36329552	137.707	200.505	0.542035	0.0042
XLOC_019685	si:dkey-188c14.4	23:25378537-25386361	104.65	154.337	0.560513	0.00215
XLOC_017758	blf	22:9996997-10045005	251.485	374.602	0.574891	0.0027
XLOC_002065	rab6a	10:37939677-37955780	17.0706	25.7937	0.595507	0.011
XLOC_019517	krt8	23:10355853-10360516	69.1623	106.412	0.621609	0.0014
XLOC_022419	rnf25	3:32808121-32817102	24.9226	39.9552	0.68093	0.0094
XLOC_013796	astn1	2:34291014-34703231	18.8851	30.7115	0.701531	0.0067
XLOC_027247	polr2j	5:64522040-64527647	88.9061	145.079	0.706482	0.0015
XLOC_001971	ptrh2	10:28988529-28991098	26.2956	44.7967	0.76857	0.00335
XLOC_000926	tnrc5	1:9554752-9796562	87.8816	151.757	0.788133	0.00225
XLOC_013841	parp2	2:37536468-37585260	36.9115	64.9544	0.815358	0.0028
XLOC_018241	calr	22:4339289-4410265	62.3562	116.083	0.896549	5.00E-05
XLOC_000408	dclk2	1:36945213-37157447	2.42099	4.71364	0.961246	0.013
XLOC_022589	mrpl12	3:47698985-47733072	28.8288	57.2678	0.990214	0.002
XLOC_009123	pabpc1a	16:58353268-58375366	423.932	893.973	1.0764	0.0003
XLOC_033123	sp3a	9:2760722-2780996	25.138	55.845	1.15156	0.00315
XLOC_030902	zfand6	7:11382753-11695541	49.8556	120.163	1.26916	5.00E-05

XLOC_002705	zgc:113625	10:42151827-42185386	0.780451	3.01801	1.95122	0.0009
XLOC_033022	tbx16	8:54012014-54031716	634.234	2679.89	2.07909	5.00E-05

Table 2. List of downregulated genes from RNA-seq in SU5402 treated dome stage zebrafish embryos

Gene_id	Gene name	Locus	Control	SU5402	log2 (fold_change)	p_value
XLOC_033433	zic2a	9:32307415-32347632	8.85475	0.250185	-5.14539	0.00185
XLOC_032018	foxd5	8:31300986-31302137	29.7986	0.870987	-5.09645	5.00E-05
XLOC_020023	-	24:3248942-3251848	13.1589	0.870875	-3.91743	5.00E-05
XLOC_008434	chd	15:46135866-46173294	14.8258	1.12629	-3.71846	5.00E-05
XLOC_010622	gsc	17:19172353-19175674	9.50265	0.86619	-3.45557	0.0001
XLOC_005517	dact2	13:44029502-44036259	11.5228	1.06819	-3.43125	5.00E-05
XLOC_002310	ca9	10:8401150-8440123	8.68257	0.92627	-3.22862	5.00E-05
XLOC_021813	foxb1.2	25:35200980-35202962	3.93178	0.428217	-3.19877	0.00155
XLOC_021648	dusp6	25:18813587-18817793	18.1931	2.13183	-3.09322	5.00E-05
XLOC_019727	sp5l	23:28267501-28270357	2.76833	0.389396	-2.82971	0.00325
XLOC_000064	spry2	1:4170918-4175021	3.51744	0.507504	-2.79303	0.00245
XLOC_003611	id1	11:19124534-19125635	204.415	30.3986	-2.74942	5.00E-05
XLOC_026377	si:dkey-256e21.1	4:57299404-57304814	8.79426	1.33225	-2.7227	0.0019
XLOC_013117	ntla	19:30633856-30637924	20.3044	3.24556	-2.64525	5.00E-05
XLOC_028741	-	6:22213497-22214102	32.4539	5.20982	-2.63909	0.0003
XLOC_029958	ENSDARG00000088259	7:7240067-7240994	10.705	1.7463	-2.61592	0.0019

XLOC_028805	amotl2a	6:27700162-27709318	21.0842	3.5945	-2.5523	5.00E-05
XLOC_028549	-	6:3874829-3875211	92.2805	16.257	-2.50497	5.00E-05
XLOC_023024	nfil3-6	3:13889404-13895597	2.78363	0.493434	-2.49604	5.00E-05
XLOC_027243	SNORA18,SNORA32,si:ch211-209a2.1	5:64397557-64418836	30.6208	5.53074	-2.46897	5.00E-05
XLOC_020582	zgc:112332	24:18997212-19016351	26.82	5.45753	-2.29699	5.00E-05
XLOC_001381	spred2a	1:51953388-51983814	1.75389	0.364064	-2.26829	0.00215
XLOC_019018	avpr2ab	23:18697745-18714285	2.03281	0.446451	-2.1869	0.013
XLOC_031203	tph1b	7:34440475-34449394	4.51986	1.00479	-2.16938	0.0004
XLOC_017982	-	22:25138396-25139659	11.0653	2.48568	-2.15433	0.00035
XLOC_021359	-	25:36014310-36015058	11.9003	2.83424	-2.06996	0.0102
XLOC_008717	efna1b	16:25521947-25537442	9.42636	2.25073	-2.06631	5.00E-05
XLOC_021556	si:ch211-157d2.1	25:9927233-10194750	72.4019	17.3439	-2.0616	0.01025
XLOC_018802	-	22:42183705-42186436	6.73296	1.63967	-2.03784	0.001
XLOC_021874	zgc:173552	25:37401186-37403067	16.2928	4.02734	-2.01634	0.013
XLOC_000757	si:ch211-114l13.11	1:58613858-58617962	6.11519	1.53228	-1.99672	0.0007
XLOC_009329	ngfr	16:18366505-18392144	2.69202	0.690123	-1.96376	0.00025
XLOC_028819	atp1b1a	6:28931187-28941283	38.27	10.2558	-1.89977	5.00E-05
XLOC_012973	-	19:20674305-20681457	8.73313	2.3777	-1.87693	0.00035
XLOC_027121	papd4	5:53911219-53925762	2.07376	0.575698	-1.84887	0.0069
XLOC_023038	si:dkey-56d12.4	3:15047005-15048990	4.42132	1.26702	-1.80304	0.002

XLOC_017056	-	21:13037353-13038544	10.1353	2.92986	-1.79048	0.00445
XLOC_000558	morc3b	1:47675504-47702364	8.85323	2.56472	-1.7874	0.0002
XLOC_027571	-	5:13049700-13050338	19.6017	5.76673	-1.76515	0.0013
XLOC_019908	cyp2aa8	23:42910749-42919521	9.5351	2.82313	-1.75595	5.00E-05
XLOC_016068	si:dkey-14a7.2	20:43428286-43434551	9.67259	2.89752	-1.73908	0.0001
XLOC_005424	arg2	13:33248148-33257976	13.2235	4.04045	-1.71051	5.00E-05
XLOC_000329	zic2b	1:28776998-28806135	145.43	44.9066	-1.69532	5.00E-05
XLOC_022703	-	3:58795593-58798348	2.60874	0.813297	-1.6815	0.0043
XLOC_010282	-	17:40014626-40026667	7.49024	2.34267	-1.67686	0.0098
XLOC_026823	histh1l	5:29077506-29078900	27.893	8.77339	-1.6687	5.00E-05
XLOC_004251	etv4	12:29107012-29139727	20.3082	6.40791	-1.66414	5.00E-05
XLOC_012906	cited4a	19:15283259-15287461	3.11137	1.02899	-1.59631	0.00095
XLOC_005321	si:ch211-223p8.8,zgc:153981	13:25053885-25061867	23.4128	7.7607	-1.59304	5.00E-05
XLOC_003575	zgc:173544	11:16402586-16406187	38.0255	12.7464	-1.57687	5.00E-05
XLOC_007242	-	14:46990938-46991549	23.1792	7.84582	-1.56284	0.0016
XLOC_021842	HIST2H3A	25:36200454-36212336	22.4742	7.70581	-1.54425	0.002
XLOC_013054	si:dkey-119m17.2	19:25920317-25950008	12.5545	4.3105	-1.54228	0.0016
XLOC_016956	rnf165a	21:5210079-5246602	21.6851	7.44862	-1.54166	0.0003
XLOC_029956	zgc:114037	7:7234272-7236228	6.55817	2.26687	-1.53259	0.0035
XLOC_003972	g6pc3	12:3895082-3904611	4.03642	1.40785	-1.51959	0.0142

XLOC_018553	si:dkey-42p8.3	22:21994397-22077298	6.6121	2.3305	-1.50447	0.00845
XLOC_016323	WDR7	21:2916640-3024116	12.4571	4.40944	-1.49831	0.00875
XLOC_011301	rgma	18:24703308-24715755	8.75645	3.11096	-1.49299	5.00E-05
XLOC_008568	ECM1 (2 of 2)	16:11307840-11319401	11.9515	4.32502	-1.46641	0.00015
XLOC_020234	adipoqa	24:27037667-27075959	3.14306	1.14928	-1.45144	0.01045
XLOC_019763	hmgn3	23:31595509-31611386	5.62182	2.05692	-1.45055	0.0052
XLOC_005995	erlec1	13:36152190-36166520	3.9244	1.44595	-1.44045	0.00055
XLOC_016968	ccng2	21:5787527-5818644	6.76755	2.49787	-1.43794	0.011
XLOC_007708	CT573389.1	15:34229853-34234424	7.7657	2.87044	-1.43584	0.00835
XLOC_020510	fam49bb,si:dkeyp-105g12.2	24:10593571-10673581	28.5046	10.7017	-1.41336	0.0067
XLOC_031375	rps4x	7:53088994-53094879	423.368	158.963	-1.41322	5.00E-05
XLOC_034359	-	Zv9_NA130:27182-28827	4.26672	1.61343	-1.403	0.0097
XLOC_025149	prickle1b	4:12957296-13060290	25.4358	9.62106	-1.40259	0.00365
XLOC_016932	-	21:4333256-4333654	47.935	18.1456	-1.40146	0.0005
XLOC_005415	osr1	13:32367971-32374045	3.7671	1.45199	-1.37543	0.0049
XLOC_012054	CABZ01070258.1	18:48164013-48172873	113.301	44.2278	-1.35714	5.00E-05
XLOC_013137	arl4ab	19:32584702-32587248	10.5374	4.12069	-1.35457	0.00025
XLOC_029182	-	6:1713354-1717445	23.166	9.06554	-1.35354	5.00E-05
XLOC_031938	sypl2b	8:25932412-25943401	6.62235	2.6563	-1.31793	0.00185
XLOC_007257	wu:fb52c12	14:48305291-48334532	1.99551	0.802413	-1.31434	0.0078

XLOC_026283	zgc:173702	4:54126518-54136531	2.88646	1.16954	-1.30337	0.0061
XLOC_029002	slc25a22	6:49036235-49047646	95.6213	38.8031	-1.30116	5.00E-05
XLOC_032504	ndufb11	8:14697014-14701374	10.1988	4.15923	-1.29402	0.01335
XLOC_008777	CBLC,CR391937.2	16:27999755-28051944	4.60906	1.88029	-1.29352	0.0022
XLOC_015388	si:ch211-102b16.4	20:42030495-42234969	71.6541	29.2443	-1.29289	0.00705
XLOC_027864	gas1b	5:33997953-34000987	5.39918	2.22144	-1.28124	0.0006
XLOC_009968	dact1	17:11022873-11032978	10.0785	4.15766	-1.27743	5.00E-05
XLOC_023422	si:dkey-106c17.1	3:38966482-38970139	5.19474	2.14476	-1.27624	0.00425
XLOC_017108	dusp4	21:18940396-18948418	12.1592	5.03198	-1.27286	0.0001
XLOC_031378	-	7:53207577-53212232	5.95893	2.47272	-1.26896	0.0009
XLOC_015303	ivns1abpa	20:34351481-34365791	2.32106	0.974753	-1.25168	0.00875
XLOC_028159	gas1a	5:46112803-46115387	4.83703	2.03534	-1.24885	0.00175
XLOC_004389	zgc:111868	12:44350787-44354919	29.2668	12.5647	-1.21989	0.00045
XLOC_008954	ccne2	16:43241773-43250825	20.5118	8.81196	-1.21892	5.00E-05
XLOC_011671	-	18:7933997-7952174	10.2616	4.41978	-1.21521	0.0087
XLOC_003814	-	11:39946632-39947242	22.7119	9.88129	-1.20068	0.0076
XLOC_022547	BX682557.1	3:42728292-42774174	2.52303	1.10104	-1.19629	0.0006
XLOC_008171	tlcd2	15:24726994-24765751	3.5673	1.56946	-1.18456	0.0017
XLOC_027022	si:dkey-193c22.2	5:41850066-41876175	2.37339	1.04696	-1.18074	0.0002
XLOC_027503	-	5:6291872-6400118	7.99404	3.62275	-1.14184	0.0002

XLOC_020581	sec61g	24:18835531-18995709	104.321	47.6464	-1.1306	0.0002
XLOC_006181	SS18L2	13:52334010-52336258	13.5003	6.21338	-1.11954	0.0047
XLOC_001826	prkab1a	10:17966646-17976383	4.93359	2.27243	-1.1184	0.01405
XLOC_022516	cln3	3:39574174-39594121	8.06872	3.72112	-1.1166	0.0041
XLOC_014558	ptch2	2:33685223-33711585	3.47015	1.60474	-1.11266	0.00025
XLOC_019125	si:dkey-151g10.6	23:25592769-25593942	100.901	46.8106	-1.10804	5.00E-05
XLOC_000361	hdhd1	1:31882590-31926772	8.51141	3.95168	-1.10693	0.00485
XLOC_013100	irx1b	19:28613318-28623012	3.66105	1.70308	-1.10411	0.0118
XLOC_027801	NPDC1 (2 of 2)	5:30510350-30552939	3.94564	1.8364	-1.10337	0.0145
XLOC_008936	trhra	16:41423503-41492749	4.84818	2.26225	-1.09969	0.00755
XLOC_032452	pim1	8:10910935-10914660	8.05573	3.77079	-1.09515	0.001
XLOC_002632	-	10:38807656-38820905	29.1977	13.7359	-1.08791	0.00285
XLOC_001845	r3hcc1	10:20426571-20482737	4.35021	2.05523	-1.08178	0.0091
XLOC_009534	dgat1b	16:33252008-33304285	8.34267	3.95253	-1.07773	0.01035
XLOC_008030	rab34a	15:14475910-14488111	9.29888	4.40578	-1.07766	0.00295
XLOC_023161	kpna2	3:25471233-25478328	13.3979	6.41551	-1.06237	0.0013
XLOC_023142	atp5g1	3:23890532-23895475	156.819	75.2494	-1.05935	5.00E-05
XLOC_021397	si:ch211-113a14.12	25:37363668-37364539	35.0772	16.9731	-1.04728	5.00E-05
XLOC_000341	metap1d	1:30002487-30030422	9.56428	4.65675	-1.03833	0.0078
XLOC_018676	BX510935.1	22:31134153-31142375	9.01818	4.39113	-1.03824	0.0046

XLOC_004319	sfxn2	12:35471297-35485230	35.6747	17.4061	-1.0353	0.0026
XLOC_009432	ELMO1 (2 of 2)	16:26840278-26884886	43.1434	21.0541	-1.03504	0.00045
XLOC_012404	rpa3	19:25950689-25952850	102.077	50.2163	-1.02343	0.0001
XLOC_010883	-	17:44050834-44057456	6.29769	3.11551	-1.01535	0.0014
XLOC_018057	pla2g6	22:31659137-31698605	7.49623	3.70988	-1.01479	0.0147
XLOC_030494	ccnd1	7:54575138-54584681	208.432	103.215	-1.01392	5.00E-05
XLOC_028165	crfb6	5:47501038-47506460	7.34479	3.65834	-1.00553	0.00415
XLOC_006114	-	13:46284424-46293003	4.16454	2.07466	-1.00528	0.00015

Table 3. ATAC-seq peaks downregulated in SU5402 treated embryos

Peak	logFC	logCPM	F	P-value	FDR
chr17:5399809-5400144	-6.348132501	2.168193545	90.74123994	8.26E-21	5.62E-15
chr2:53655293-53655556	4.969166958	1.951903808	85.67686081	1.08E-19	3.67E-14
chr15:31176334-31176608	8.998511063	1.185862537	43.80366756	2.99E-19	6.78E-14
chr16:58385570-58385838	4.543364931	2.125372475	81.65185277	7.16E-19	1.22E-13
chr10:42194940-42195098	8.948974456	1.133987871	42.48342256	9.97E-19	1.36E-13
chr25:9720300-720610	8.850809435	1.037077987	40.02147472	9.40E-18	1.07E-12
chr7:3060509-3060956	5.350145265	1.356662723	72.51910738	5.26E-17	5.11E-12
chr2:49791898-49792129	5.049528791	1.380235543	69.6702136	2.17E-16	1.85E-11
chr15:26516153-26516351	5.54496493	1.151834065	67.60308681	4.71E-16	3.56E-11
chr2:12387515-12387795	8.653044942	0.807264905	34.63774599	1.23E-15	8.36E-11
chr12:33859946-33860325	3.557297579	2.634479151	65.14749798	1.46E-15	9.05E-11

chr13:52475260-52475728	3.746062932	2.187904969	65.49702899	1.86E-15	1.05E-10
chr1:37417377-37417994	-5.630364144	1.561603498	64.40442181	3.25E-15	1.70E-10
chr2:34337689-34337942	8.488147832	0.695109703	31.5408488	2.14E-14	1.03E-09
chr2:56732077-56732307	4.176988121	1.517882536	60.40114673	2.26E-14	1.03E-09
chr7:32384305-32384457	4.823581721	1.140286004	59.21396191	2.96E-14	1.26E-09
chr6:49670091-49670348	4.249726775	1.404487875	58.77495853	4.69E-14	1.88E-09
chr3:13957412-13957730	-5.448358218	1.394557568	57.65588855	8.07E-14	3.05E-09
chr7:35964638-35964766	4.956524373	1.004245466	55.863842	1.33E-13	4.76E-09
chr6:15204717-15204972	4.301183466	1.263105105	56.10537864	1.56E-13	5.11E-09
chr1:2120223-2120690	3.106602754	3.576929215	54.47304694	1.58E-13	5.11E-09
chr4:41624931-41625407	3.093343081	2.96124157	53.83306028	2.66E-13	8.21E-09
chr17:27782360-27782770	3.770098071	1.587730092	54.9619929	3.36E-13	9.95E-09
chr22:2087376-2087597	3.537027354	1.79634889	54.05079729	5.51E-13	1.56E-08
chr7:13421986-13422187	4.298003312	1.142867622	51.91439659	1.11E-12	3.03E-08
chr6:49452481-49452697	4.887087853	0.853743461	50.80501455	1.37E-12	3.59E-08
chr3:30385032-30385215	5.136040879	0.775816258	50.02548993	1.81E-12	4.57E-08
chr18:35742-36022	3.156571285	5.184851601	49.30364566	2.19E-12	5.33E-08
chr1:37873232-37873587	-8.475928555	0.90987174	26.45996803	4.72E-12	1.11E-07
chr22:37794187-37794565	4.385622496	0.967981563	48.5016132	5.05E-12	1.14E-07
chr22:37782063-37782294	-8.470962205	0.903730609	26.35604043	5.18E-12	1.14E-07
chr10:45425670-45425926	5.072008245	0.729817151	47.74448551	5.38E-12	1.14E-07

chr3:30371003-30371151	8.215595404	0.442296044	25.71521366	6.80E-12	1.40E-07
chr11:11548215-11548474	5.470785999	0.611792439	46.63170237	8.57E-12	1.67E-07
chr20:3934520-3934750	3.284293818	1.750581772	48.4465351	8.58E-12	1.67E-07
chr17:5398326-5398628	-3.491080044	1.936803527	48.28805584	9.29E-12	1.76E-07
chr10:2643472-2643873	-5.129558208	1.061546309	46.21192114	1.76E-11	3.24E-07
chr22:5252249-5253052	2.814279025	4.111102014	45.13621542	1.84E-11	3.29E-07
chr3:126097-126349	-3.224614417	2.308759773	46.35583806	2.13E-11	3.72E-07
chr1:58427653-58428245	-3.875413952	1.596210711	46.3177593	2.36E-11	3.96E-07
chr22:25826208-25826500	3.173024306	1.772077218	46.37118145	2.38E-11	3.96E-07
chr24:43116589-43117068	3.025092046	2.009314117	45.66274832	3.34E-11	5.41E-07
chr3:32491718-32491902	8.125934999	0.350071466	23.76718325	4.77E-11	7.54E-07
chr22:1927104-1927454	3.358508017	1.463409298	44.56787612	5.32E-11	8.22E-07
chr10:30818487-30819152	2.694035587	3.194345157	42.99521984	5.49E-11	8.30E-07
chr25:3184724-3185239	2.997250255	1.936914299	44.23730037	6.81E-11	1.01E-06
chr9:21032805-21033178	2.868903426	2.145854691	43.48067445	9.45E-11	1.37E-06
chr25:1327376-1327629	3.743200883	1.068755096	42.34163028	1.23E-10	1.74E-06
chr1:55814211-55814436	3.716715481	1.089034175	42.33841777	1.25E-10	1.74E-06
chr13:8497838-8498010	8.032677568	0.286967922	22.28630566	2.10E-10	2.85E-06
chr7:34499262-34499606	2.725775745	2.356906069	41.61878057	2.16E-10	2.89E-06
chr22:29645215-29645625	-4.960769206	0.913842773	40.81605365	2.27E-10	2.97E-06
chr22:5251748-5252021	3.689974111	1.046075183	40.82518312	2.57E-10	3.30E-06

chr2:57873734-57874114	-3.708078595	1.496798683	41.34958299	2.64E-10	3.33E-06
chr2:56985123-56985456	2.712383727	2.351610198	41.09324419	2.82E-10	3.49E-06
chr22:24247949-24248466	-4.906268543	0.932295292	40.02988949	3.44E-10	4.17E-06
chr1:58680177-58680452	-2.929833426	2.326808575	40.51680258	3.80E-10	4.53E-06
chr19:42741350-42741527	5.964560802	0.328750724	39.08485216	4.06E-10	4.76E-06
chr7:5322190-5322529	3.65740091	1.018301958	39.81852054	4.15E-10	4.79E-06
chr12:33860535-33860879	3.022208583	1.591674667	40.44293081	4.27E-10	4.84E-06
chr11:18064950-18065172	-2.687180583	2.967338557	39.19734724	4.39E-10	4.90E-06
chr15:14134321-14134546	5.26401552	0.425866206	38.87711603	4.51E-10	4.95E-06
chr19:17573981-17574266	3.642764546	1.009905913	39.40161312	5.08E-10	5.49E-06
chr10:42116318-42116524	5.232175993	0.429991158	38.44507647	5.63E-10	5.98E-06
chr1:44364500-44364730	4.147275558	0.708073499	38.52789706	5.71E-10	5.98E-06
chr4:4054355-4054699	3.425544408	1.138375187	39.32810552	5.87E-10	6.05E-06
chr7:3757431-3757687	-3.786409394	1.358279252	39.54153951	6.08E-10	6.16E-06
chr1:44365032-44365211	4.835493546	0.490717803	38.22741605	6.30E-10	6.16E-06
chr16:36309709-36310408	-3.557012351	1.465945741	39.56931025	6.30E-10	6.16E-06
chr7:46087284-46087455	7.981826965	0.230040848	21.17953057	6.34E-10	6.16E-06
chr18:28877724-28878110	2.891848158	1.73451258	39.56000848	6.79E-10	6.51E-06
chr16:56712011-56712209	3.633342416	0.967826947	38.61819844	7.25E-10	6.78E-06
chr12:11585481-11585713	2.72877023	2.070702324	39.38676914	7.27E-10	6.78E-06
chr17:385874-386711	-2.604026788	4.005438704	37.8672385	7.57E-10	6.96E-06

chr7:7240058-7240293	2.644044691	2.329579821	39.08024438	7.73E-10	7.01E-06
chr13:10363694-10363955	2.55321582	2.648799435	38.62105969	7.95E-10	7.11E-06
chr9:53467316-53467458	3.534191884	1.038955445	38.4553653	8.39E-10	7.41E-06
chr25:9719527-9719828	2.632994316	2.303950942	38.87929342	8.64E-10	7.47E-06
chr25:36458353-36458681	2.873956522	1.741807714	39.06696413	8.67E-10	7.47E-06
chr5:35071235-35071429	3.684387649	0.939456911	38.13476334	9.00E-10	7.65E-06
chr9:46618685-46619005	-3.772431076	1.257710708	38.37108187	1.03E-09	8.63E-06
chr17:9276150-9276707	-2.668896676	2.746795961	37.91022082	1.05E-09	8.69E-06
chr22:3565853-3566202	-3.346992614	1.556578582	38.48026502	1.12E-09	9.14E-06
chr14:39106639-39106953	2.511204886	2.763406987	37.66240653	1.17E-09	9.48E-06
chr17:20533145-20533413	5.228126917	0.369134628	36.96750048	1.20E-09	9.62E-06
chr1:37688748-37688948	-4.813949817	0.850205101	37.19815583	1.32E-09	1.05E-05
chr5:1833066-1833295	-3.093618772	1.825623723	38.17453702	1.35E-09	1.05E-05
chr25:4126876-4127076	3.042100395	1.449927535	37.99872852	1.36E-09	1.05E-05
chr16:1726229-1726400	-8.105756805	0.568674421	20.39232729	1.39E-09	1.06E-05
chr14:23858034-23858319	2.751747127	1.871580008	37.94884975	1.51E-09	1.15E-05
chr10:44075959-44076315	2.681167238	2.044302701	37.88445618	1.54E-09	1.15E-05
chr17:15816979-15817375	2.494015945	2.752680279	37.12272487	1.55E-09	1.15E-05
chr25:37413670-37413861	3.292420527	1.159553194	37.32337123	1.62E-09	1.19E-05
chr21:26533699-26533881	-4.802066613	0.83030475	36.68067183	1.68E-09	1.22E-05
chr22:17704715-17704960	3.317082145	1.108386621	37.04509741	1.80E-09	1.29E-05

chr1:2113785-2114055	2.511141804	2.561340766	37.07840455	1.83E-09	1.30E-05
chr10:276791-277212	2.446091425	3.803940718	36.08842274	1.89E-09	1.32E-05
chr11:12832632-12832941	3.450412197	1.020203491	36.54428773	2.16E-09	1.50E-05
chr17:1173241-1173586	-3.70138489	1.238728462	36.62695996	2.42E-09	1.66E-05